Fall 2019

Cationic Cobaltocene Derivatives and Polyelectrolyte Membranes for Energy Storage Applications

Tianyu Zhu

CATIONIC COBALTOCENE DERIVATIVES AND POLYELECTROLYTE MEMBRANES FOR ENERGY STORAGE APPLICATIONS

by

Tianyu Zhu

Bachelor of Science
Nanjing University, 2015

Submitted in Partial Fulfillment of the Requirements

For the Degree of Doctor of Philosophy in

Chemistry

College of Arts and Sciences

University of South Carolina

2019

Accepted by:

Chuanbing Tang, Major Professor

Brian C. Benicewicz, Chair, Examining Committee

Dmitry V. Peryshkov, Committee Member

Kevin Huang, Committee Member

Cheryl L. Addy, Vice Provost and Dean of the Graduate School

ACKNOWLEDGEMENTS

First and foremost, I would like to express my deepest appreciation to my advisor, Prof. Chuanbing Tang, who carefully guided me in both of my life and research over the past years. His enthusiasm and altitude towards science influenced me a lot and there is still much I want to learn from him in the future.

Then I want to thank Dr. Brian C. Benicewicz, Dr. Dmitry V. Peryshkov, Dr. Kevin Huang, Dr. Harry J. Ploehn and Dr. John Weidner for not only serving as my committee members, but also providing tremendous guidance and support for my research. I want to thank Dr. Benicewicz for guiding me in the research of polymer-grafted nanoparticles, and his group members for fuel cell related study. Also, I want to mention Dr. Huang and his postdoc for the collaborative work on rechargeable batteries.

In addition, I want to express my gratitude to past and present members in Tang group, department friends and colleagues, all my collaborators; It is a great pleasure to work and share happiness with all of you.

Finally, I would like to thank my family for their moral and financial support during my graduate study.

ABSTRACT

Metal-containing polyelectrolytes (or metallo-polyelectrolytes) represent a new class of polymeric materials with distinct properties compared to traditional organo-polyelectrolytes or neutral metallopolymers. This emerging class of synthetic materials is ubiquitous for a myriad of utilities ranging from traditional electrolyte chemistry to biomedicals to sustainable applications, to name just a few. This dissertation work is focused on the design, synthesis, characterization and application of advanced metallo-cations and metallo-polyelectrolytes for energy storage applications. First, a template method to prepare metallo-polyelectrolytes based on cationic cobaltocene and polyethylene backbone was described. The resulting membranes are mechanically tough, ionically conductive and chemically inert. Second, a family of substituted cobaltocenium cations and their derivatives was designed by theoretical calculation and experimentally synthesized for the first time. The redox behaviors and chemical stability of these metallo-cations were systematically examined and complemented those of state-of-the-art organic cations. Furthermore, substituted cobaltocene cation was integrated to construct solid polyelectrolyte membranes for energy storage devices (e.g. solid-state alkaline fuel cells). The device performance of these polyelectrolytes under highly basic and oxidative environments is also discussed.

Table of Contents

Acknowledgements iii

Abstract iv

List of Tables vii

List of Figures viii

List of Symbols xii

List of Abbreviations xiii

Chapter 1: General Introduction 1

1.1 Metallo-Polyelectrolytes and Their Diverse Topologies 2

1.2 Electronic, Bonding, and Redox Properties 4

1.3 Metallo-Polyelectrolytes for Ion Transport 10

1.4 Dissertation Outline 14

1.5 References 15

Chapter 2: Cationic Metallo-Polyelectrolytes for Robust Alkaline Anion-Exchange Membranes 22

2.1 Abstract 23

2.2 Introduction 23

2.3 Results And Discussion 26

2.4 Conclusions 34

2.5 Experimental Details 34

2.6 References 38

CHAPTER 3: THE FIRST SYNTHESIS OF A COMPLETE SET OF METALLO-CATIONS 45

3.1 ABSTRACT.....46

3.2 INTRODUCTION.....46

3.3 RESULTS AND DISCUSSION 47

3.4 CONCLUSIONS 56

3.5 EXPERIMENTAL DETAILS 56

3.6 REFERENCES 73

CHAPTER 4: REDOX- AND ALKALINE-STABLE METALLO-POLYELECTROLYTES FOR ENERGY STORAGE DEVICES.....79

4.1 ABSTRACT.....80

4.2 INTRODUCTION.....80

4.3 RESULTS AND DISCUSSION 81

4.4 CONCLUSIONS 88

4.5 EXPERIMENTAL DETAILS 88

4.6 REFERENCES 94

CHAPTER 5: SUMMARY AND OUTLOOK.....98

5.1 DISSERTATION SUMMARY.....99

5.2 FUTURE DIRECTION 100

5.3 REFERENCES 102

APPENDIX A: PERMISSION TO REPRINT.....104

APPENDIX B: CRYSTAL STRUCTURES 107

LIST OF TABLES

Table 2.1. Compositions and IECs of cobaltocenium AEMs. 31

Table 2.2. Mechanical properties of cobaltocenium AEM samples. 31

Table 3.1. BDE of various cobaltocenium cations by DFT calculations. 49

Table 3.2. Metal-counterion bonding strength and distance of various cobaltocenium cations by DFT calculations.....50

Table B.1. Crystal data and structure refinement for $Co(C_5H_5)_2(PF_6)$.....110

Table B.2. Crystal data and structure refinement for $[Co(C_5H_3(CH_3)_2)_2][PF_6]$ 113

Table B.3. Crystal data and structure refinement for $[Co(C_5H_2(CH_3)_3)_2][PF_6]$ 116

Table B.4. Crystal data and structure refinement for $[Co(C_5H(CH_3)_4)_2][PF_6]$.....119

Table B.5. Crystal data and structure refinement for $[Co(C_5H_4C(CH_3)_3)_2](PF_6)$.....121

Table B.6. Crystal data and structure refinement for $[Co(C_5H_3(C(CH_3)_3)_2)_2](PF_6)$.....123

LIST OF FIGURES

Figure 1.1. Diverse topologies of metallo-polyelectrolytes: **a.** metal ions attached to the side chain of organic polyelectrolytes through electrostatic interaction; **b.** neutral metal complexes at the side chain of polyelectrolytes; **c.** charged metal complexes at the side chain by covalent bonding; **d.** charged metal complexes at the side chain through coordination; **e.** main chain metallo-polyelectrolytes formed by coordination; **f.** main chain metallo-polyelectrolytes formed by covalent bonding. 3

Figure 1.2. Metallo-polyelectrolyte interactions with oppositely charged molecular substrates at three different levels. **a**. small molecules, **b**. macromolecules, and **c**. membranes or crosslinked networks. 6

Figure 1.3. a. Primary degradation mechanisms of quaternary ammonium cations; **b.** alkaline stable metal-containing cations for AEMs. 11

Figure 1.4. Metallo-polyelectrolytes for ion transport. Synthesis of metallo-polyelectrolytes by ROMP with metal complexes at the side-chain: **a.** heteroleptic bis(terpyridine) Ru(II) complex;[2] **b.** nickel-containing complex;[4] Metallo-polyelectrolytes by polycondensation: **c.** permethyl cobaltocenium-containing polysulfone;[17] **d.** cobaltocenium-containing polybenzimidazole;[18] **e.** illustration of single ion site migration inside alkaline anion-exchange membranes; **f.** a highly preferred phase separated morphology containing continuous hydrophilic ion transport channels and a hydrophobic matrix. 13

Figure 2.1. a. Synthesis of cobaltocenium monomer **2**, copolymer **3** and hydrogenated polymer **4** as AEMs; **b**. images of transparent and flexible cobaltocenium AEMs; **c**. proposed structures of cobaltocenium-containing AEMs in a hydroxide solution. 26

Figure 2.2. ^{1}H NMR spectra of cobaltocenium monomer **2** (top), copolymer **3** (middle) and hydrogenated polymer **4** (bottom). 28

Figure 2.3. a. UV-Vis spectra of unsubstituted cobaltocenium in a solution of NaOH at pH=14 over time; **b.** UV-Vis spectra of unsubstituted cobaltocenium in a solution of HCl at pH=1.5 over time; **c.** UV-Vis spectra of cobaltocenium monomer **2** with chloride ion

after immersing in 1 M NaOH at 80 ˚C for 1 h and 10 d; **d.** peak intensity of UV-Vis absorption at 282 nm (Red) and 346 nm (Blue) for cobaltocenium monomer **2** with chloride ion in 1 M NaOH at 80 °C. 29

Figure 2.4. Cobaltocenium AEMs: **a**. TGA and DTG curves; **b**. SAXS profiles; **c**. hydroxide conductivity of membranes as a function of temperature in fully hydrated condition; **d**. room temperature conductivity as a function of immersion time of membranes in 1 M NaOH solution at 80 ˚C.....33

Figure 2.5 Synthesis of cobaltocenium AEMs.....36

Figure 3.1 Bonding of cobaltocenium cations by DFT calculations. **a.** illustration of metal-Cp bond dissociation; **b.** DFT calculation of bond dissociation energy (BDE) as a function of number of substituents; **c.** comparison of optimized structures by DFT calculation, metal-Cp and metal-counterion distance for unsubstituted, octa-methyl and tetra-*tert*-butyl cobaltocenium. (Hydrogen atoms are omitted for clarity; **cc** represents unsubstituted cobaltocenium; **dmcc**, **tmcc**, **hmcc**, **omcc**, **dtcc**, and **ttcc** represent cobaltocenium with di-methyl, tetra-methyl, hexa-methyl, octa-methyl, di-*tert*-butyl, and tetra-*tert*-butyl substituents, respectively.) 48

Figure 3.2. Synthetic pathways of cobaltocenium derivatives by methyl and *tert*-butyl substitution: derivatives with even number of alkyl groups are prepared by oxidative reactions between substituted cyclopentadiene and $CoBr_2$ in the presence of $NaPF_6$; those with odd number of substituted groups are prepared by nucleophilic addition and endo-hydride abstraction of derivatives with even number of alkyl groups. (The center number box indicates the number of substituents).....52

Figure 3.3. Redox properties and chemical stability of cobaltocenium cations. **a.** chemical structures of cobaltocenium derivatives, and two organo-cations used in this study for comparison; **b**. cyclic voltammetry curves for cobaltocenium cations and organo-cations at a scan of 100 mV/s in acetonitrile with 0.1 M tetra-butyl-ammonium hexafluorophosphate as the supporting electrolyte, shadows represent HOR and ORR potentials; **c**. Stability of cobaltocenium cations and organo-cations (0.025 M) in 5M KOH/CD_3OH at 80 °C under air.....55

Figure 3.4. Synthesis of cationic cobaltocene derivatives 59

Figure 4.1. Schematic illustration of **a.** an AEMFC device; **b.** ion transport, ORR and HOR reactions in an AEMFC; **c.** the voltage changes in an AEMFC. 82

Figure 4.2. Synthesis of octamethyl cobaltocenium polyelectrolytes as AEMs. (synthesis details. **i**: HBr/HAc; **ii**: NaN_3, DMF, 70 ˚C; **iii**: ethynyltrimethylsilane, *n*-BuLi, THF; **iv**: triphenylcarbenium hexafluorophosphate, DCM; **v**: $CuSO_4$, Na ascorbate, THF/H_2O; **vi**: Grubbs III catalyst, DMAc/xylenes, *p*-toluenesulfonyl hydrazide, Bu_3N; **vii**: aqueous NH_4Cl, ion-exchange resin, 60 ˚C).....83

Figure 4.3. ^1H NMR spectrum of hydrogenated octamethyl cobaltocenium polymer in DMSO-d_6. 84

Figure 4.4. a. Stress-strain curves of omccAEM membrane in a dry state and a hydrated condition; **b.** WADX pattern of omccAEM membrane (red line: experimental data; grey line: fitting sum curve; green and blue lines: fitting multi-peaks, where blue line is considered as a crystalline peak); **c.** SAXS profile of omccAEM membrane; **d.** water uptake and swelling ratio for omccAEM membrane at different temperature; **e.** Arrhenius plots for conductivity of omccAEM with chloride and hydroxide as a function of temperature under fully hydrated conditions; **f.** room temperature conductivity as a function of immersion time of omccAEM in 3M KOH aqueous solution at 60 ˚C.....86

Figure 4.5. a. Polarization curves and power densities for omccAEM in a H_2/O_2 fuel cell (Anode: 0.8 mg PtRu/C cm^{-2}, Cathode: 0.49 mg Pt/C cm^{-2} on 5% PTFE GDL); **b.** high frequency resistance curves for omccAEM in a H_2/O_2 fuel cell under constant voltage at 55 ˚C.....87

Figure 4.6. Synthesis of octamethyl cobaltocenium AEMs.....94

Figure A.1. Copyright release for Chapter 1 and Chapter 5. 105

Figure A.2. Copyright release for Chapter 2.....106

Figure B.1. Molecular structure of **1** showing displacement ellipsoids drawn at the 60% probability level. Both Co centers on crystallographic inversion centers. Cp rings of Co2 disordered over two equally populated orientations. 111

Figure B.2. Molecular structure of **2b** showing displacement ellipsoids drawn at the 40% probability level. Images of one possible Me2Cp grouping arrangement in the cation. .114

Figure B.3. Molecular structure of **S17** showing displacement ellipsoids drawn at the 50% probability level.Co1A and Co1B cations are enantiomers. Counterions are omitted for clarity. 117

Figure B.4. Molecular structure of **2c** showing displacement ellipsoids drawn at the 50% probability level. Counterions are omitted for clarity.....120

Figure B.5. Molecular structure of **3a** showing displacement ellipsoids drawn at the 50% probability level. Superscripts denote symmetry-equivalent atoms. Both species have C2h point symmetry. 122

Figure B.6. Molecular structure of **3b** displacement ellipsoids drawn at the 40% probability level. Counterions are omitted for clarity.....125

.

List of Symbols

M_n	Number average molecular weight
$Đ$	Dispersity
T_g	Glass transition temperature
T_m	Melting temperature
T_d	Temperature at 5% weight loss

List of Abbreviations

AEM ..... Anion Exchange Membrane

AEMFC ..... Anion Exchange Membrane Fuel Cell

AFM ..... Atomic Force Microscopy

ATRP ..... Atom Transfer Radical Polymerization

BDE ..... Bond Dissociation Energy

DCM ..... Dichloromethane

DLS ..... Dynamic Light Scattering

DMF ..... *N*,*N*-Dimethylformamide

DSC ..... Differential Scanning Calorimetry

GPC ..... Gel Permeation Chromatography

FTIR ..... Fourier-Transform Infrared Spectroscopy

IEC ..... Ion-Exchange Capacity

MW ..... Molecular Weight

NMR ..... Nuclear Magnetic Resonance Spectroscopy

PEC ..... Polyelectrolyte complex

RAFT ..... Reversible Addition-Fragmentation Chain-Transfer

ROMP ..... Ring-Opening Metathesis Polymerization

SAXS ..... Small-Angle X-ray Scattering

SEM ..... Scanning Electron Microscope

TBACl ..... Tetrabutyl Ammonium Chloride

TGA ..... Thermal Gravitational Analysis

THF ..... Tetrahydrofuran

TMS ..... Trimethylsilyl

UV-Vis ..... Ultraviolet-Visible

CHAPTER 1

GENERAL INTRODUCTION[1]

[1] Zhu, T.; Sha, Y.; Yan, J.; Pageni, P.; Rahman, M. A.; Yan, Y.; Tang, C., Metallo-Polyelectrolytes as A Class of Ionic Macromolecules for Functional Materials. *Nat. Commun.*, **2018**, *9*, 4329. Adapted with permission from Springer Nature. Copyright © 2018 Springer Nature

1.1 Metallo-Polyelectrolytes and Their Diverse Topologies

Polyelectrolytes are a class of macromolecules containing charged groups, either positively, negatively or both.[3] Equally important to uncharged neutral polymers, polyelectrolytes have been widely used for a myriad of applications, ranging from genetic coding to synthetic membranes for separation to drug delivery, to name just a few.[5-7] Quaternary ammonium-based cationic and organic acid-based anionic polymers are among the most common polyelectrolytes. While polyelectrolytes continue to attract attention in the areas of chemistry, physics, engineering, biology, and pharmaceutics, it is appealing for both academia and industry to design charged macromolecules toward unprecedented properties and functions to address problems that the world is facing regarding health, energy, environments and sustainability in the 21st century.[8-11]

The fields of polymer and macromolecular sciences have enjoyed a unique combination of metals and soft organic frameworks in the name of metallopolymers, metal-containing polymers or organometallic polymers since the middle of 20th century.[12-15] When metallopolymers carry charged groups, they form a class of polyelectrolytes or metallo-polyelectrolytes. This is also an emerging area that is particularly well suited for manufacturing functional materials.

Depending on the metal location and the nature of chemical bonding of metals, metallo-polyelectrolytes have a variety of topologies as summarized in **Figure 1.1**. In the case of metals as a pendant group, metal cations can be counterions to anionic polyelectrolytes (**Figure 1.1 a**). Polyelectrolyte frameworks could also carry neutral metal centers (**Figure 1.1 b**). On the other hand, metal cations can coordinate or covalently complex at the side chain to form metallo-polyelectrolytes (**Figure 1.1 c** & **d**). Similarly,

main chain metallo-polyelectrolytes can be also fabricated via coordination or covalent bonding (**Figure 1.1 e** & **f**). Organo-polyelectrolytes utilize covalent bonding to form the ionic charged groups as an integral part of macromolecules. However, the formation of ionic centers via coordination chemistry is rare in this kind of polyelectrolytes.

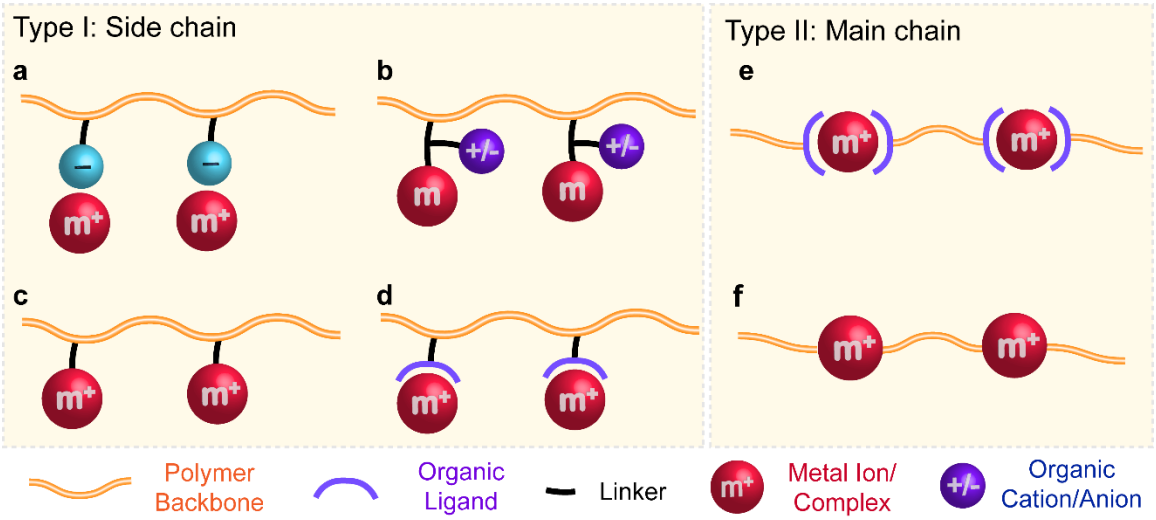

Figure 1.1. Diverse topologies of metallo-polyelectrolytes: **a.** metal ions attached to the side chain of organic polyelectrolytes through electrostatic interaction; **b.** neutral metal complexes at the side chain of polyelectrolytes; **c.** charged metal complexes at the side chain by covalent bonding; **d.** charged metal complexes at the side chain through coordination; **e.** main chain metallo-polyelectrolytes formed by coordination; **f.** main chain metallo-polyelectrolytes formed by covalent bonding.

Based on different architectures of metallo-polyelectrolytes, there are two major approaches to integrate metals into macromolecules: (1) metal ions attached to conventional polyelectrolytes through electrostatic interaction (**Figure 1.1 a**) or neutral metals (or metal complexes) added onto conventional polyelectrolytes (**Figure 1.1 b**), in which the charged groups behave most likely the same way as organo-polyelectrolytes, though the metals could provide additional functions; (2) charged metals integrated into organic frameworks (**Figure 1.1 c-f**), in which the properties of polyelectrolytes would be

mostly dictated by the ionic metal centers. The latter scenario is expected to be substantially different from traditional organo-polyelectrolytes.

1.2 Electronic, Bonding, and Redox Properties

Polyelectrolytes are ionic macromolecules that can complex with a variety of oppositely charged substrates. The ionic groups and polymeric backbone are the most important components for polyelectrolytes. When mixing with substrates carrying oppositely charged ions, it typically encounters enthalpy-driven electrostatic interactions. The association between oppositely charged molecules simultaneously initiates entropic changes by the loss of counterions. Most often, the entropic change drives the complexation, while the attractive Coulombic interactions between opposite charges are favorable in terms of enthalpy change. On the other hand, complexes between two oppositely charged polyelectrolytes, often referred to polyelectrolyte complexes (PECs), are mostly studied.[18-19] Depending on the strength of complexation, PECs often undergo phase separation, with the formation of either solid precipitates or liquid-like coacervates.[20-21]

While there are many similarities to organo-polyelectrolytes, metallo-polyelectrolytes provide a new level of electrolyte chemistry and physics. Noticeable difference is the presence of transition metals that allow unique electronic properties such as lipophobicity, ionic binding strength and redox chemistry.[22-23] The tunable oxidation state of metal cations would offer unprecedented redox chemistry that organo-ions typically cannot. This property could open up many new applications for metallo-polyelectrolytes beyond traditional organo-polyelectrolytes.[11, 24] In addition, metal cations may exhibit significantly distinct behaviors in thermal and chemical stability for some

applications.[2, 25] On the other hand, metals are generally used as cationic centers for building polyelectrolytes, thus it is fair to compare metallo-polyelectrolytes with cationic organo-polyelectrolytes, particularly the most studied quaternary ammonium-based counterparts.

Electronic properties of metallo-polyelectrolytes.

The ionic binding for both metal-containing cations and organo-ions first encounters with electrostatic Coulombic interactions. The intrinsic electron configuration of transition metals often involves incompletely filled d-orbitals, which could have dramatically different electronic and possibly solvophilic effects in comparison with nitrogen and phosphorous atoms in organo-ions, when complexing with oppositely charged molecules. In the case of organometallic cations, the size of these cations matters. The Pearson theory of hard and soft acids and bases (HSAB theory) could provide a basic foundation to compare the ionic binding strength.[26-28] Strong binding occurs between hard acids and hard bases, similarly between soft acids and soft bases. Small quaternary ammonium is a hard acid and prefers to interact with small anions. In comparison, most metallo-polyelectrolytes carry large metal cations (or large organometallic cations), a kind of soft acids. Thus, they would favor to bind with soft bases, large anionic substrates.[22] Although there is lack of quantitative data on ionic binding strength in literature, the qualitative difference between organic and metal-containing ions should be considered for choosing counterions, whenever appropriate.

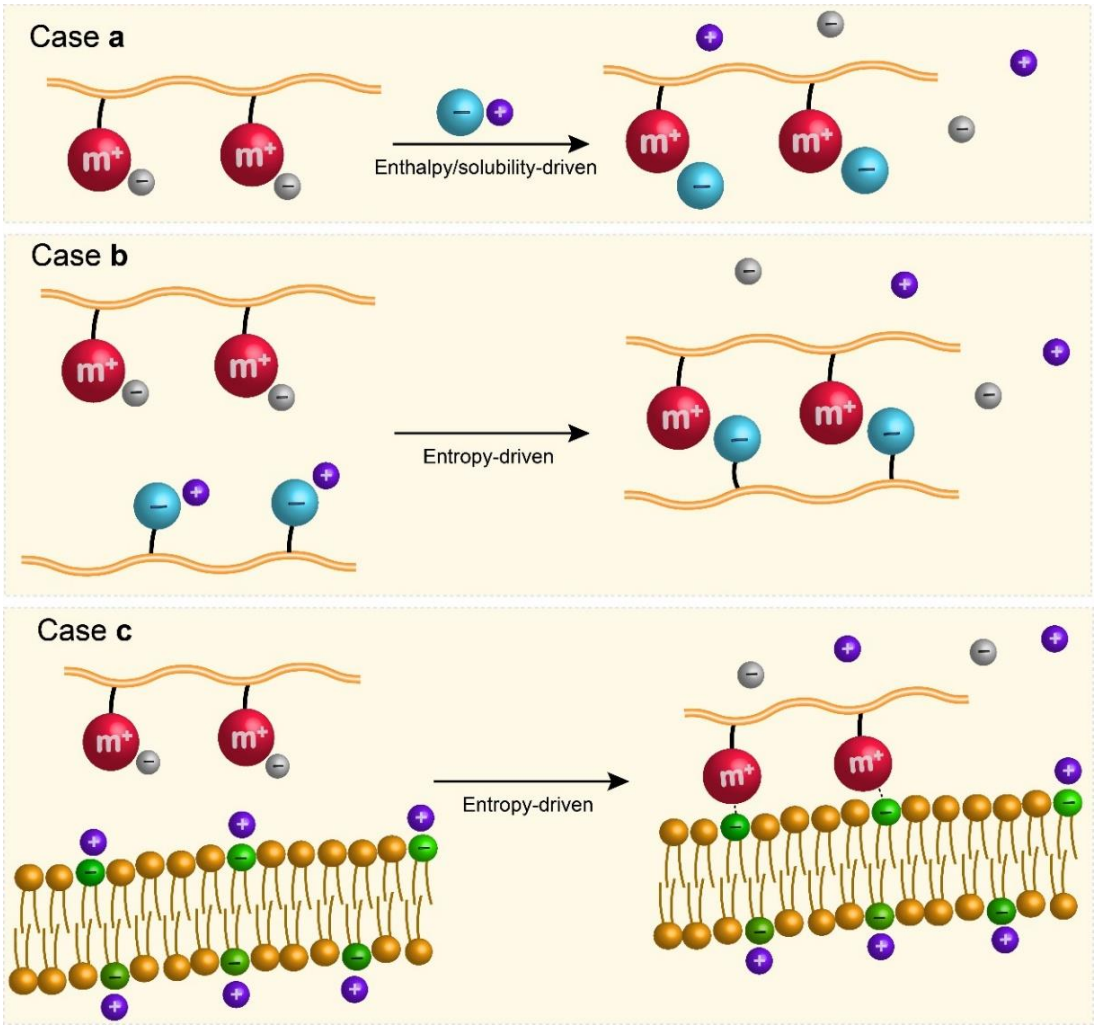

Figure 1.2. Metallo-polyelectrolyte interactions with oppositely charged molecular substrates at three different levels. **a**. small molecules, **b**. macromolecules, and **c**. membranes or crosslinked networks.

Ionic binding of metallo-polyelectrolytes.

We examine interactions of metallo-polyelectrolytes with several oppositely charged substrates, which provide a general picture to illustrate various scenarios. Specific comparisons with organo-polyelectrolytes are given in following sections outlining functional materials. There are three levels of oppositely charged molecular substrates for interactions relevant to the functions of metallo-polyelectrolytes: small molecules, macromolecules, and membranes or crosslinked networks (**Figure 1.2**). All these

interactions are associated with changes of enthalpy, entropy, and in many cases dehydration (e.g. reduced solubility with loss of water).

In the case of molecular anions (**Case a**), the entropic change with the release of counterions associated with metal cations is generally small.[29] Thus, the enthalpic change would play a greater role in driving ion exchange. It has been demonstrated that the type of charges appears to be more important.[30] For example, carboxylates associate with cations weaker than sulfonates. The aromatic sulfonates associate more strongly than the aliphatic ones. The presence of π-system on anions increases the affinity for cationic metal centers significantly. This is mostly attributed to Coulombic interactions. Another driving force would be the reduction of solubility in solutions, in some case even leading to phase separation. The complexation of metallo-polyelectrolytes with molecular anions is essentially an equilibrium process, which could be dramatically shifted with the significant reduction of solubility or precipitation of newly formed complexes. For example, a phase-transfer ion-exchange strategy was developed to prepare cationic cobaltocenium polyelectrolytes using tetrabutyl ammonium halide salts to replace a hexafluorophosphate counterion.[31] The dramatically reduced solubility crashes out newly formed halide-paired polyelectrolytes in acetonitrile. On the other hand, halide-paired polyelectrolytes were reported to ion-exchange with antibiotics to form bioconjugates.[32] The exchange is favorable, possibly due to the small gain of entropy, as antibiotics have a significantly larger size than halides. In addition, one should consider the Pearson HSAB theory on soft acids and bases.[26-28] In the case of ion-exchange from chloride to β-lactam antibiotics, the anionic antibiotics are a relatively softer base than chloride, thus favorable for interaction with a soft acid like cobaltocenium.

When metallo-polyelectrolytes interact with negatively charged macromolecules, it is the situation of **Case b** for the formation of PECs. While the complexation starts with attractive electrostatic interactions, it is the favorable entropic change to drive the mixing by releasing their respective small counterions. The loss of configurational and translational entropy of the long chains of polyelectrolytes upon the formation of PECs would contribute positively to the entropy change. The PEC formation is dictated by many factors such as molecular weight, charge density, molar ratio, Van der Waals forces, hydrophobic interactions, hydrogen bonding, etc. Typically, polymers with a longer chain and higher charge densities tend to form PECs. It has been quantitatively compared with ionic binding strength between oppositely charged polyelectrolytes.[30, 33] We reported the complexation of cobaltocenium-containing methacrylate polymers with poly(acrylic acid). The level of complexation was monitored by the release of their counterions. The gradual increase of turbidity indicated the formation of liquid-like coacervates.[32] However, when these metallo-polyelectrolytes interacted with phosphate-containing macromolecules (e.g. lipoteichoic acid), it was observed with the formation of precipitates. In addition, when complexed with the same anionic polyelectrolytes (e.g. poly(styrene sulfonate)), cobaltocenium-containing polyelectrolytes exhibited stronger binding strength than quaternary ammonium-containing counterparts.[22]

The ionic binding strength can be evaluated by the extent to which ion pairs between PECs are torn apart by a common salt, KBr.[30, 34] With the addition of salt, ion pairs in PECs are surrounded by the free ions via diffusion. With the increase of salt concentration, the PECs dissociate progressively. The complexation would be completely suppressed above a critical ionic strength, which depends on the type of ionic groups and

charge density in polyelectrolytes as well as their chain length. Thus, ionic strength is always an important factor regarding polyelectrolyte complexation.

As a membrane or a crosslinked charged network possesses even lower translational and rotational configurations than a single polyelectrolyte (**Case c**), it is expected that the positive gain of entropy change would greatly favor its complexation with metallo-polyelectrolytes via releasing highly mobile counterions. On the other hand, the strong complexation might have a negative impact on the diffusion of polyelectrolytes across the network. The choice of ionic groups and charge density would become more important for tuning the complexation. It has been demonstrated that diffusion of ionic sites within PEC films is much faster than polyelectrolytes themselves (probably over 2 orders of magnitude).[35] This is quite straightforward as it is a local rearrangement of ionic units vs. PEC assembly in all of their forms. Such diffusion becomes more relevant when the networks are cell membranes, which will be elaborated in a section below about antimicrobial biomaterials.

Redox chemistry of metallo-polyelectrolytes.

Research on redox active polyelectrolytes can be traced to early 1980s.[36-43] For metallo-polyelectrolytes, metal-containing cations can be well utilized with their reduction and oxidation chemistry,[44] which is usually not possessed by organo-ions. For example, many research groups have extensively investigated the redox behaviors of ferrocenium and cobaltocenium-containing polyelectrolytes, including dendrimers and block copolymers.[45-52] The formation of PECs can be tuned by changing the oxidation state of metal-containing cations, in some cases, even fully destroyed. In the section below regarding multilayers, redox chemistry of metallo-polyelectrolytes could be utilized to

modulate the assembly and disassembly processes. In biological systems, metal cations could participate metabolisms involving enzymes, such as oxidative stress.[53-54] Fenton chemistry is another common redox chemistry producing super radical species,[55] which has been reported in designing antimicrobial metallo-polyelectrolytes to induce oxidative stress on bacterial cells,[56-57] as elaborated below.

1.3 Metallo-Polyelectrolytes for Ion Transport.

Ion-exchange in polyelectrolyte-based membranes has a broad range of applications in energy conversion/storage devices, such as alkaline fuel cells,[58-59] redox flow batteries,[60] electrodialysis and electrolyzers.[61] It mainly takes the advantage of the ability of binding to small ions (like hydroxide, halide, carbonate ions) and redox stability under operational potentials. However, it remains a challenge to develop advanced anion-exchange membranes (AEMs) with sufficient chemical stability and high anionic conductivity under extremely harsh, highly basic conditions in alkaline fuel cells. The major issues that limit the performance of AEMs include the degradation of polymers under caustic conditions and lower intrinsic mobility of hydroxide ions. This section summarizes recent progress on the design of metallo-polyelectrolytes to improve ion exchange as well as cation stability under alkaline conditions.

Traditional quaternary ammonium-based organo-polyelectrolytes are used for anion-exchange and transport.[62-64] Some other organic cations include imidazolium,[65-66] phosphonium,[67-68] pyridinium,[69-70] and guanidinium,[71-72] while poor chemical and thermal stability is the major concern for many of these cations and their organo-polyelectrolytes. The primary mechanisms of degradation for the well-studied benzyl trimethylammonium

cation involve Hofmann elimination and nucleophilic substitution by hydroxide ions, as well as the formation of Ylide or chemical rearrangements (**Figure 1.3 a**).[59, 73]

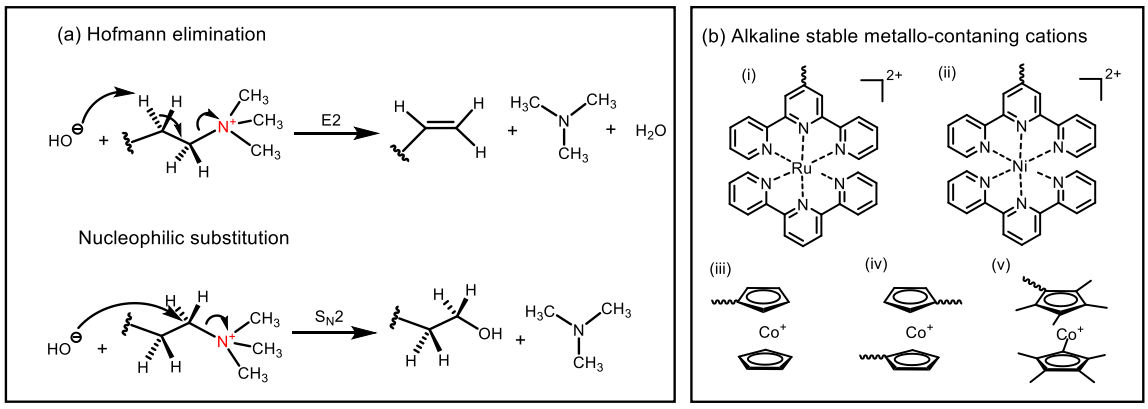

Figure 1.3. a. Primary degradation mechanisms of quaternary ammonium cations; **b.** alkaline stable metal-containing cations for AEMs.

Compared to conventional organic cations, many metal complexes (or metal cations) exhibit good physiochemical stability under strong basic conditions (**Figure 1.3 b**). For example, cationic Ru complexes exhibited excellent stability in NaOH solution at room temperature over six months.[2] Similarly, no significant changes were observed for cobaltocenium cyclooctene monomer in 1 M NaOH solution at 80 °C for two weeks.[25] Only 7% of dimethyl cobaltocenium cation degraded after storing in 1M KOH at 80 °C for 30 days.[17] Permethyl cobaltocenium cation showed a much longer lifetime than many other organic cations under high temperature (only 8.5% degraded at 140 °C in 1 M NaOD/D_2O after 6 weeks).[74] In addition, both mono-substituted and permethyl cobaltocenium-containing polyelectrolytes showed excellent thermal stability with decomposition temperature over 300 °C, which is significantly higher than most ammonium or imidazole-functionalized polyelectrolytes.[16, 25] However, more rigorous tests are required to reveal the stability of these metal complexes under highly basic and also highly oxidative conditions, especially at the device level.[75] In addition to metal-containing ions, polymeric

frameworks are equally important to maintain structural and mechanical integrity of the entire polyelectrolytes.

On the other hand, to obtain higher ion conductivity, elucidation of the ion diffusion mechanisms inside polyelectrolyte membranes is vital.[30, 76] In the case of alkaline fuel cells, free hydroxide ions are produced by oxygen reduction reaction in the cathode. Then, hydroxide ions can hop from one cationic site to another, as seen in **Figure 1.4 e**, which is similar to proton transport through the ionic domains in Nafion. Finally, free hydroxide ions transport through membranes to the anode side and participate the oxidation reaction with fuels. We reported cobaltocenium-containing copolymers with a hydrophobic polyethylene backbone for maintaining mechanical stability and hydrophilic cobaltocenium side chains for achieving rapid hydroxide transport.[25] To date, metallo-polyelectrolytes for ion-exchange membranes can be separated into two categories: polymers with non-aromatic based backbones and aromatic backbones.

Non-Aromatic Based Polymer Backbones.

This class of metallo-polyelectrolytes is mostly built from norbornene/cyclooctene-functionalized monomers, as shown in **Figure 1.4 a-c**. Hickner, Tew and co-workers reported multivalent metal-cation-based polyelectrolytes in 2012,[2] which were synthesized by copolymerization of a bis(terpyridine)Ru(II) complex-functionalized norbornene monomer with dicyclopentadiene, the latter monomer is a crosslinker (**Figure 1.4 a**). These membranes exhibited good hydroxide conductivity (28.6 mS/cm at 30 °C) with mechanical properties comparable to traditional quaternary ammonium-based polyelectrolytes. In early 2018, they further developed crosslinked nickel-containing polyelectrolytes using thiol-ene reactions (**Figure 1.4 b**).[4] In this case, the nickel cation functions as both an ion conductor

and a crosslinker. Although the formation of ion clusters was observed, high water uptake (> 150%) and extreme brittleness of membranes were the major drawbacks.

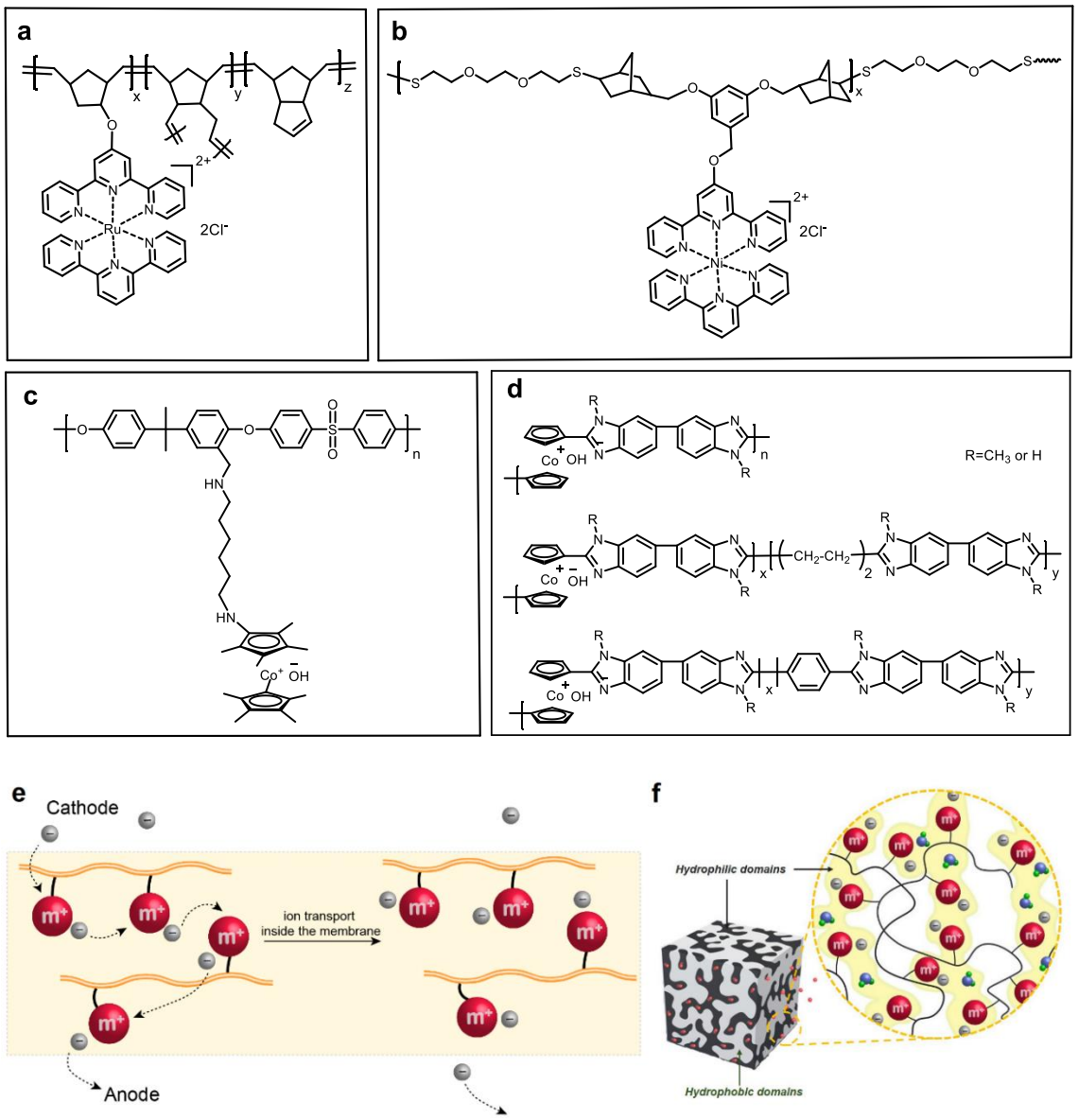

Figure 1.4. Metallo-polyelectrolytes for ion transport. Synthesis of metallo-polyelectrolytes by ROMP with metal complexes at the side-chain: **a.** heteroleptic bis(terpyridine) Ru(II) complex;[2] **b.** nickel-containing complex;[4] Metallo-polyelectrolytes by polycondensation: **c.** permethyl cobaltocenium-containing polysulfone;[16] **d.** cobaltocenium-containing polybenzimidazole;[17] **e.** illustration of single ion site migration inside alkaline anion-exchange membranes; **f.** a highly preferred phase separated morphology containing continuous hydrophilic ion transport channels and a hydrophobic matrix.

Aromatic Based Polymer Backbones.

The second type of metallo-polyelectrolytes contains aromatic polymer backbones. These polymers are typically prepared by polycondensation reactions. The Yan group reported permethyl cobaltocenium as an ultra-stable cation for ion transport.[16] The bulky hydrophilic cations were linked to a rigid hydrophobic polysulfone backbone via a flexible diamine linker (**Figure 1.4 c**). The membrane exhibited excellent thermal stability, high tensile strength (40 MPa with 10% elongation at break) and good conductivity (22 mS/cm at room temperature). However, earlier work demonstrated that polysulfone-based membranes would have cation-triggered backbone degradation,[73] which remains a concern for durability of these materials. Polybenzimidazole membranes with cobaltocenium on the backbone were prepared by microwave polycondensation, as reported by Zhu and co-workers (**Figure 1.4 d**).[17] These membranes exhibited hydroxide conductivity of 37.5 mS/cm at 90 °C and over 80% hydroxide conductivity retention for nearly one month.

Ideally, a phase-separated morphology in membranes is favorable to facilitate the ion transport and improve the electrochemical performance, especially under partially hydrated conditions, as illustrated in **Figure 1.4 f**.[77] Well-connected hydrophilic domains or nanochannels for faster ion migration were also observed in many polymer architectures like block copolymers and comb-shaped polymers.[78] On the other hand, hydrophobic components could serve as the matrix to maintain structural and mechanical integrity during ion transport and device fabrication.

1.4 Dissertation Outline

The central theme of this thesis is to investigate novel metallo-cations and metallo-polyelectrolyte membranes for energy storage applications. It generally includes the

design, synthesis, characterization of small molecules and polymers, as well as their electrochemical behavior in alkaline anion-exchange membrane fuel cells.

Chapter 2 describes the preparation of cobaltocenium-containing cyclooctene monomers and their polymerization via ring-opening metathesis polymerization (ROMP). The physiochemical and electrochemical properties of cobaltocenium-containing copolymers are carefully investigated.

Chapter 3 focuses on the design, preparation and characterization of a set of substituted cobaltocenium cations by a combination of computational and experimental study. The redox and chemical stability of these new metallo-cations were investigated and correlated with their chemical structures.

Chapter 4 discusses the synthesis of metallo-polyelectrolytes with octamethyl cobaltocenium cations. The polyelectrolyte membranes showed excellent mechanical properties, chemical stability, microphase separated morphology as well as good performance in an anion-exchange membrane fuel cell.

In the last Chapter, we conclude with challenges and prospects in our research and related area.

1.5 References

1. Zhu, T.; Sha, Y.; Yan, J.; Pageni, P.; Rahman, M. A.; Yan, Y.; Tang, C., Metallo-polyelectrolytes as a class of ionic macromolecules for functional materials. *Nat. Commun.* **2018,** *9* (1), 4329.

2. Zha, Y.; Disabb-Miller, M. L.; Johnson, Z. D.; Hickner, M. A.; Tew, G. N., Metal-cation-based anion exchange membranes. *J. Am. Chem. Soc.* **2012,** *134* (10), 4493-4496.

3. Hara, M., *Polyelectrolytes: science and technology*. CRC Press: New York, 1992.

4. Kwasny, M. T.; Zhu, L.; Hickner, M. A.; Tew, G. N., Utilizing thiol–ene chemistry for crosslinked nickel cation-based anion exchange membranes. *J. Polym. Sci. A* **2018,** *56* (3), 328-339.

5. Hiller, J. A.; Mendelsohn, J. D.; Rubner, M. F., Reversibly erasable nanoporous anti-reflection coatings from polyelectrolyte multilayers. *Nat. Mater.* **2002,** *1* (1), 59-63.

6. Pack, D. W.; Hoffman, A. S.; Pun, S.; Stayton, P. S., Design and development of polymers for gene delivery. *Nat. Rev. Drug Discov.* **2005,** *4* (7), 581-593.

7. Viovy, J.-L., Electrophoresis of DNA and other polyelectrolytes: Physical mechanisms. *Rev. Mod. Phys* **2000,** *72* (3), 813.

8. Dobrynin, A. V.; Rubinstein, M., Theory of polyelectrolytes in solutions and at surfaces. *Prog. Polym. Sci.* **2005,** *30* (11), 1049-1118.

9. Jiang, H.; Taranekar, P.; Reynolds, J. R.; Schanze, K. S., Conjugated polyelectrolytes: synthesis, photophysics, and applications. *Angew. Chem. Int. Ed.* **2009,** *48* (24), 4300-4316.

10. Mecerreyes, D., Polymeric ionic liquids: Broadening the properties and applications of polyelectrolytes. *Prog. Polym. Sci.* **2011,** *36* (12), 1629-1648.

11. Yan, Y.; Zhang, J.; Ren, L.; Tang, C., Metal-containing and related polymers for biomedical applications. *Chem. Soc. Rev.* **2016,** *45* (19), 5232-5263.

12. Whittell, G. R.; Hager, M. D.; Schubert, U. S.; Manners, I., Functional soft materials from metallopolymers and metallosupramolecular polymers. *Nat. Mater.* **2011,** *10* (3), 176-188.

13. Beck, J. B.; Rowan, S. J., Multistimuli, multiresponsive metallo-supramolecular polymers. *J. Am. Chem. Soc.* **2003,** *125* (46), 13922-13923.

14. Williams, K. A.; Boydston, A. J.; Bielawski, C. W., Main-chain organometallic polymers: synthetic strategies, applications, and perspectives. *Chem. Soc. Rev.* **2007,** *36* (5), 729-744.

15. Hailes, R. L. N.; Oliver, A. M.; Gwyther, J.; Whittell, G. R.; Manners, I., Polyferrocenylsilanes: synthesis, properties, and applications. *Chem. Soc. Rev.* **2016,** *45* (19), 5358-5407.

16. Gu, S.; Wang, J.; Kaspar, R. B.; Fang, Q.; Zhang, B.; Bryan Coughlin, E.; Yan, Y., Permethyl Cobaltocenium (Cp*2Co+) as an Ultra-Stable Cation for Polymer Hydroxide-Exchange Membranes. *Sci. Rep.* **2015,** *5*, 11668.

17. Chen, N.; Zhu, H.; Chu, Y.; Li, R.; Liu, Y.; Wang, F., Cobaltocenium-containing polybenzimidazole polymers for alkaline anion exchange membrane applications. *Poly. Chem.* **2017,** *8* (8), 1381-1392.

18. Philipp, B.; Dautzenberg, H.; Linow, K.-J.; Kötz, J.; Dawydoff, W., Polyelectrolyte complexes—recent developments and open problems. *Prog. Polym. Sci.* **1989,** *14* (1), 91-172.

19. Thünemann, A. F.; Müller, M.; Dautzenberg, H.; Joanny, J.-F.; Löwen, H., Polyelectrolyte complexes. In *Polyelectrolytes with defined molecular architecture II*, Schmidt, M., Ed. Springer: 2004; pp 113-171.

20. Wang, Q.; Schlenoff, J. B., The Polyelectrolyte Complex/Coacervate Continuum. *Macromolecules* **2014,** *47* (9), 3108-3116.

21. Chollakup, R.; Smitthipong, W.; Eisenbach, C. D.; Tirrell, M., Phase Behavior and Coacervation of Aqueous Poly(acrylic acid)−Poly(allylamine) Solutions. *Macromolecules* **2010,** *43* (5), 2518-2528.

22. Pageni, P.; Kabir, M. P.; Yang, P.; Tang, C., Binding of Cobaltocenium-Containing Polyelectrolytes with Anionic Probes. *J. Inorg. Organomet. Polym.* **2017,** *27* (4), 1100-1109.

23. Ma, Y.; Dong, W. F.; Hempenius, M. A.; Möhwald, H.; Vancso, G. J., Redox-controlled molecular permeability of composite-wall microcapsules. *Nat. Mater.* **2006,** *5* (9), 724-9.

24. Wang, S.; Xu, Z.; Wang, T.; Xiao, T.; Hu, X.-Y.; Shen, Y.-Z.; Wang, L., Warm/cool-tone switchable thermochromic material for smart windows by orthogonally integrating properties of pillar [6] arene and ferrocene. *Nat. commun.* **2018,** *9*, DOI: 10.1038/s41467-018-03827-3.

25. Zhu, T.; Sha, Y.; Adabi, H.; Peng, X.; Cha, Y.; Dissanayake, D. M. M. M.; Smith, M.; Vannucci, A.; Mustain, W. E.; Tang, C., The First Synthesis of a Complete Set of Metallo-Cations Toward Redox- and Alkaline-Stable Metallo-Polyelectrolytes. *Manuscript submitted* **2019**.

26. Pearson, R. G., Hard and soft acids and bases. *J. Am. Chem. Soc.* **1963,** *85* (22), 3533-3539.

27. Pearson, R. G., Hard and soft acids and bases, HSAB, part II: Underlying theories. *J. Chem. Educ.* **1968,** *45* (10), 643.

28. Pearson, R. G., Recent advances in the concept of hard and soft acids and bases. *J. Chem. Educ.* **1987,** *64* (7), 561.

29. Van der Gucht, J.; Spruijt, E.; Lemmers, M.; Stuart, M. A. C., Polyelectrolyte complexes: bulk phases and colloidal systems. *J. Colloid Interface Sci* **2011,** *361* (2), 407-422.

30. Fu, J.; Fares, H. M.; Schlenoff, J. B., Ion-Pairing Strength in Polyelectrolyte Complexes. *Macromolecules* **2017,** *50* (3), 1066-1074.

31. Zhang, J. Y.; Yan, Y.; Chance, M. W.; Chen, J. H.; Hayat, J.; Ma, S. G.; Tang, C. B., Charged Metallopolymers as Universal Precursors for Versatile Cobalt Materials. *Angew. Chem. In. Ed.* **2013,** *52* (50), 13387-13391.

32. Zhang, J. Y.; Chen, Y. P.; Miller, K. P.; Ganewatta, M. S.; Bam, M.; Yan, Y.; Nagarkatti, M.; Decho, A. W.; Tang, C. B., Antimicrobial Metallopolymers and Their Bioconjugates with Conventional Antibiotics against Multidrug-Resistant Bacteria. *J. Am. Chem. Soc.* **2014,** *136* (13), 4873-4876.

33. Bucur, C. B.; Sui, Z.; Schlenoff, J. B., Ideal Mixing in Polyelectrolyte Complexes and Multilayers: Entropy Driven Assembly. *J. Am. Chem. Soc.* **2006,** *128* (42), 13690-13691.

34. Chollakup, R.; Beck, J. B.; Dirnberger, K.; Tirrell, M.; Eisenbach, C. D., Polyelectrolyte Molecular Weight and Salt Effects on the Phase Behavior and Coacervation of Aqueous Solutions of Poly(acrylic acid) Sodium Salt and Poly(allylamine) Hydrochloride. *Macromolecules* **2013,** *46* (6), 2376-2390.

35. Fares, H. M.; Schlenoff, J. B., Diffusion of Sites versus Polymers in Polyelectrolyte Complexes and Multilayers. *J. Am. Chem. Soc.* **2017,** *139* (41), 14656-14667.

36. Flanagan, J. B.; Margel, S.; Bard, A. J.; Anson, F. C., Electron transfer to and from molecules containing multiple, noninteracting redox centers. Electrochemical oxidation of poly(vinylferrocene). *J. Am. Chem. Soc.* **1978,** *100* (13), 4248-4253.

37. Denisevich, P.; Willman, K. W.; Murray, R. W., Unidirectional current flow and charge state trapping at redox polymer interfaces on bilayer electrodes: principles, experimental demonstration, and theory. *J. Am. Chem. Soc.* **1981,** *103* (16), 4727-4737.

38. Chidesy, C. E. D.; Murray, R. W., Electroactive Polymers and Macromolecular Electronics. *Science* **1986,** *231* (4733), 25-31.

39. Willner, I.; Riklin, A.; Lapidot, N., Electron-transfer communication between a redox polymer matrix and an immobilized enzyme: activity of nitrate reductase in a viologen-acrylamide copolymer. *J. Am. Chem. Soc.* **1990,** *112* (17), 6438-6439.

40. Anson, F. C.; Saveant, J. M.; Shigehara, K., New model for the interior of polyelectrolyte coatings on electrode surfaces. Mechanisms of charge transport through protonated poly(L-lysine) films containing FeIII(edta)- and FeII(edta)2- as counterions. *J. Am. Chem. Soc.* **1983,** *105* (5), 1096-1106.

41. Methenitis, C.; Morcellet-Sauvage, J.; Morcellet, M., The interaction of poly (N-methacryloyl-L-alanine) with copper (II). *Polymer Bulletin* **1984,** *12* (2), 133-139.

42. Heller, A., Electrical wiring of redox enzymes. *Acc. Chem. Res* **1990,** *23* (5), 128-134.

43. Degani, Y.; Heller, A., Electrical communication between redox centers of glucose oxidase and electrodes via electrostatically and covalently bound redox polymers. *J. Am. Chem. Soc.* **1989,** *111* (6), 2357-2358.

44. Connelly, N. G.; Geiger, W. E., Chemical redox agents for organometallic chemistry. *Chem. Rev.* **1996,** *96* (2), 877-910.

45. Wang, Y.; Rapakousiou, A.; Astruc, D., ROMP Synthesis of Cobalticenium–Enamine Polyelectrolytes. *Macromolecules* **2014,** *47* (12), 3767-3774.

46. Kazutake, T.; J., D. D.; D., A. H.; Isabel, C.; Blanca, G.; M., C. C.; Beatriz, A.; Moisés, M.; José, L., Cobaltocenium-Functionalized Poly(propylene imine) Dendrimers: Redox and Electromicrogravimetric Studies and AFM Imaging. *Chem.: Eur. J* **2001,** *7* (5), 1109-1117.

47. Gu, H.; Ciganda, R.; Castel, P.; Moya, S.; Hernandez, R.; Ruiz, J.; Astruc, D., Tetrablock Metallopolymer Electrochromes. *Angew. Chem. In. Ed.* **2018,** *57* (8), 2204-2208.

48. Casado, C. M.; González, B.; Cuadrado, I.; Alonso, B.; Morán, M.; Losada, J., Mixed ferrocene–cobaltocenium dendrimers: the most stable organometallic redox systems combined in a dendritic molecule. *Angew. Chem.* **2000,** *112* (12), 2219-2222.

49. Cuadrado, I.; Casado, C. M.; Lobete, F.; Alonso, B.; González, B.; Losada, J.; Amador, U., Preparation and Redox Properties of Novel Polymerizable Pyrrole- and Allyl-Functionalized Cobaltocenium Monomers and Siloxane-Based Cobaltocenium Polymers. *Organometallics* **1999,** *18* (24), 4960-4969.

50. Staff, R. H.; Gallei, M.; Mazurowski, M.; Rehahn, M.; Berger, R.; Landfester, K.; Crespy, D., Patchy Nanocapsules of Poly(vinylferrocene)-Based Block Copolymers for Redox-Responsive Release. *ACS Nano* **2012,** *6* (10), 9042-9049.

51. Daniel, S.; Moritz, v. d. L.; Markus, G., Synthesis of Breathing Metallopolymer Hollow Spheres for Redox-Controlled Release. *Macromol. Rapid Commun* **2016,** *37* (19), 1573-1580.

52. Rabiee Kenaree, A.; Gilroy, J. B., Synthesis and characterization of metal-rich phosphonium polyelectrolytes and their use as precursors to nanomaterials. *Dalton Transactions* **2016,** *45* (45), 18229-18240.

53. Apel, K.; Hirt, H., Reactive oxygen species: metabolism, oxidative stress, and signal transduction. *Annu. Rev. Plant Biol.* **2004,** *55*, 373-399.

54. Yakes, F. M.; Van Houten, B., Mitochondrial DNA damage is more extensive and persists longer than nuclear DNA damage in human cells following oxidative stress. *Proc. Natl. Acad. Sci. U.S.A.* **1997,** *94* (2), 514-519.

55. Hayyan, M.; Hashim, M. A.; AlNashef, I. M., Superoxide ion: generation and chemical implications. *Chem. Rev.* **2016,** *116* (5), 3029-3085.

56. Lemire, J. A.; Harrison, J. J.; Turner, R. J., Antimicrobial activity of metals: mechanisms, molecular targets and applications. *Nat. Rev. Microbiol.* **2013,** *11* (6), 371.

57. Abd-El-Aziz, A. S.; Agatemor, C.; Etkin, N., Antimicrobial resistance challenged with metal-based antimicrobial macromolecules. *Biomaterials* **2017,** *118*, 27-50.

58. Varcoe, J. R.; Slade, R. C., Prospects for alkaline anion-exchange membranes in low temperature fuel cells. *Fuel cells* **2005,** *5* (2), 187-200.

59. Couture, G.; Alaaeddine, A.; Boschet, F.; Ameduri, B., Polymeric materials as anion-exchange membranes for alkaline fuel cells. *Prog. Polym. Sci.* **2011,** *36* (11), 1521-1557.

60. Li, X.; Zhang, H.; Mai, Z.; Zhang, H.; Vankelecom, I., Ion exchange membranes for vanadium redox flow battery (VRB) applications. *Energy Environ. Sci.* **2011,** *4* (4), 1147-1160.

61. Xu, T., Ion exchange membranes: state of their development and perspective. *J. Membr. Sci* **2005,** *263* (1-2), 1-29.

62. Robertson, N. J.; Kostalik IV, H. A.; Clark, T. J.; Mutolo, P. F.; Abruña, H. c. D.; Coates, G. W., Tunable high performance cross-linked alkaline anion exchange membranes for fuel cell applications. *J. Am. Chem. Soc.* **2010,** *132* (10), 3400-3404.

63. Clark, T. J.; Robertson, N. J.; Kostalik IV, H. A.; Lobkovsky, E. B.; Mutolo, P. F.; Abruna, H. D.; Coates, G. W., A ring-opening metathesis polymerization route to alkaline anion exchange membranes: development of hydroxide-conducting thin films from an ammonium-functionalized monomer. *J. Am. Chem. Soc.* **2009,** *131* (36), 12888-12889.

64. Pham, T. H.; Olsson, J. S.; Jannasch, P., N-spirocyclic quaternary ammonium ionenes for anion-exchange membranes. *J. Am. Chem. Soc.* **2017,** *139* (8), 2888-2891.

65. Hugar, K. M.; Kostalik IV, H. A.; Coates, G. W., Imidazolium cations with exceptional alkaline stability: A systematic study of structure–stability relationships. *J. Am. Chem. Soc.* **2015,** *137* (27), 8730-8737.

66. Fan, J.; Wright, A. G.; Britton, B.; Weissbach, T.; Skalski, T. J.; Ward, J.; Peckham, T. J.; Holdcroft, S., Cationic Polyelectrolytes, Stable in 10 M KOHaq at 100° C. *ACS Macro Lett.* **2017,** *6* (10), 1089-1093.

67. Noonan, K. J.; Hugar, K. M.; Kostalik IV, H. A.; Lobkovsky, E. B.; Abruña, H. c. D.; Coates, G. W., Phosphonium-functionalized polyethylene: a new class of base-stable alkaline anion exchange membranes. *J. Am. Chem. Soc.* **2012,** *134* (44), 18161-18164.

68. Gu, S.; Cai, R.; Luo, T.; Jensen, K.; Contreras, C.; Yan, Y., Quaternary phosphonium-based polymers as hydroxide exchange membranes. *ChemSusChem* **2010,** *3* (5), 555-558.

69. Sata, T.; Yamane, Y.; Matsusaki, K., Preparation and properties of anion exchange membranes having pyridinium or pyridinium derivatives as anion exchange groups. *J. Polym. Sci. A* **1998,** *36* (1), 49-58.

70. Wang, J.; Zhao, Y.; Setzler, B. P.; Rojas-Carbonell, S.; Yehuda, C. B.; Amel, A.; Page, M.; Wang, L.; Hu, K.; Shi, L., Poly (aryl piperidinium) membranes and ionomers for hydroxide exchange membrane fuel cells. *Nat. Energy* **2019,** *4* (5), 392.

71. Kim, D. S.; Labouriau, A.; Guiver, M. D.; Kim, Y. S., Guanidinium-functionalized anion exchange polymer electrolytes via activated fluorophenyl-amine reaction. *Chem. Mater.* **2011,** *23* (17), 3795-3797.

72. Zhang, Q.; Li, S.; Zhang, S., A novel guanidinium grafted poly (aryl ether sulfone) for high-performance hydroxide exchange membranes. *ChemComm* **2010,** *46* (40), 7495-7497.

73. Arges, C. G.; Ramani, V., Two-dimensional NMR spectroscopy reveals cation-triggered backbone degradation in polysulfone-based anion exchange membranes. *Proc. Natl. Acad. Sci. U.S.A.* **2013,** *110* (7), 2490-2495.

74. Gu, S.; Wang, J.; Kaspar, R. B.; Fang, Q.; Zhang, B.; Bryan Coughlin, E.; Yan, Y., Permethyl Cobaltocenium (Cp*2Co+) as an Ultra-Stable Cation for Polymer Hydroxide-Exchange Membranes. *Sci. Rep.* **2015,** *5*, 11668.

75. Varcoe, J. R.; Atanassov, P.; Dekel, D. R.; Herring, A. M.; Hickner, M. A.; Kohl, P. A.; Kucernak, A. R.; Mustain, W. E.; Nijmeijer, K.; Scott, K.; Xu, T.; Zhuang, L., Anion-exchange membranes in electrochemical energy systems. *Energy Environ. Sci.* **2014,** *7* (10), 3135-3191.

76. Kwasny, M. T.; Zhu, L.; Hickner, M. A.; Tew, G. N., Thermodynamics of Counterion Release Is Critical for Anion Exchange Membrane Conductivity. *J. Am. Chem. Soc.* **2018,** *140* (25), 7961–7969.

77. Shin, D. W.; Guiver, M. D.; Lee, Y. M., Hydrocarbon-based polymer electrolyte membranes: importance of morphology on ion transport and membrane stability. *Chem. Rev.* **2017,** *117* (6), 4759-4805.

78. Li, N.; Yan, T.; Li, Z.; Thurn-Albrecht, T.; Binder, W. H., Comb-shaped polymers to enhance hydroxide transport in anion exchange membranes. *Energy Environ. Sci.* **2012,** *5* (7), 7888-7892.

CHAPTER 2

CATIONIC METALLO-POLYELECTROLYTES FOR ROBUST ALKALINE ANION-EXCHANGE MEMBRANES[1]

[1] Zhu, T.; Xu, S.; Rahman, M. A.; Dogdibegovic, E.; Yang, P.; Pageni, P.; Kabir, M. P.; Zhou, X.; Tang, C., Cationic Metallo-Polyelectrolytes for Robust Alkaline Anion-Exchange Membranes. *Angew. Chem. Int. Ed.*, **2018**, *57*, 2388-2392. Adapted with permission from Wiley. Copyright © 2018 Wiley-VCH Verlag GmbH & Co. KGaA, Weinheim

2.1 Abstract

Chemically inert, mechanically tough, cationic metallo-polyelectrolytes were conceptualized and designed as durable anion-exchange membranes (AEMs). Ring-opening metathesis polymerization (ROMP) of cobaltocenium-containing cyclooctene with triazole as the only linker group, followed by backbone hydrogenation, led to a new class of AEMs with a polyethylene-like framework and alkaline-stable cobaltocenium cation for ion transport. These AEMs exhibited excellent thermal, chemical and mechanical stability, as well as high ion conductivity.

2.2 Introduction

Polyelectrolytes have vast applications ranging from coating to biomedical materials.[2-3] Among them, cationic polyelectrolytes are widely pursued as anion-exchange membranes (AEMs) in alkaline fuel cells for converting fuels into electricity,[4-16] which can be operated below 100 ˚C and thus are more attractive as energy conversion devices for electric vehicles and powering portable devices.

Commonly, AEMs are copolymers containing cations that are covalently linked to hydrophobic polymer backbones.[4-5, 16-17] The most popular approach is the use of quaternary ammonium cation (QAC)-containing polymers. However, QACs are prone to degradation through Hofmann elimination (E2) or nucleophilic substitution (S_N2) under highly basic conditions. Over the past few years, several strategies have been adopted to improve the alkaline stability of AEM backbones: (i) protect ammonium cations using steric protection, conformational restrictions or inductive effects;[18-26] (ii) explore alternative stable cations such as benzyl quaternary guanidinium,[27-28] imidazolium,[29-31] and

phosphonium[32-35] to slow down degradation. However, these methods have either sacrificed ion conductivity or still faced challenges on achieving long-term stability.

Of equal importance, other components of polyelectrolytes as AEMs are also required to be stable for withstanding harsh chemical environments. A degradation or deterioration of chemical compositions of polyelectrolytes would have a catastrophic impact on membrane performance. It is essential to design novel cationic polyelectrolytes with high cation stability and superior chemical durability of the polymer framework.

Herein we report a new class of robust AEMs based on cobaltocenium-containing polyelectrolytes that bear promising hydroxide conductivity as well as mechanical, thermal and chemical stability. These novel membranes exhibited long-term stability that is unprecedented over many reported polymeric systems. Specifically, we developed side-chain cobaltocenium-containing vinyl polymers, which have non-hydrolysable hydrocarbon backbones and extraordinarily stable side chains, yet with high modulus and toughness.

We along with others have discovered that cationic cobaltocenium exhibits good stability toward harsh chemical environments in both strong acidic and basic conditions.[36-42] As shown in **Figure 2.3 a & b**, there is negligible change in characteristic UV absorption corresponding to cobaltocenium after it was dissolved in a solution of NaOH (pH = 14) or HCl (pH = 1.5) for two weeks. Moreover, published work by Yan[43] and Zhu[44] both demonstrated that cobaltocenium cations with substituent group in Cp ring had superior thermal and chemical stability over other reported cations. Such extraordinary stability of cationic cobaltocenium motivated us to design ultra-stable polyelectrolytes in both cations and other compositions of frameworks for AEMs. To construct the new polymeric systems,

we need to avoid the integration of functional groups (e.g. ester, amide, anhydride, carbonate, etc.) and linkers that are susceptible to degradation under strong basic conditions for a prolonged period of time. Due to the instabilities of ester or imide group, most cobaltocenium polymers reported in literature could not be used as stable AEMs directly.[45-53]

To place our work in context, metal cations have been used for AEMs. Hickner and Tew reported the synthesis of AEMs functionalized with bis(terpyridine)-ruthenium(II) complexes.[15] These membranes exhibited good ion conductivity and mechanical properties. However, the decline of conductivity in alkaline condition over a long term was a concern. Yan and coworkers reported permethyl cobaltocenium-containing polysulfone as AEMs that exhibited extraordinary stability of cations and chemical stability of polymers.[43] The ion conductivity was mediocre, partially due to the steric hindrance for the pentamethyl group. These polymers were quite brittle with elongation at break only about 10%. Later Zhu and coworkers synthesized polybenzimidazole polymers with cobaltocenium cations in the main-chain.[44] These membranes showed improved thermal stability and ion-exchange capacity, but the mechanical and alkaline stability of these AEMs were inferior because of the poor stability of linkage groups and the rigid polymer backbones. Both approaches adopted condensation polymerization to prepare rigid polymers with relatively limited molecular weight. In addition, the synthesis was particularly laborious with low yields.

In this work, we followed three design principles: (1) eliminate any hydrolysable functionalities; (2) maximize the content of hydrocarbon in the compositions; (3) enable polymers with controlled molecular weight. Specifically, we used highly efficient click

chemistry to attach cobaltocenium onto a cyclic vinyl monomer, which was executed for ring-opening metathesis polymerization (ROMP).[54-55] The resultant polymer has only one triazole group as a linker between cobaltocenium and the polymer backbone. This powerful synthetic tool allows the preparation of high molecular weight toward mechanically flexible and tough polymers. In addition, these polymers have a polyethylene-like backbone to warrant mechanical integrity and chemical stability under harsh basic conditions.

2.3 Results and Discussion

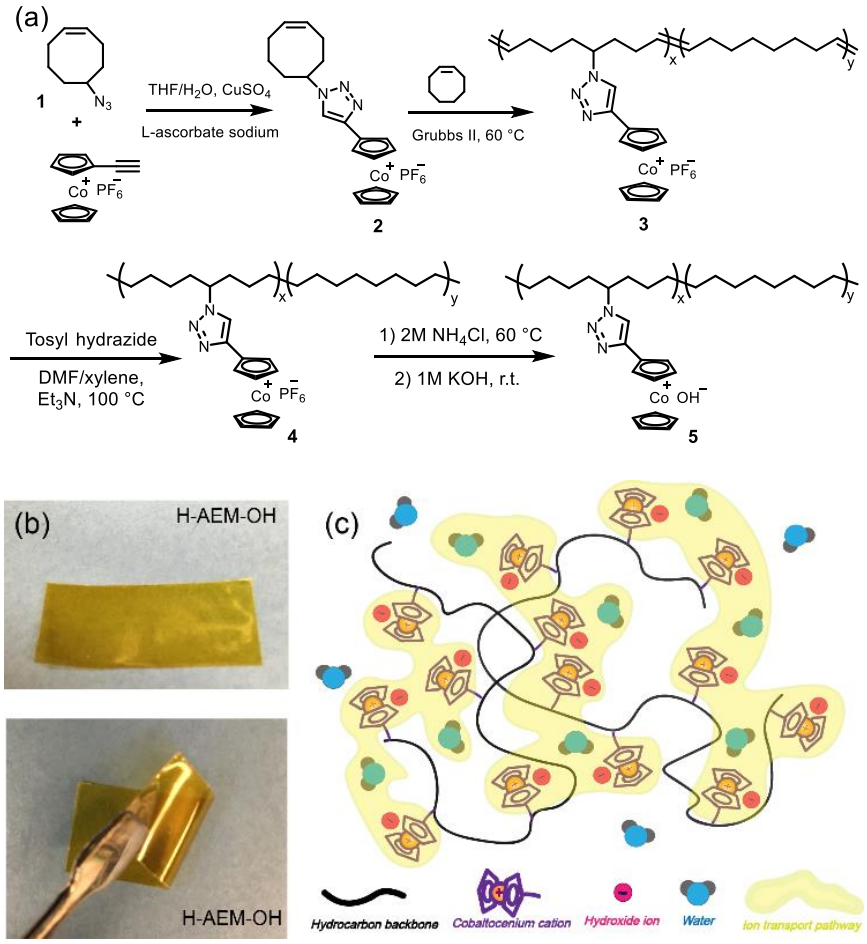

Figure 2.1. a. Synthesis of cobaltocenium monomer **2**, copolymer **3** and hydrogenated polymer **4** as AEMs; **b**. images of transparent and flexible cobaltocenium AEMs; **c**. proposed structures of cobaltocenium-containing AEMs in a hydroxide solution.

We prepared cobaltocenium-containing cyclooctene that was subject to ROMP, as illustrated in **Figure 2.1 a**. 5-Bromocyclooct-1-ene was derived from cyclooctadiene,[35] and then converted to 5-azidocyclooct-1-ene (**1**). A copper-catalyzed click reaction between **1** and ethynylcobaltocenium hexafluorophosphate yielded cobaltocenium cyclooctene with a triazole as the linker (**2**), which was subsequently carried out for ROMP with cyclooctene as a co-monomer with the aid of Grubbs II catalyst to get a copolymer **3**. The molecular weight was well controlled by adjusting the molar ratio of monomers to catalysts. In this study, we chose a polymer with molecular weight at 80,000 g/mol, which is sufficiently high to warrant the formation of flexible membranes. The cobaltocenium monomer and cationic copolymers in hexafluorophosphate form were characterized by ^{1}H NMR spectroscopy (**Figure 2.2**), which unambiguously confirmed their structures with specific assignments to each proton. The presence of unsaturated bonds in the backbone of polymer **3** could be a concern on the long-term stability in alkaline conditions. The alkaline stability of this copolymer was improved by hydrogenation of the backbone. The reduction of double bonds could be confirmed with ^{1}H NMR (**Figure 2.2**) and disappearance of characteristic absorption in the range of 1686~1796 cm^{-1} in FTIR spectrum. These hydrogenated copolymers were subsequently carried out ion-exchange from hexafluorophosphate (PF_6^-) to chloride (Cl^-) and then to hydroxide (OH^-) ion, and further fabricated to form anion exchange membranes H-AEM$_x$-OH (**5**) (x represents the molar fraction of cobaltocenium units in a polymer composition).

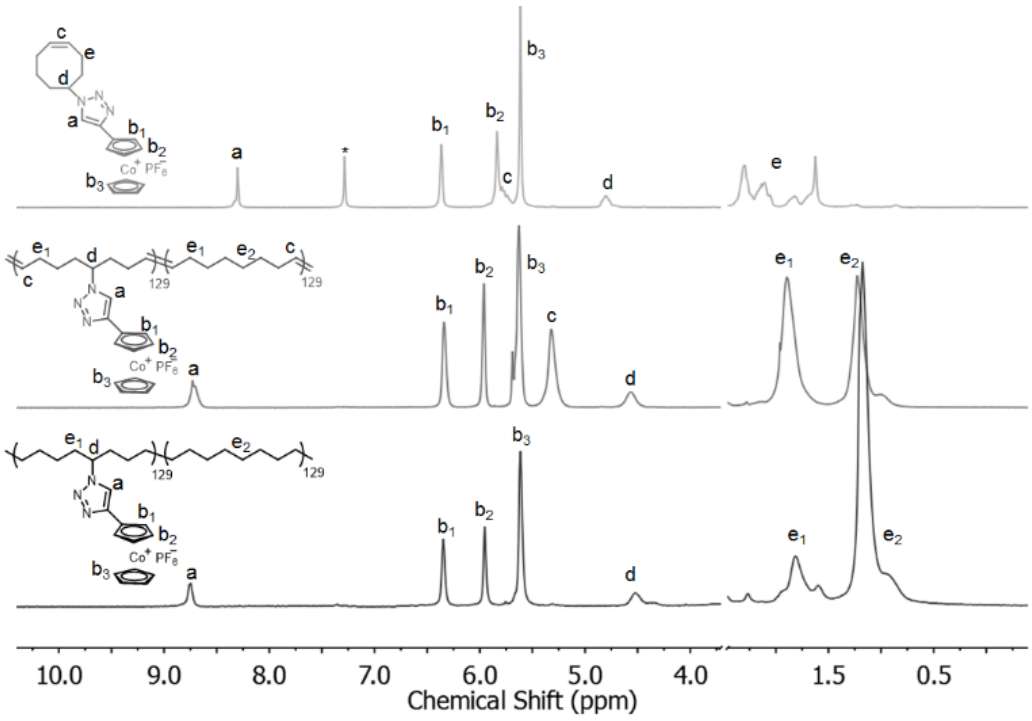

Figure 2.2. ^{1}H NMR spectra of cobaltocenium monomer **2** (top), copolymer **3** (middle) and hydrogenated polymer **4** (bottom).

Cobaltocenium monomer **2** with Cl^{-} anion was evaluated for its alkaline stability by UV-vis spectroscopy, as cobaltocenium has a characteristic UV absorption at ~ 282 nm (**Figure 2.3 c**).[36-37] The monomer was dissolved in 1 M NaOH at 80 ˚C and then collected for time-dependent UV-vis spectra. Two representative absorption peaks appeared at 282 nm and 346 nm, characteristically originated from the cobaltocenium and triazole groups respectively. The absorption spectrum obtained after 10 days perfectly overlapped with the initial one (**Figure 2.3 d**). Both peaks maintained nearly 100% of initial intensity even after 10 d, unambiguously indicating excellent alkaline stability of cobaltocenium and triazole at elevated pH and temperatures. Furthermore, the stability of cobaltocenium monomer **2** was confirmed by ^{1}H NMR and mass spectrum after exposure in alkaline conditions. We noticed that proton-deuterium exchange occurred on protons from both aromatic rings and alkenes in the monomer structure, while no signals indicated any degraded products. As

investigated recently by the Patric group,[56] this kind of proton-deuterium exchange is reversible and does not lead to any structural degradation. All above stability tests suggested cobaltocenium is a stable cation suitable for AEM applications.

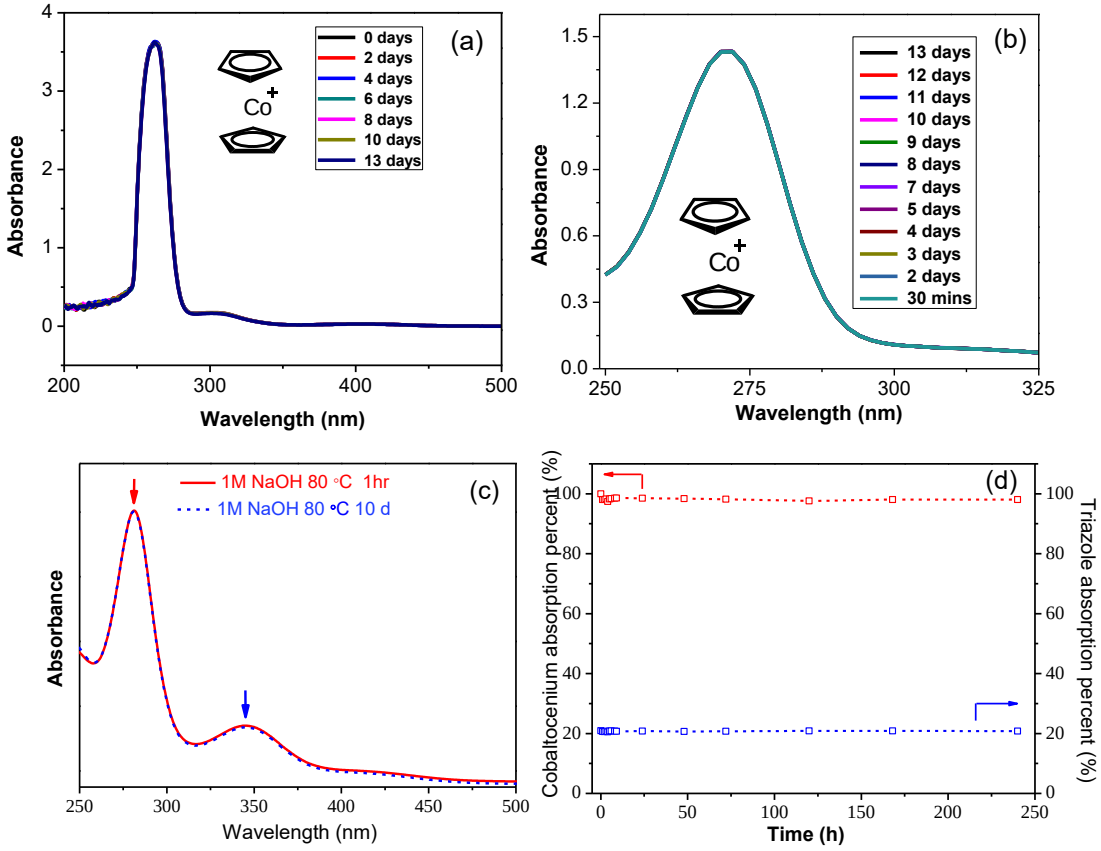

Figure 2.3. a. UV-Vis spectra of unsubstituted cobaltocenium in a solution of NaOH at pH=14 over time; **b.** UV-Vis spectra of unsubstituted cobaltocenium in a solution of HCl at pH=1.5 over time; **c.** UV-Vis spectra of cobaltocenium monomer **2** with chloride ion after immersing in 1 M NaOH at 80 ˚C for 1 h and 10 d; **d.** peak intensity of UV-Vis absorption at 282 nm (Red) and 346 nm (Blue) for cobaltocenium monomer **2** with chloride ion in 1 M NaOH at 80 °C.

For cobaltocenium-containing polymers, direct anion exchange from hydrophobic PF_6^- to hydrophilic OH^- was challenging.[15, 43] We resolved this problem by first exchange to Cl^- in 2 M aqueous solution of NH_4Cl at 60 ˚C. Then, exchange from Cl^- to OH^- was carried out by immersing polymer membranes into 1 M NaOH solution. Complete ion-exchange was confirmed by ion exchange capacity (IEC) titration (**Table 2.1**) and Energy

Dispersive X-ray (EDX) characterization. These membranes were in yellow color, flexible and transparent (**Figure 2.1 b**). All membranes after anion exchange were not soluble in water or other polar aprotic solvents like dimethylacetamide and acetonitrile.

The thermal stability of cobaltocenium-containing polymers was studied by thermogravimetric analysis (TGA) (**Figure 2.4 a**). The decomposition of hydrogenated H-AEM_x-OH membranes under N_2 atmosphere consisted of two different stages and occurred only well above 300 ˚C. The 5% weight-loss decomposition temperature (T_d) of H-AEM_{40}-OH and H-AEM_{50}-OH were 347 ˚C and 328 ˚C, respectively. In comparison, many reported AEMs with ammonium or imidazole cations have much lower decomposition temperature for their cations (< 200 ˚C).[57-59] Our results suggested both cobaltocenium cations and the hydrocarbon backbone have excellent thermal stability.

Mechanical properties of AEMs are largely dependent on the choice of polymer backbones. For well-studied poly(p-phenylene oxide), polybenzimidazole, and polystyrene based AEMs, the tensile strain at break is usually lower than 80% due to their rigid aromatic backbones. While for flexible poly(4-methyl-1-pentene) based films,[60] the tensile strength is relatively low. We intended cobaltocenium polymers to be tough, flexible and strong. Mechanical properties of cobaltocenium AEMs were characterized at 80% RH and under ambient temperature. Both H-AEM_{40}-OH and H-AEM_{50}-OH retained tensile strain over 120% attributed to the existence of a highly flexible backbone (**Table 2.2**).

These cobaltocenium membranes were expected to have phase separation due to immiscibility of the hydrophobic backbone and hydrophilic side chain in the copolymers. Small-angle X-ray scattering (SAXS) was used to investigate the morphology of cobaltocenium membranes (**Figure 2.4 b**). Both of the membranes exhibited a broad

primary scattering peak around q^* = 1.28 and 1.54 nm^{-1} with a d spacing ($2\pi/q^*$) of 4.9 and 4.1 nm. The lack of higher orders of scattering peaks implied that the phase separation is probably short-range correlated,[61-62] which is reasonable given the membranes are not block copolymers. Atomic force microscopy (AFM) images also confirmed the microphase separation between hydrophilic and hydrophobic domains under spin casting conditions. The dark areas represent the soft matrix from polyethylene backbone, whereas the brighter ones represent hard domains from cobaltocenium side chains. Such phase-separated morphology is essential for anion exchange materials with desirable properties. The hydrophobic backbone provided mechanically flexible and chemically stable scaffold, whereas the hydrophilic side-chains facilitated ion transport through connected ionic channels.

Table 2.1. Compositions and IECs of cobaltocenium AEMs.

Sample	x[a]	y[a]	IEC_{theo} (mmol/g)	IEC_{titr} (mmol/g)	λ
H-AEM_{40}-OH	40	60	1.81	1.53	11.2
H-AEM_{50}-OH	50	50	2.02	1.86	11.6

[a] x and y represent molar fractions of cobaltocenium and cyclooctene units respectively.

Table 2.2. Mechanical properties of cobaltocenium AEM samples.

Sample	Tensile strength (MPa)	Elongation at break (%)	Toughness (MJ/m^3)
H-AEM_{40}-OH	8.15	153	10.1
H-AEM_{50}-OH	8.44	120	6.53

The water uptake and swelling ratio of hydrogenated membranes was measured in DI water at different temperature. Even under high cation loading, side-chain cobaltocenium AEMs still exhibited relatively low water uptake and swelling ratio

especially at room temperature, which can be explained by the hydrophobic nature of polyethylene-like backbone. Furthermore, the number of absorbed water molecules per cobaltocenium cation was calculated to be in the range of 11.2 to 11.6, and showed a tendency of slight increase with higher IEC. Hence, both cobaltocenium copolymers showed good resistance to water uptake at various temperature. Such water management property could play a critical role in forming ion conducting pathways (**Figure 2.1 c**) and ensure the membranes to be dimensionally stable over a long term. While for many quaternary ammonium or phosphonium polymers, high cation loading for better electrical property makes them much more hydrophilic and absorbs excess water, which in turn sacrifices the overall stability.[35, 57, 63-64] Our study on cobaltocenium AEMs indicated the possibility of simultaneously making high IEC and having good water management property.

The hydroxide conductivity of membranes with different loading of cobaltocenium cation as a function of temperature is shown in **Figure 2.4 c**. Both membranes showed steadily increased conductivity at elevated temperature likely due to higher water uptake and faster ion migration. The hydroxide conductivity of H-AEM$_{40}$-OH and H-AEM$_{50}$-OH reached pretty high value at 90 ˚C: 72 and 90 mS/cm, respectively. Considering the processability and durability of membranes, we only incorporated up to 50 mol% cobaltocenium in copolymers at this stage. It could be possible to achieve even higher hydroxide conductivity by increasing the IEC and optimizing the compositions of copolymers. Moreover, the hydroxide conductivity at different temperature generally followed an Arrhenius relationship. The activation energy for ion transport was calculated to be 19.2 to 20.2 kJ/mol.

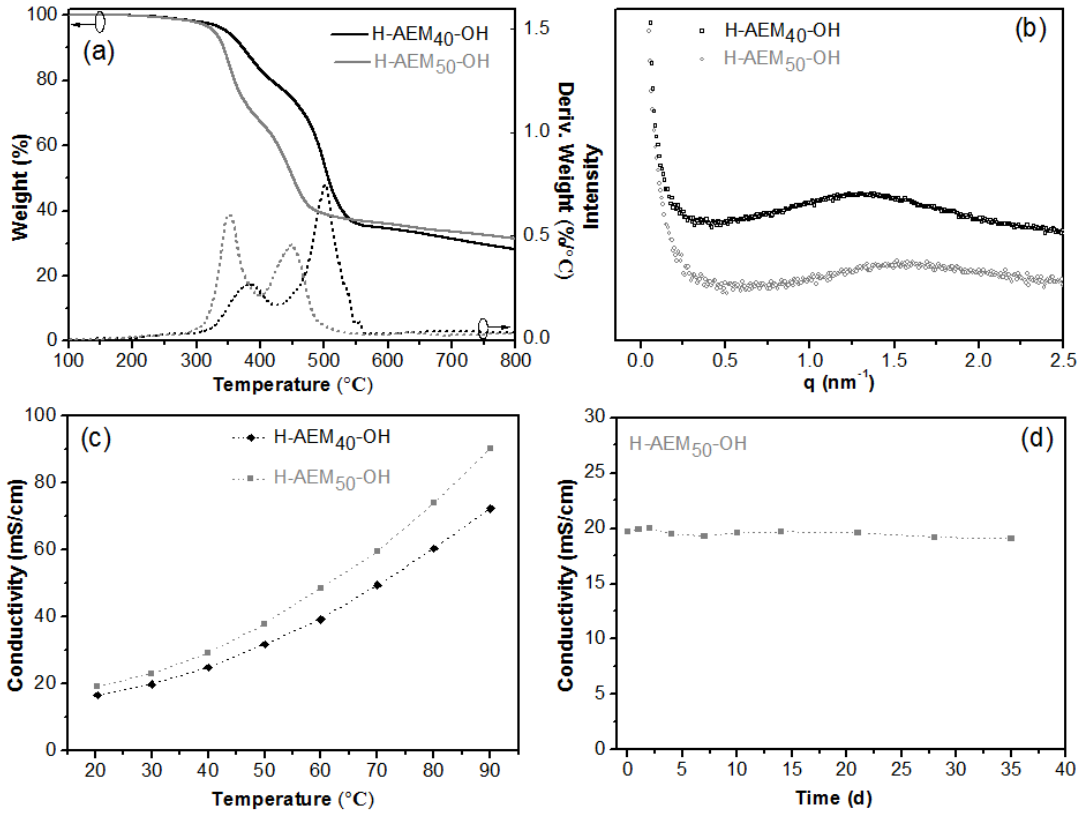

Figure 2.4. Cobaltocenium AEMs: **a**. TGA and DTG curves; **b**. SAXS profiles; **c**. hydroxide conductivity of membranes as a function of temperature in fully hydrated condition; **d**. room temperature conductivity as a function of immersion time of membranes in 1 M NaOH solution at 80 ˚C.

The alkaline stability at high operating temperature has always been a key concern for AEMs. For polymers prepared via ROMP, the unsaturated double bond in repeating units is considered to not only limit the chain flexibility, but also make membranes less stable in harsh basic conditions. We employed direct hydrogenation to reduce the double bonds in the polymer backbone. In addition, polymers with polyethylene-like backbone exhibited improved durability and ductility. H-AEM$_{50}$-OH was chosen for the long-term stability test because of its higher ion capacity and hydroxide conductivity. FTIR spectra showed that all chemical structures of membranes remained almost unchanged before and after the test. Moreover, initial hydroxide conductivity of hydrated membranes was

maintained over 95% after soaking in 1 M NaOH at 80 ˚C for one month, indicating their superior chemical and mechanical stability (**Figure 2.4 d**).

2.4 Conclusions

In summary, a new design for anion-exchange membranes was achieved using metallo-polyelectrolytes containing cationic cobaltocenium with a polyethylene-like backbone and a non-hydrolysable linker. These copolymers were prepared via ROMP in conjunction with hydrogenation of polymer backbones. These membranes exhibited long-term durability with excellent mechanical toughness and flexibility, great chemical stability of cations and other polymer compositions, as well as good ion conductivity. This work demonstrated that side-chain cobaltocenium polymers can be used as a candidate for new-generation anion-exchange membrane materials in fuel cell applications.

2.5 Experimental Details

Materials

1,5-Cyclooctadiene (99%), hydrobromic acid solution (33% in acetic acid), *p*-toluenesulfonyl hydrazide (97%), ethyl vinyl (99%) ether and Grubbs II catalyst were purchased from Sigma-Aldrich and used as received. Sodium azide (99%), cobaltocenium hexafluorophosphate (98%), anhydrous *N*,*N*-dimethylacetamide (99.8%), standardized hydrochloric acid (0.1 N) and potassium hydroxide solutions (0.1 N) were purchased from VWR. Cyclooctene (>95%) was purchased from TCI. 5-Bromocyclooct-1-ene and ethynylcobaltocenium hexafluorophosphate were synthesized and characterized according to the literature procedure.[65-67] 5-Bromocyclooct-1-ene has been reported before but a modified synthetic route was used here.[35, 68]

Characterization

^{1}H NMR (300 MHz), ^{13}C NMR (75 MHz) and ^{19}F NMR (282 MHz) spectra were recorded on a Varian Mercury 300 spectrometer using $CDCl_3$ or DMSO-d_6 as solvents. All chemical shifts in ^{1}H and ^{13}C NMR were compared to tetramethylsilane (TMS) as the reference. ESI mass spectra were collected at the University of South Carolina mass spectrometry center. Atomic force microscopy (AFM) was accomplished using a Multimode Nanoscope V system (Bruker, Santa Barbara, CA). Tapping mode AFM was used to map the topography by tapping the surface using an oscillating tip. The measurements were achieved using commercial Si cantilevers with a nominal spring constant and resonance frequency at 20~80 N/m and 230~410 kHz, respectively (TESP, Bruker AFM Probes, Santa Barbara, CA). Fourier transform infrared spectroscopy (FTIR) was recorded on a PerkinElmer spectrum 100 FTIR spectrometer using an attenuated total reflection method. The UV-Vis spectra were recorded by a Shimadzu UV-2450 spectrophotometer. Energy Dispersive X-ray (EDX) analysis was acquired by a Zeiss Ultraplus thermal field emission scanning electron microscope. A Biologic VMP3 potentiostat with electrochemical impedance spectroscopy (EIS) capability was used for electrochemical measurements of polymer membranes.

Synthetic Procedures

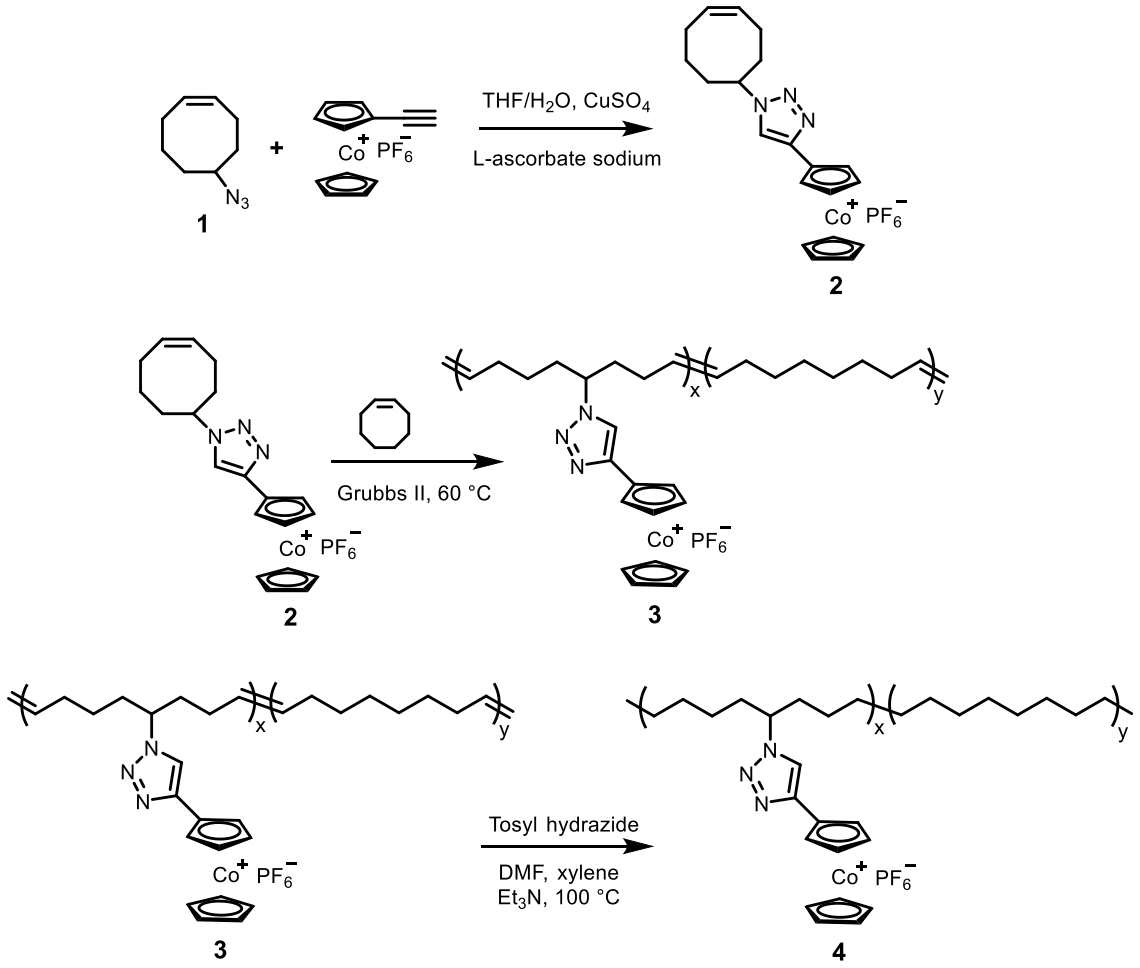

Figure 2.5. Synthesis of cobaltocenium AEMs.

Synthesis of cobaltocenium monomer 2.

5-Azidocyclooct-1-ene (**1**) (465 mg, 3.07 mol, 1 equvi.) and ethynylcobaltocenium hexafluorophosphate (1.10 g, 3.07 mmol, 1 equvi.) were dissolved in a 250 mL flask containing 150 mL of tetrahydrofuran (THF)/water (3 : 2). 1M aqueous solution of $CuSO_4$ (3.07 mmol, 1 equvi.) was added and purge N_2 for 30 min. At 0 ˚C, a freshly-prepared 1 M aqueous solution of sodium ascorbate (6.14 mmol, 2 equvi.) was added dropwise, and then the solution was allowed to react at room temperature under stirring for 12 h. 3 mL aqueous solution of ammonia was added to the mixture and stirred for another 10 min. The solvent

was extracted with dichloromethane (100 mL × 2). The organic phase was collected, filtered through celite, dried with anhydrous $MgSO_4$ and evaporated. The crude product was dissolved with 8 mL dichloromethane and precipitated in cold diethyl ether. Cobaltocenium monomer **2** could be obtained as yellow solid in a yield of 85%. ^{1}H NMR ($CDCl_3$): δ 1.38~2.35 (m, 10H, 3-, 4-, 6-, 7-, 8-C*H*$_2$), 4.74~4.86 (m, 1H, 5-*H*), 5.68~5.82 (m, 2H, C*H*=C*H*), 5.55~5.70 (m, 5*H*, Cp), 5.79~5.92 (t, 2H, C*H*$_2$=CH$_2$ on the Cp ring), 6.32~6.44 (t, 2H, CH$_2$=C*H*$_2$ on the Cp ring), 8.25~8.35 (s, 1H, triazole *H*). ^{13}C NMR ($CDCl_3$, ppm): 130.76, 128.88, 95.47, 85.98, 84.36, 80.61, 62.27, 34.90, 25.90, 22.79. ^{19}F NMR ($CDCl_3$, ppm): δ=−70.83,−72.72. ESI$^+$-MS: m/z= 364 [M]$^+$.

Synthesis of cobaltocenium copolymer 3.

Cobaltocenium-containing cyclooctene copolymers were synthesized by ring-opening metathesis polymerization (ROMP). Cobaltocenium monomer **2** (100 mg, 0.196 mmol) and cyclooctene (21.6 mg, 0.196 mmol) were dissolved in 2 mL dimethylacetamide (DMAc) and purged with nitrogen for 20 min. The reaction temperature increased to 65 ºC, and then Grubbs II catalyst was added into the reaction mixture. Several drops of ethyl vinyl ether were added to stop the polymerization after 60 min after the full conversion of monomer was confirmed by ^{1}H NMR. The polymers were obtained by precipitation three times in methanol and dried overnight under vacuum (yield: 85%). Other copolymers with different cobaltocenium contents were prepared in a similar way. ^{1}H NMR (DMSO-d$_6$): δ 0.67-2.06 (broad, backbone C*H*$_2$), 4.36-4.69 (broad, 1H, -C*H*-), 5.09~5.45 (broad, C*H*=C*H*), 5.55~5.70 (m, 5H, Cp), 5.87~6.04 (broad, 2H, C*H*$_2$=CH$_2$ on the Cp ring), 6.20~6.44 (broad, 2H, CH$_2$=C*H*$_2$ on the Cp ring), 8.64~8.88 (broad, 1H, triazole *H*). The target molecular weight was 80,000 g/mol for hydrogenated polymers.

Synthesis of cobaltocenium copolymer **3**.

Synthesis of hydrogenated cobaltocenium copolymer 4

A flask loaded with copolymer **3** (200 mg) and 10 mL of DMF/xylene (1 : 1) was purged nitrogen for 20 min. Then, *p*-toluenesulfonyl hydrazide (5.0 equiv. per double bond) and triethylamine (5.0 equiv. per double bond) were added into the reaction solution. The reaction mixture was heated to 100 ºC for 5 h. The solution was cooled to room temperature and precipitated into 100 mL methanol. Finally, the yellow polymer precipitate was washed three times with methanol and dried overnight under vacuum (yield 95%). ^{1}H NMR (DMSO-d_6): δ 0.67-2.09 (broad, backbone C*H*$_2$), 4.29-4.63 (broad, 1H, -C*H*-), 5.42~5.74 (m, 5H, Cp), 5.81~6.04 (broad, 2H, C*H*$_2$=CH$_2$ on the Cp ring), 6.21~6.44 (broad, 2H, CH$_2$=C*H*$_2$ on the Cp ring), 8.63~8.89 (broad, 1H, triazole *H*).

2.6 References

1. Zhu, T.; Xu, S.; Rahman, A.; Dogdibegovic, E.; Yang, P.; Pageni, P.; Kabir, M. P.; Zhou, X. d.; Tang, C., Cationic Metallo-Polyelectrolytes for Robust Alkaline Anion-Exchange Membranes. *Angew. Chem. Int. Ed.* **2018,** *57* (9), 2388-2392.

2. Zhai, L.; Cebeci, F. Ç.; Cohen, R. E.; Rubner, M. F., Stable Superhydrophobic Coatings from Polyelectrolyte Multilayers. *Nano Lett.* **2004,** *4* (7), 1349-1353.

3. Pack, D. W.; Hoffman, A. S.; Pun, S.; Stayton, P. S., Design and development of polymers for gene delivery. *Nat Rev Drug Discov* **2005,** *4* (7), 581-593.

4. Varcoe, J. R.; Slade, R. C. T., Prospects for Alkaline Anion-Exchange Membranes in Low Temperature Fuel Cells. *Fuel Cells* **2005,** *5* (2), 187-200.

5. Hickner, M. A.; Herring, A. M.; Coughlin, E. B., Anion exchange membranes: Current status and moving forward. *J. Polym. Sci., Part B: Polym. Phys.* **2013,** *51* (24), 1727-1735.

6. Merle, G.; Wessling, M.; Nijmeijer, K., Anion exchange membranes for alkaline fuel cells: A review. *J. Membr. Sci.* **2011,** *377* (1–2), 1-35.

7. Couture, G.; Alaaeddine, A.; Boschet, F.; Ameduri, B., Polymeric materials as anion-exchange membranes for alkaline fuel cells. *Prog. Polym. Sci.* **2011,** *36* (11), 1521-1557.

8. Robertson, N. J.; Kostalik, H. A.; Clark, T. J.; Mutolo, P. F.; Abruña, H. D.; Coates, G. W., Tunable High Performance Cross-Linked Alkaline Anion Exchange Membranes for Fuel Cell Applications. *J. Am. Chem. Soc.* **2010,** *132* (10), 3400-3404.

9. John, J.; Hugar, K. M.; Rivera-Meléndez, J.; Kostalik, H. A.; Rus, E. D.; Wang, H.; Coates, G. W.; Abruña, H. D., An Electrochemical Quartz Crystal Microbalance Study of a Prospective Alkaline Anion Exchange Membrane Material for Fuel Cells: Anion Exchange Dynamics and Membrane Swelling. *J. Am. Chem. Soc.* **2014,** *136* (14), 5309-5322.

10. Clark, T. J.; Robertson, N. J.; Kostalik Iv, H. A.; Lobkovsky, E. B.; Mutolo, P. F.; Abruña, H. D.; Coates, G. W., A Ring-Opening Metathesis Polymerization Route to Alkaline Anion Exchange Membranes: Development of Hydroxide-Conducting Thin Films from an Ammonium-Functionalized Monomer. *J. Am. Chem. Soc.* **2009,** *131* (36), 12888-12889.

11. Tanaka, M.; Fukasawa, K.; Nishino, E.; Yamaguchi, S.; Yamada, K.; Tanaka, H.; Bae, B.; Miyatake, K.; Watanabe, M., Anion Conductive Block Poly(arylene ether)s: Synthesis, Properties, and Application in Alkaline Fuel Cells. *J. Am. Chem. Soc.* **2011,** *133* (27), 10646-10654.

12. Thomas, O. D.; Soo, K. J. W. Y.; Peckham, T. J.; Kulkarni, M. P.; Holdcroft, S., A Stable Hydroxide-Conducting Polymer. *J. Am. Chem. Soc.* **2012,** *134* (26), 10753-10756.

13. Chen, C.; Tse, Y.-L. S.; Lindberg, G. E.; Knight, C.; Voth, G. A., Hydroxide Solvation and Transport in Anion Exchange Membranes. *J. Am. Chem. Soc.* **2016,** *138* (3), 991-1000.

14. Li, N.; Leng, Y.; Hickner, M. A.; Wang, C.-Y., Highly Stable, Anion Conductive, Comb-Shaped Copolymers for Alkaline Fuel Cells. *J. Am. Chem. Soc.* **2013,** *135* (27), 10124-10133.

15. Zha, Y.; Disabb-Miller, M. L.; Johnson, Z. D.; Hickner, M. A.; Tew, G. N., Metal-Cation-Based Anion Exchange Membranes. *J. Am. Chem. Soc.* **2012,** *134* (10), 4493-4496.

16. Shin, D. W.; Guiver, M. D.; Lee, Y. M., Hydrocarbon-Based Polymer Electrolyte Membranes: Importance of Morphology on Ion Transport and Membrane Stability. *Chem. Rev.* **2017,** *117* (6), 4759-4805.

17. Pan, J.; Chen, C.; Zhuang, L.; Lu, J., Designing Advanced Alkaline Polymer Electrolytes for Fuel Cell Applications. *Acc. Chem. Res.* **2012,** *45* (3), 473-481.

18. Mohanty, A. D.; Bae, C., Mechanistic analysis of ammonium cation stability for alkaline exchange membrane fuel cells. *J. Mater. Chem. A* **2014,** *2* (41), 17314-17320.

19. Marino, M. G.; Kreuer, K. D., Alkaline Stability of Quaternary Ammonium Cations for Alkaline Fuel Cell Membranes and Ionic Liquids. *ChemSusChem* **2015,** *8* (3), 513-523.

20. Pham, T. H.; Jannasch, P., Aromatic Polymers Incorporating Bis-N-spirocyclic Quaternary Ammonium Moieties for Anion-Exchange Membranes. *ACS Macro Lett.* **2015,** *4* (12), 1370-1375.

21. Dang, H.-S.; Jannasch, P., Alkali-stable and highly anion conducting poly(phenylene oxide)s carrying quaternary piperidinium cations. *J. Mater. Chem. A* **2016,** *4* (30), 11924-11938.

22. Yang, Z.; Guo, R.; Malpass-Evans, R.; Carta, M.; McKeown, N. B.; Guiver, M. D.; Wu, L.; Xu, T., Highly Conductive Anion-Exchange Membranes from Microporous Tröger's Base Polymers. *Angew. Chem.* **2016,** *128* (38), 11671-11674.

23. Lee, W.-H.; Kim, Y. S.; Bae, C., Robust Hydroxide Ion Conducting Poly(biphenyl alkylene)s for Alkaline Fuel Cell Membranes. *ACS Macro Lett.* **2015,** *4* (8), 814-818.

24. Yang, Z.; Zhou, J.; Wang, S.; Hou, J.; Wu, L.; Xu, T., A strategy to construct alkali-stable anion exchange membranes bearing ammonium groups via flexible spacers. *J. Mater. Chem. A* **2015,** *3* (29), 15015-15019.

25. Liu, Y.; Zhang, B.; Kinsinger, C. L.; Yang, Y.; Seifert, S.; Yan, Y.; Mark Maupin, C.; Liberatore, M. W.; Herring, A. M., Anion exchange membranes composed of a poly(2,6-dimethyl-1,4-phenylene oxide) random copolymer functionalized with a bulky phosphonium cation. *J. Membr. Sci.* **2016,** *506*, 50-59.

26. Dang, H.-S.; Weiber, E. A.; Jannasch, P., Poly (phenylene oxide) functionalized with quaternary ammonium groups via flexible alkyl spacers for high-performance anion exchange membranes. *J. Mater. Chem. A* **2015,** *3* (10), 5280-5284.

27. Chen, D.; Hickner, M. A., Degradation of Imidazolium- and Quaternary Ammonium-Functionalized Poly(fluorenyl ether ketone sulfone) Anion Exchange Membranes. *ACS Appl. Mater. Interfaces* **2012,** *4* (11), 5775-5781.

28. Kim, D. S.; Labouriau, A.; Guiver, M. D.; Kim, Y. S., Guanidinium-Functionalized Anion Exchange Polymer Electrolytes via Activated Fluorophenyl-Amine Reaction. *Chem.Mater.* **2011,** *23* (17), 3795-3797.

29. Hugar, K. M.; Kostalik, H. A.; Coates, G. W., Imidazolium Cations with Exceptional Alkaline Stability: A Systematic Study of Structure–Stability Relationships. *J. Am. Chem. Soc.* **2015,** *137* (27), 8730-8737.

30. Aitken, B. S.; Buitrago, C. F.; Heffley, J. D.; Lee, M.; Gibson, H. W.; Winey, K. I.; Wagener, K. B., Precision Ionomers: Synthesis and Thermal/Mechanical Characterization. *Macromolecules* **2012,** *45* (2), 681-687.

31. Lin, B.; Dong, H.; Li, Y.; Si, Z.; Gu, F.; Yan, F., Alkaline Stable C2-Substituted Imidazolium-Based Anion-Exchange Membranes. *Chem. Mater.* **2013,** *25* (9), 1858-1867.

32. Gu, S.; Cai, R.; Luo, T.; Chen, Z.; Sun, M.; Liu, Y.; He, G.; Yan, Y., A Soluble and Highly Conductive Ionomer for High-Performance Hydroxide Exchange Membrane Fuel Cells. *Angew. Chem. Int. Ed.* **2009,** *48* (35), 6499-6502.

33. Gu, S.; Cai, R.; Luo, T.; Jensen, K.; Contreras, C.; Yan, Y., Quaternary Phosphonium-Based Polymers as Hydroxide Exchange Membranes. *ChemSusChem* **2010,** *3* (5), 555-558.

34. Gu, S.; Cai, R.; Yan, Y., Self-crosslinking for dimensionally stable and solvent-resistant quaternary phosphonium based hydroxide exchange membranes. *ChemComm* **2011,** *47* (10), 2856-2858.

35. Noonan, K. J. T.; Hugar, K. M.; Kostalik, H. A.; Lobkovsky, E. B.; Abruña, H. D.; Coates, G. W., Phosphonium-Functionalized Polyethylene: A New Class of Base-Stable Alkaline Anion Exchange Membranes. *J. Am. Chem. Soc.* **2012,** *134* (44), 18161-18164.

36. Hardy, C. G.; Zhang, J.; Yan, Y.; Ren, L.; Tang, C., Metallopolymers with transition metals in the side-chain by living and controlled polymerization techniques. *Prog Polym Sci* **2014,** *39* (10), 1742-1796.

37. Yan, Y.; Pageni, P.; Kabir, M. P.; Tang, C., Metallocenium Chemistry and Its Emerging Impact on Synthetic Macromolecular Chemistry. *Synlett* **2016,** *27*, 984-1005.

38. Ornelas, C.; Ruiz, J.; Astruc, D., Giant Cobalticinium Dendrimers. *Organometallics* **2009,** *28*, 276-2723.

39. Sheats, J. E.; Rausch, M. D., Synthesis and properties of cobalticinium salts. I. Synthesis of monosubstituted cobalticinium salts. *J. Org. Chem.* **1970,** *35* (10), 3245-3249.

40. Wilkinson, G., The Preparation and Some Properties of the Cobalticinium Salts. *J. Am. Chem. Soc.* **1952,** *74* (23), 6148-6149.

41. Zhao, L.; Liu, X.; Zhang, L.; Qiu, G.; Astruc, D.; Gu, H., Metallomacromolecules containing cobalt sandwich complexes: Synthesis and functional materials properties. *Coord. Chem. Rev.* **2017,** *337*, 34-79.

42. Gu, H.; Ciganda, R.; Castel, P.; Ruiz, J.; Astruc, D., Living ROMP Syntheses and Redox Properties of Triblock Metallocopolymer Redox Cascades. *Macromolecules* **2016,** *49* (13), 4763-4773.

43. Gu, S.; Wang, J.; Kaspar, R. B.; Fang, Q.; Zhang, B.; Bryan Coughlin, E.; Yan, Y., Permethyl Cobaltocenium (Cp*2Co+) as an Ultra-Stable Cation for Polymer Hydroxide-Exchange Membranes. *Sci. Rep.* **2015,** *5*, 11668.

44. Chen, N.; Zhu, H.; Chu, Y.; Li, R.; Liu, Y.; Wang, F., Cobaltocenium-containing polybenzimidazole polymers for alkaline anion exchange membrane applications. *Poly. Chem.* **2017,** *8* (8), 1381-1392.

45. Ren, L.; Hardy, C. G.; Tang, C., Synthesis and Solution Self-Assembly of Side-Chain Cobaltocenium-Containing Block Copolymers. *J. Am. Chem. Soc.* **2010,** *132* (26), 8874-8875.

46. Ren, L.; Hardy, C. G.; Tang, S.; Doxie, D. B.; Hamidi, N.; Tang, C., Preparation of Side-Chain 18-e Cobaltocenium-Containing Acrylate Monomers and Polymers. *Macromolecules* **2010,** *43* (22), 9304-9310.

47. Ren, L.; Zhang, J.; Bai, X.; Hardy, C. G.; Shimizu, K. D.; Tang, C., Preparation of cationic cobaltocenium polymers and block copolymers by "living" ring-opening metathesis polymerization. *Chem. Sci.* **2012,** *3* (2), 580-583.

48. Zhang, J.; Chen, Y. P.; Miller, K. P.; Ganewatta, M. S.; Bam, M.; Yan, Y.; Nagarkatti, M.; Decho, A. W.; Tang, C., Antimicrobial Metallopolymers and Their Bioconjugates with Conventional Antibiotics against Multidrug-Resistant Bacteria. *J. Am. Chem. Soc.* **2014,** *136* (13), 4873-4876.

49. Gilroy, J. B.; Patra, S. K.; Mitchels, J. M.; Winnik, M. A.; Manners, I., Main-Chain Heterobimetallic Block Copolymers: Synthesis and Self-Assembly of Polyferrocenylsilane-b-Poly(cobaltoceniumethylene). *Angew. Chem. Int. Ed.* **2011,** *50* (26), 5851-5855.

50. Mayer, U. F. J.; Gilroy, J. B.; O'Hare, D.; Manners, I., Ring-Opening Polymerization of 19-Electron [2]Cobaltocenophanes: A Route to High-Molecular-Weight, Water-Soluble Polycobaltocenium Polyelectrolytes. *J. Am. Chem. Soc.* **2009,** *131* (30), 10382-10383.

51. Yan, Y.; Zhang, J.; Ren, L.; Tang, C., Metal-containing and related polymers for biomedical applications. *Chem. Soc. Rev.* **2016,** *45* (19), 5232-5263.

52. Ciganda, R.; Gu, H.; Castel, P.; Zhao, P.; Ruiz, J.; Hernández, R.; Astruc, D., Living ROMP Synthesis and Redox Properties of Diblock Ferrocene/Cobalticenium Copolymers. *Macromol. Rapid Commun.* **2016,** *37* (1), 105-111.

53. Gu, H.; Ciganda, R.; Hernandez, R.; Castel, P.; Zhao, P.; Ruiz, J.; Astruc, D., Diblock Polyelectrolytic Copolymers Containing Cationic Iron and Cobalt Sandwich Complexes: Living ROMP Synthesis and Redox Properties. *Macromol. Rapid Commun.* **2016,** *37* (7), 630-636.

54. Zhang, J.; Yan, Y.; Chance, M. W.; Chen, J.; Hayat, J.; Ma, S.; Tang, C., Charged Metallopolymers as Universal Precursors for Versatile Cobalt Materials. *Angew. Chem. Int. Ed.* **2013,** *52* (50), 13387-13391.

55. Wei, J.; Ren, L.; Tang, C.; Su, Z., Electric-stimulus-responsive multilayer films based on a cobaltocenium-containing polymer. *Poly. Chem.* **2014,** *5* (22), 6480-6488.

56. Pham, T. H.; Olsson, J. S.; Jannasch, P., N-Spirocyclic Quaternary Ammonium Ionenes for Anion-Exchange Membranes. *J. Am. Chem. Soc.* **2017,** *139* (8), 2888-2891.

57. Guo, D.; Lai, A. N.; Lin, C. X.; Zhang, Q. G.; Zhu, A. M.; Liu, Q. L., Imidazolium-Functionalized Poly(arylene ether sulfone) Anion-Exchange Membranes Densely Grafted with Flexible Side Chains for Fuel Cells. *ACS Appl. Mater. Interfaces* **2016,** *8* (38), 25279-25288.

58. Wu, H.; Jia, W.; Liu, Y., An imidazolium-type hybrid alkaline anion exchange membrane with improved membrane stability for alkaline fuel cells applications. *J. Mater. Sci.* **2017,** *52* (3), 1704-1716.

59. Ge, Q.; Ran, J.; Miao, J.; Yang, Z.; Xu, T., Click Chemistry Finds Its Way in Constructing an Ionic Highway in Anion-Exchange Membrane. *ACS Appl. Mater. Interfaces* **2015,** *7* (51), 28545-28553.

60. Zhang, M.; Shan, C.; Liu, L.; Liao, J.; Chen, Q.; Zhu, M.; Wang, Y.; An, L.; Li, N., Facilitating Anion Transport in Polyolefin-Based Anion Exchange Membranes via Bulky Side Chains. *ACS Appl. Mater. Interfaces* **2016,** *8* (35), 23321-23330.

61. Li, N.; Wang, L.; Hickner, M., Cross-linked comb-shaped anion exchange membranes with high base stability. *ChemComm* **2014,** *50* (31), 4092-4095.

62. Tsai, T.-H.; Ertem, S. P.; Maes, A. M.; Seifert, S.; Herring, A. M.; Coughlin, E. B., Thermally Cross-Linked Anion Exchange Membranes from Solvent Processable Isoprene Containing Ionomers. *Macromolecules* **2015,** *48* (3), 655-662.

63. Ren, X.; Price, S. C.; Jackson, A. C.; Pomerantz, N.; Beyer, F. L., Highly Conductive Anion Exchange Membrane for High Power Density Fuel-Cell Performance. *ACS Appl. Mater. Interfaces* **2014,** *6* (16), 13330-13333.

64. Pan, J.; Lu, S.; Li, Y.; Huang, A.; Zhuang, L.; Lu, J., High-Performance Alkaline Polymer Electrolyte for Fuel Cell Applications. *Adv. Funct. Mater.* **2010,** *20* (2), 312-319.

65. Blencowe, A.; Qiao, G. G., Ring-Opening Metathesis Polymerization with the Second Generation Hoveyda–Grubbs Catalyst: An Efficient Approach toward High-Purity Functionalized Macrocyclic Oligo(cyclooctene)s. *J. Am. Chem. Soc.* **2013,** *135* (15), 5717-5725.

66. Vanicek, S.; Kopacka, H.; Wurst, K.; Müller, T.; Schottenberger, H.; Bildstein, B., Chemoselective, Practical Synthesis of Cobaltocenium Carboxylic Acid Hexafluorophosphate. *Organometallics* **2014,** *33* (5), 1152-1156.

67. Yan, Y.; Zhang, J.; Qiao, Y.; Tang, C., Facile Preparation of Cobaltocenium-Containing Polyelectrolyte via Click Chemistry and RAFT Polymerization. *Macromol. Rapid Commun.* **2014,** *35* (2), 254-259.

68. Demonceau, A.; Stumpf, A. W.; Saive, E.; Noels, A. F., Novel Ruthenium-Based Catalyst Systems for the Ring-Opening Metathesis Polymerization of Low-Strain Cyclic Olefins. *Macromolecules* **1997,** *30* (11), 3127-3136.

CHAPTER 3

THE FIRST SYNTHESIS OF A COMPLETE SET OF METALLO-CATIONS [1]

[1] Zhu, T.; Sha, Y.; Adabi, H.; Peng, X.; Cha, Y.; Dissanayake, D. M. M. M.; Smith, M. D.; Vannucci, A. K.; Mustain, W. E.; Tang, C., The First Synthesis of a Complete Set of Metallo-Cations Toward Redox- and Alkaline-Stable Metallo-Polyelectrolytes. *Manuscript submitted*, **2019.**

3.1 Abstract

Cations are crucial components in emerging functional polyelectrolytes for a myriad of applications. Rapid development in this area necessitates the exploration of new cations with advanced properties. Herein we describe a combination of computational and experimental design of cobaltocene metallo-cations that have distinct electronic and redox properties.

3.2 Introduction

Charged polyelectrolytes are widely used in a variety of areas, ranging from biological systems to commodity materials to membranes for energy applications.[2-4] At the advent of the 100th anniversary of the 'Macromolecular Hypothesis' by Hermann Staudinger, polymer science has overseen a distinct existence of metallopolymers that have a unique combination of inorganic metal centers and organic skeletons.[5-9] Among them, cationic metallo-polyelectrolytes have contributed fascinating optoelectronic and physicochemical properties and functions that could revolutionize areas such as biomedicines, energy conversion and water purification.[10-13]

The central piece of a polyelectrolyte resides on charged groups, which are the most critical in dictating properties of polymeric frameworks. Thus, there is an ingenious impetus in discovering and designing novel ionic moieties in the hope of achieving unprecedented properties in advanced materials. In conventional organo-polyelectrolytes, there are a few classes of cations such as quaternary ammonium and phosphonium, that have been well explored with a wide spectrum of derivatives to suit various needs. However, there are very few choices of metallo-polyelectrolytes, in a large extent due to the lack of tunability of metal cations. Herein we report the first complete synthesis of

cobaltocene cations with 1 to 10 substituents and further evaluate their redox and chemical properties. The methodology in this work could be the first realization of rational design of metallo-cations towards metallo-polyelectrolytes with similar levels of vigor to organo-polyelectrolytes.

The key dogma is to address a critical challenge how to design metallo-cations with a full spectrum of structures with tunable physiochemical properties. Recent work has showed that metal centers can endow metallo-polyelectrolytes with diverse electrochemical redox behavior, rich electrochromic properties, as well as fascinating ionic binding with macromolecular/biological substrates.[14-15] These physiochemical properties rely on understanding of structures and chemical bonding of metallo-cations. In this work we demonstrate the first rational design of cobaltocene cations utilizing density functional theory (DFT) calculation, synthesize a spectrum of derivatives based on modular alkylation and chemoselective alkynylation, and evaluate their redox potentials and chemical stability.

3.3 Results and Discussion

Bonding of cobaltocenium cations by DFT calculations.

Compared with 18-e ferrocene, the isoelectronic cobaltocene cation (commonly called cobaltocenium) is known for its chemical stability. It has been reported to behave much like a large alkali metal ion in aqueous solution.[16] Although structural modifications to the cyclopentadienyl ligands in neutral metallocenes have been extensively explored,[17-21] there is a lack of a rational design of metallocene cations. In this work, we designed cobaltocenium cations by systemically installing methyl and tert-butyl groups and correlated electronic and steric effects on the stability of cations.

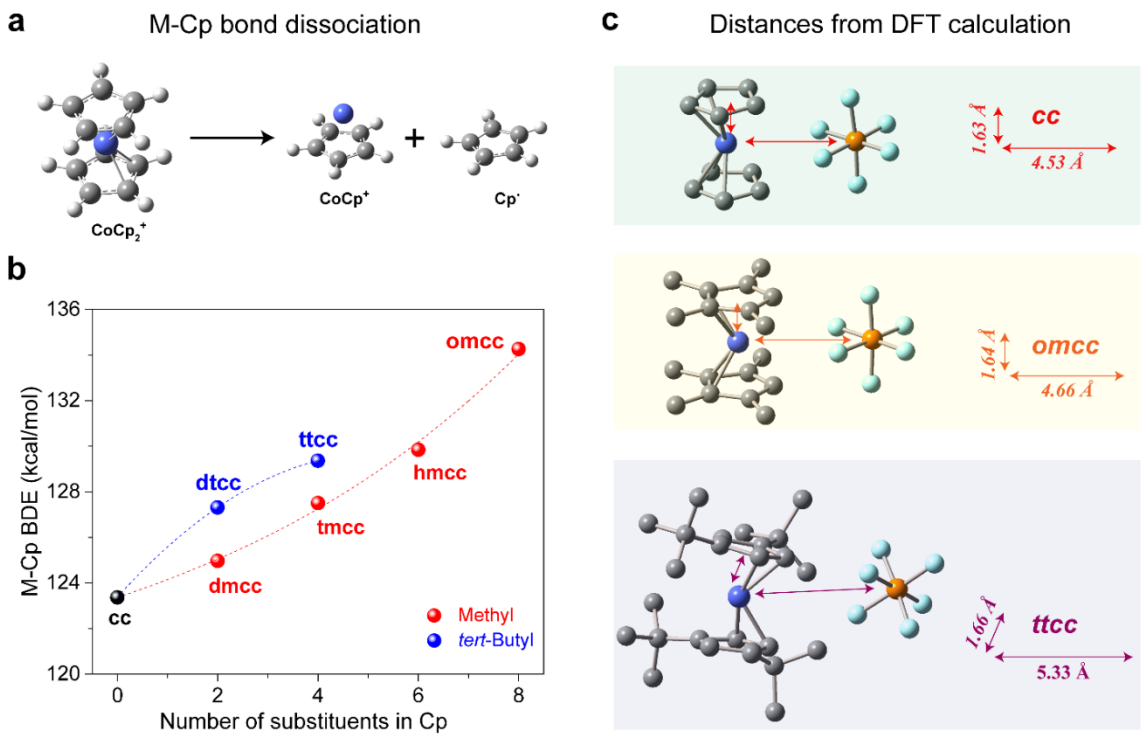

Figure 3.1 Bonding of cobaltocenium cations by DFT calculations. **a.** illustration of metal-Cp bond dissociation; **b.** DFT calculation of bond dissociation energy (BDE) as a function of number of substituents; **c.** comparison of optimized structures by DFT calculation, metal-Cp and metal-counterion distance for unsubstituted, octa-methyl and tetra-*tert*-butyl cobaltocenium. (Hydrogen atoms are omitted for clarity; **cc** represents unsubstituted cobaltocenium; **dmcc**, **tmcc**, **hmcc**, **omcc**, **dtcc**, and **ttcc** represent cobaltocenium with di-methyl, tetra-methyl, hexa-methyl, octa-methyl, di-*tert*-butyl, and tetra-*tert*-butyl substituents, respectively.)

DFT calculations facilitate the understanding of thermochemistry of cobaltocenium cations, mostly bond dissociation energies (BDEs) of the metal-Cp bond (**Figure 3.1 a**), which is closely related with redox potential and chemical stability.[22-23] As shown in **Figure 3.1 b**, the increase of methyl or *tert*-butyl groups on Cp ligands generally results in higher BDEs of multi-substituted cobaltocenium derivatives. In the case of methyl substitution, this can be rationalized by the electron-donating nature of methyl group, which leads to more overlapped electronic wave functions of binding partners between the metal and Cp.[24] Though the electron-donating effect of *tert*-butyl increases the BDEs of di- and tetra-substituted cobaltocenium, the steric effect results in significantly tilted Cp

planes when there are four tert-butyl groups. With further substitution of the bulky group, for example, in the case of hexa-*tert*-butyl cobaltocenium, the paramount steric repulsion from *tert*-butyl groups over the electronic effect makes BDE of metal-Cp inversely reduced (113.6 kcal/mol, not drawn in **Figure 3.1 b**), even lower than unsubstituted cobaltocenium (123.4 kcal/mol).

Table 3.1 BDE of various cobaltocenium cations by DFT calculations.

Substituents	Number of substituents	E_{PF6^-} (au)	$E_{Cobaltocenium}$ (au)	$E_{Complex}$ (au)	$E_{ionic\ bonding}$ (kcal/mol)	Distance [a] (Å)
methyl	0	-939.8874604	-1769.10252	-2709.133063	89.87213573	4.34042
	2	-939.8874604	-1847.646596	-2787.673607	87.65303354	4.34042
	4	-939.8874604	-1926.190208	-2866.216339	87.10016796	4.37388
	6	-939.8874604	-2004.73271	-2944.761603	88.83517091	4.38839
	8	-939.8874604	-2083.275822	-3023.299832	85.76811443	4.45786
	10	-939.8874604	-2161.817714	-3101.831555	79.38073067	4.86480
tert-butyl	2	-939.8874604	-2083.237031	-3023.265951	88.85224423	4.37008
	4	-939.8874604	-2397.363695	-3337.379867	80.84492601	5.13565
	6	-939.8874604	-2711.428528	-3651.443435	80.0507709	5.32601

In addition to the metal-Cp bonding, one needs to consider the interaction between cobaltocenium cation and counterion. Using PF_6^- as a counterion, we calculated the cobalt-counterion bonding strength and the cobalt-phosphorous distance (**Tables 3.1 & 3.2**). Three representative structures are shown in **Figure 3.1 c**. Introducing methyl substituents only results in a slight increase in the metal-counterion distance, e.g. only 0.13 Å difference between unsubstituted and octa-methyl cobaltocenium. In the case of tetra-*tert*-butyl cobaltocenium, this difference increases to 0.80 Å. In general, the increase of both methyl and *tert*-butyl substituents, ionic bonding strength weakens. As described in later sections, the larger metal-counterion distance and weaker ionic bonding strength could indicate a

better protection of the cationic cobalt center from nucleophilic attack by anions, thus enhancing stability of metallo-cations under caustic environments such as high alkaline solution (e.g. hydroxide ions as nucleophile).

Table 3.2 Metal-counterion bonding strength and distance of various cobaltocenium cations by DFT calculations.

Substituents	Number of substituents	Cp (au)	Cp (ZPE au)	$CpCo^+$ (au)	$CpCo^+$ (ZPE au)	Cp_2Co^+ (au)	Cp_2Co^+ (ZPE au)	BDE (kcal/mol)
methyl	0	-193.1792287	0.076140368	-1576.32223	0.080730537	-1769.707831	0.166556656	123.3653
	2	-232.4461745	0.103930103	-1615.59231	0.107404219	-1848.246521	0.220120853	124.9693
	4	-271.712020	0.13082859	-1654.86111	0.134195883	-1926.784636	0.273241817	127.5020
	6	-310.9764794	0.157271089	-1694.12985	0.160667081	-2005.323464	0.328048022	129.8461
	8	-350.2398767	0.184365683	-1733.39838	0.187592672	-2083.861941	0.381575549	134.2651
	10	-389.5011909	0.210776295	-1772.6663	0.214800466	-2162.400726	0.437280974	138.9461
tert-butyl	2	-350.2176222	0.186454298	-1733.36965	0.189518662	-2083.799748	0.385481737	127.3015
	4	-507.2576082	0.295760591	-1890.41894	0.298397666	-2397.893195	0.604577414	129.3509
	6	-664.2827192	0.406866919	-2047.45329	0.406866919	-2711.930635	0.829408013	113.6480

Synthesis of substituted cobaltocenium cations.

Unsubstituted cobaltocenium (**cc**) and cobaltocenium derivatives with even number of methyl (**dmcc**, **tmcc, hmcc, omcc**) or *tert*-butyl substituents (**dtcc**, **ttcc**) on Cp rings were prepared by the reaction of $CoBr_2$ and different cyclopentadienyl ligands. The complete synthetic procedures are shown in **Figure 2**. No column chromatography was required during the synthesis of these compounds, and all cations can be prepared in gram scales. Chemical structures of these compounds were confirmed by nuclear magnetic resonance, UV-vis spectrometry, high-resolution mass spectrometry, and single-crystal X-ray diffraction. Although crystal structures of **cc** and **dtcc** were previously reported and identical to our results, structures of **tmcc**, **hmcc**, **omcc** and **ttcc** have not been reported

yet.[25-26] From the X-ray characterization, cobaltocenium cations with different methyl substituents exhibit two parallel Cp rings, while four bulky *tert*-butyl substituents induce steric repulsion between Cp rings and hence lead to a tilted structure for **ttcc**. These structures are consistent with optimized results by DFT calculations (**Figure 3.1 c**). Further introducing *tert*-butyl substituents was unsuccessful largely due to too high steric hindrance and unstable metal-Cp bonding.

Synthesis of cobaltocenium derivatives with direct substitution of odd number of alkyl groups was not carried out, as it requires tedious separation from derivatives with even number of substituents as a result of statistical reactions involving a mixture of two cyclopentadienyl ligands (one with odd numbers of alkyl groups, the other with even numbers of alkyl groups), often with extremely low yields (e.g. the synthesis monomethyl cobaltocenium has a yield of only 5-10%).[27-28] However, recently we and others demonstrated chemo-selective synthesis of mono-substituted cobaltocenium with high yields (e.g. 50-80%) *via* one-pot nucleophilic addition and endo-hydride abstraction.[29-30] We extended this strategy to prepare cobaltocenium derivatives with odd number of substituents using the above-mentioned cobaltocenium with even number of alkyl groups as substrates by introducing an alkyne group (alkynylation) (**Figure 3.2**). Simply, cobaltocenium derivatives were mixed with trimethylsilylacetylene in the presence of butyl lithium, followed by the addition of trityl cation. This one-pot reaction typically involves the transitions of η^5-η^4-η^5 sandwich structures. The overall yields of these derivatives with odd number of substituents were over 70%. For the first time, a full spectrum of cobaltocenium derivatives from unsubstituted to complete substitution were prepared,

which could serve as an ideal platform to explore their physiochemical properties and discover potential applications.

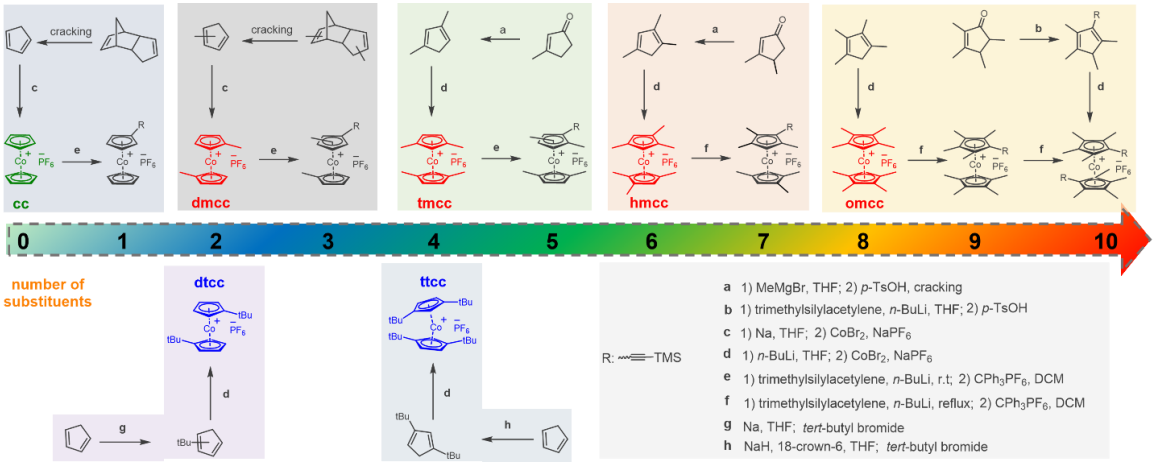

Figure 3.2. Synthetic pathways of cobaltocenium derivatives by methyl and *tert*-butyl substitution: derivatives with even number of alkyl groups are prepared by oxidative reactions between substituted cyclopentadiene and $CoBr_2$ in the presence of $NaPF_6$; those with odd number of substituted groups are prepared by nucleophilic addition and endo-hydride abstraction of derivatives with even number of alkyl groups. (The center number box indicates the number of substituents).

Redox properties and chemical stability.

Redox potential and chemical stability are among the most essential properties of metallo-cations to dictate their utilities.[31] Compared to traditional organo-cations, transition metal complexes possess unique metal-ligand bonding and usually exhibit a few redox states due to their variable oxidation states of metals. This allows broad applications of metal complexes, ranging from catalysis to photochromic and electrochromic devices.[14, 32-33]

We first examined electrochemical properties of these alkylated cobaltocenium derivatives by cyclic voltammetry (CV) in acetonitrile using tetra-butyl-ammonium hexafluorophosphate as a supporting electrolyte. In all cases as shown in **Figure 3.3 b**, CV scans exhibited a one-electron reversible reduction ascribing to the redox couple of

cobaltocenium (Co^{III})/cobaltocene (Co^{II}).[34] The secondary reduction from Co^{II} to Co^{I} was only observed for unsubstituted cobaltocenium (**1**) over the investigated potential window. Due to the inductive donation of electrons from the methyl or *tert*-butyl groups, all multi-substituted cobaltocenium cations exhibited lower reduction potentials than **1**. There is almost a linear decrease of the reduction potential of every ~110 mV by the addition of a pair of methyl groups in Cp rings. In the case of the *tert*-butyl substitution, the decrease in reduction potential becomes smaller (from 95 mV to 70 mV) when more *tert*-butyl groups were introduced. This is probably due to steric effects, as there is a lower energy level of LUMO orbital for tilted cobaltocenium. An earlier study by Manners and coworkers also showed the distinct shift to less negative reduction potential with increasing tilting for [2]cobaltoceniumphane and [3]cobaltoceniumphane.[35]

Chemical stability of metallo-cations is critical for many utilities such as energy storage, catalysis, and biological metabolism.[36] Coates, Noonan and coworkers have investigated the long-term stability of various organic cations in the presence of nucleophilic hydroxide or alkoxide anions.[37-40] In comparison, comprehensive evaluation of stability of metallo-cations has not been done, largely due to the lack of a meaningful set of derivatives.[8, 41-46] Herein we evaluated methylated and *tert*-butylated cobaltocenium cations under high alkaline conditions (5 M KOH/CD_3OH at 80 °C) and attempted to compare them with organo-cations. It is worthwhile to note that the tests were done under oxidative atmosphere (with constant charging of air), while most reported alkaline stability has been done under inert atmosphere, which is far from the real scenarios in many applications that operate under oxidative conditions.

CD_3OH was used as a reaction medium for KOH instead of deuterated water to preclude the undesirable hydrogen/deuterium exchange process involving the Cp rings (a hurdle for NMR analysis), and it also provides more aggressive reaction conditions to accelerate potential degradation of cations.[37-38, 43-44] We monitored the stability of cations by NMR spectroscopy. Initially, we explored the methyl substituent effect on the stability of cobaltocenium cations (**Figure 3.3 c**). Di, tetra, octa-methyl cobaltocenium cations with chloride as the counterion were prepared due to their good solubility in methanol. Previous studies have reported good alkaline stability of unsubstituted cobaltocenium under inert atmosphere (e.g. under nitrogen protection).[8, 16, 47] However, under air purging, it lost over 40% within 232 hours. Dimethyl cobaltocenium was observed to behave similarly to the unsubstituted cobaltocenium. The degradation was unable to monitor by NMR after 232 hours, due to the formation of paramagnetic cobalt salts. The introduction of four methyl groups resulted in considerable improvement in stability, with 37.4% cation loss after 392 hours. Further increasing the number of substituents to eight methyl groups (**2c**) produced a much more inert cation, and the octamethyl cobaltocenium only degraded by 10.9% and 18.5% after 553 hours and 1025 hours, respectively.

We then investigated the steric effect on the stability of *tert*-butyl cobaltocenium (**Figure 3.3 c**). We hypothesized that the presence of *tert*-butyl groups makes cobaltocenium more resistant to nucleophilic attack from hydroxide anions by keeping them away from the cationic metal center. Di-*tert*-butyl cobaltocenium cation (**3a**) exhibited a substantial alkaline stability with 26.6% loss after 1025 hours. The cation with the best alkaline stability is tetra-*tert*-butyl cobaltocenium (**3b**), which showed a minimal

degradation over 1025 hours under harsh oxidative and high alkaline conditions (only ~ 8.2% cation loss).

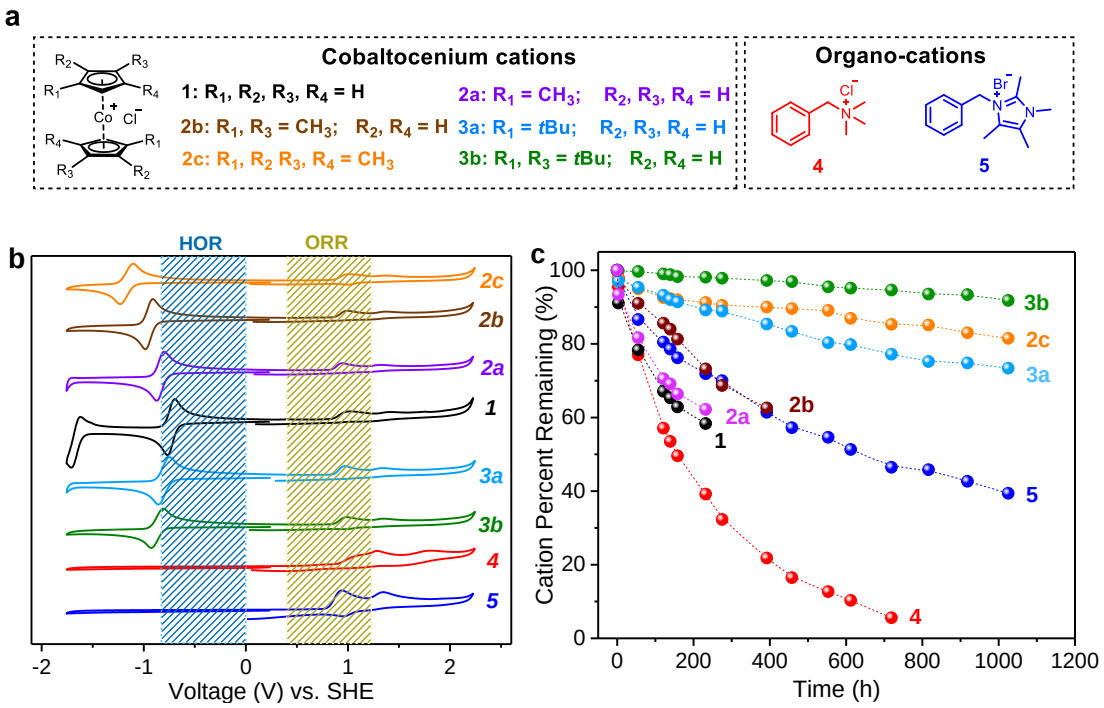

Figure 3.3. Redox properties and chemical stability of cobaltocenium cations. **a.** chemical structures of cobaltocenium derivatives, and two organo-cations used in this study for comparison; **b**. cyclic voltammetry curves for cobaltocenium cations and organo-cations at a scan of 100 mV/s in acetonitrile with 0.1 M tetra-butyl-ammonium hexafluorophosphate as the supporting electrolyte, shadows represent HOR and ORR potentials; **c**. Stability of cobaltocenium cations and organo-cations (0.025 M) in 5M KOH/CD_3OH at 80 °C under air.

Furthermore, we compared the stability of these cobaltocenium cations with conventional organo-cations, benzyl trimethylammonium (**4**) and multi-substituted imidazole cation (**5**) (**Figure 3.3 c**).[37, 48-49] Cation **4** degrades rapidly under oxidative alkaline conditions, with more than 50% of cations degraded within the first week. Cation **5** is considered to be a signature organo-cation for its excellent alkaline stability under inert conditions.[37, 39-40] However, it lost about 60.6% under oxidative conditions after 1025 hours, much less stable than cobaltocenium cations **2c**, **3a**, and **3b**.

Taken together, it was concluded that the chemical stability and redox property of these new metallo-cations can be modulated by the substituent effect. For cobaltocenium with the same type of substituents, both alkaline and redox stability has the same trend with the BDEs, i.e., **2c**>**2b**>**2a**>**1** and **3b**>**3a**>**1**. However, it is not the most thermodynamically stable cobaltocenium with eight methyl groups (**2c**), but the one with four steric *tert*-butyl groups (**3b**) to have the highest alkaline stability, indicating that the steric effect plays an important role in determining the alkaline stability, while the electronic effect governs more on the redox property.

3.4 Conclusions

In summary, we have combined computational and experimental studies, for the first time, toward a complete set of substituted cobaltocenium cations with tunable electronic and redox properties. The synthesis enabled the substitution of even numbers of methyl and *tert*-butyl groups followed by chemoselective nucleophilic addition and hydride abstraction. The selection of electron-donating alkyl groups allowed the design of highly stable metallo-cations under harsh conditions.

3.5 Experimental Details

Materials

Dicyclopentadiene, methylcyclopentadiene dimer, 3-methyl-2-cyclopentenone, methylmagnesium bromide solution (3.0 M in diethyl ether), p-toluenesulfonic acid monohydrate, n-butyllithium solution (2.5 M in hexanes), sodium hexafluorophosphate, 2-bromo-2-methylpropane, 1,2,3,4-tetramethyl-1,3-cyclopentadiene (~85%), sodium hydride (60% dispersion in mineral oil), benzyl trimethylammonium, sodium (cubes stored

in mineral oil), 18-crown-6, cis-cyclooctene, isopropyl alcohol, crotonic acid, sulfuric acid (95-98%), polyphosphoric acid (115% H_3PO_4 basis), and methanol-d_3 were purchased from Sigma-Aldrich and used as received. Cobalt(II) bromide (anhydrous) was purchased from Beantown Chemical. Acetonitrile, hexane, methanol, dichloromethane, tetrahydrofuran, xylenes, tributylamine, anhydrous copper(II) sulfate, sodium ascorbate and acetone were purchased from VWR. Chloroform-d, acetone-d_6, acetonitrile-d_3, and dimethyl sulfoxide DMSO-d_6 were purchased from Cambridge Isotope Laboratories. Ion exchange procedures to prepare small molecules and polyelectrolytes with hydrophilic counterions (Cl^- and OH^-) followed our early work.[8, 50] Multi-substituted imidazolium (**5**) was prepared according to the literature.[37]

Characterization

^1H NMR (300 MHz) and ^{13}C NMR (75 MHz) spectra were recorded on a Varian Mercury 300 spectrometer using chloroform-d_3 ($CDCl_3$), methanol-d_3 (CD_3OH), acetone-d_6 (CD_3COCD_3), acetonitrile-d_3 (CD_3CN) or dimethyl sulfoxide(DMSO-d_6) as solvents. All chemical shifts in ^1H and ^{13}C NMR were compared to deuterated solvents or tetramethylsilane (TMS) as a reference. High-resolution mass spectra (HRMS) and ESI mass spectra (MS) were collected at the University of South Carolina mass spectrometry center. The UV-Vis spectra were recorded by a Shimadzu UV-2450 spectrophotometer.

Solvent suppression and quantitative ^1H NMR spectra analysis: The –OH signal in partially deuterated solvent CD_3OH was suppressed by presaturation delay. ^1H NMR spectra were acquired with 60 second relaxation delay before normal 16 scans for each analysis. The spectra were processed using MestReNova Version 12.0.0-20080 (Mestrelab

Research S.L.). Residual signals between 6.0 to 6.5 ppm often derive from solvent suppression. Baseline correction and phase correction were applied for all spectra.

A basic deuterated solution was firstly prepared by dissolving base (5 M KOH) and internal standard (0.025M 3-(trimethylsilyl)-1-propanesulfonic acid sodium salt) in CD_3OH. The model compound (0.025M) was then dissolved in the deuterated solution (0.5 mL) and transferred into NMR tubes. The system was sealed and analyzed for the initial data point. The tube was heated in a heating block setting at 80 °C. The solutions were cooled to room temperature and analyzed by ^1H NMR spectroscopy every 2 days. Pressured air was charged into the solutions in tubes for at least 5 min and the tubes were sealed again for each time-dependent test. The remaining cation percentage of cobaltocenium model compounds was calculated by the integration change of protons in Cp rings compared to the internal standard. The cation remaining percentage of organic cations was calculated using the method reported by Coates and coworkers.[37]

Cyclic voltammetry (CV) studies were carried out in an H-cell separated by a fine glass frit, using a CH Instruments potentiostat with a three-electrode setup. A glassy carbon electrode was used as a working electrode, Pt as a counter electrode and saturated calomel electrode (SCE) as a reference electrode. The cyclic voltammograms were obtained at a scan rate of 100 mV s^{-1}. Solutions were 1.0 mmol L^{-1} of cobaltocenium derivatives and 0.1 mol L^{-1} in tetrabutylammonium hexafluorophosphate as a supporting electrolyte; acetonitrile was used as solvent; all CV measurements were under N_2 atmosphere.

Synthetic Procedures

Unsubstituted cobaltocenium hexafluorophosphate.

Unsubstituted cobaltocenium (**1**) was prepared according to the literature.[27, 51] **^{1}H NMR** (300 MHz, acetone-d_6): δ= 5.91 (s, *Cp*, 5H). **^{13}C NMR** (75 MHz, acetone-d_6): δ= 85.93 (*Cp*). **MS** *m/z* calculated for $C_{10}H_{10}Co^{+}(M^{+})$ 189.12, found 189.

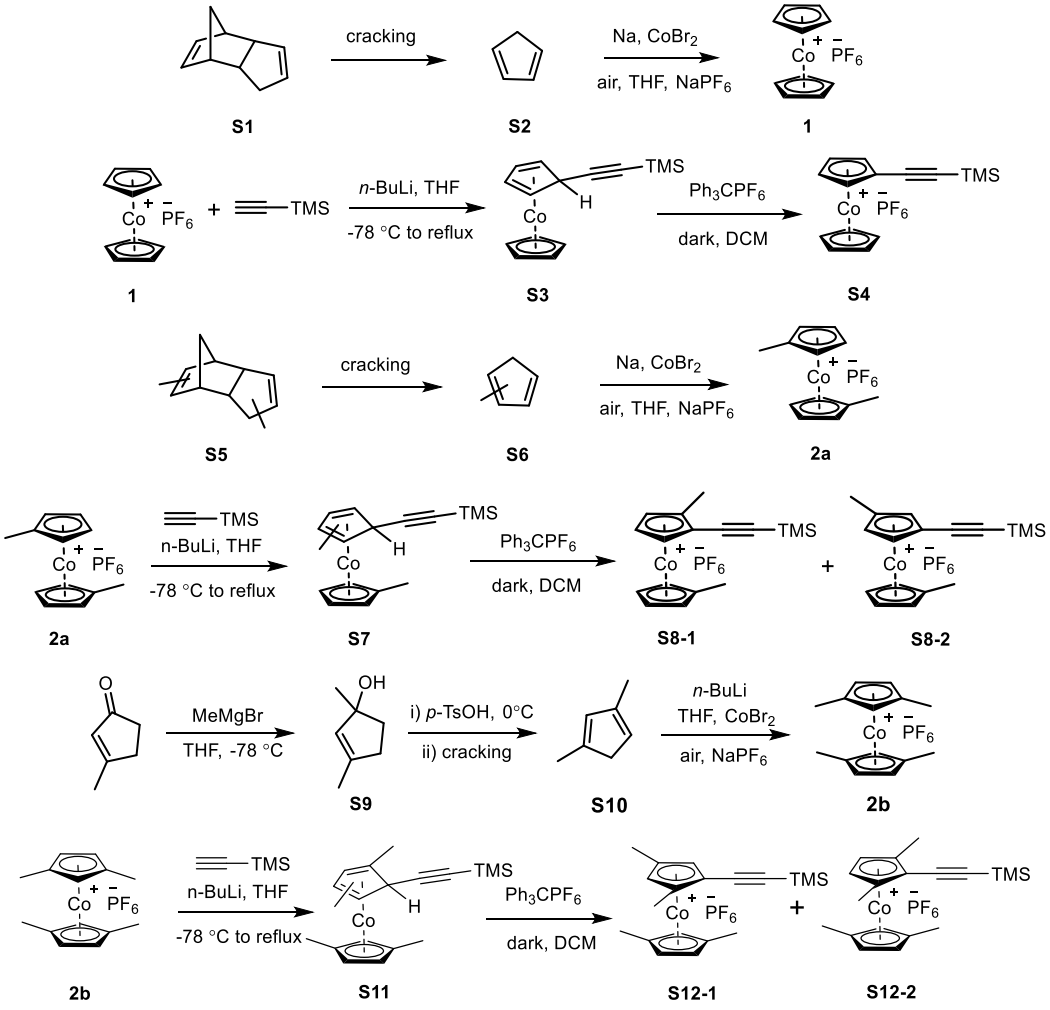

Continued

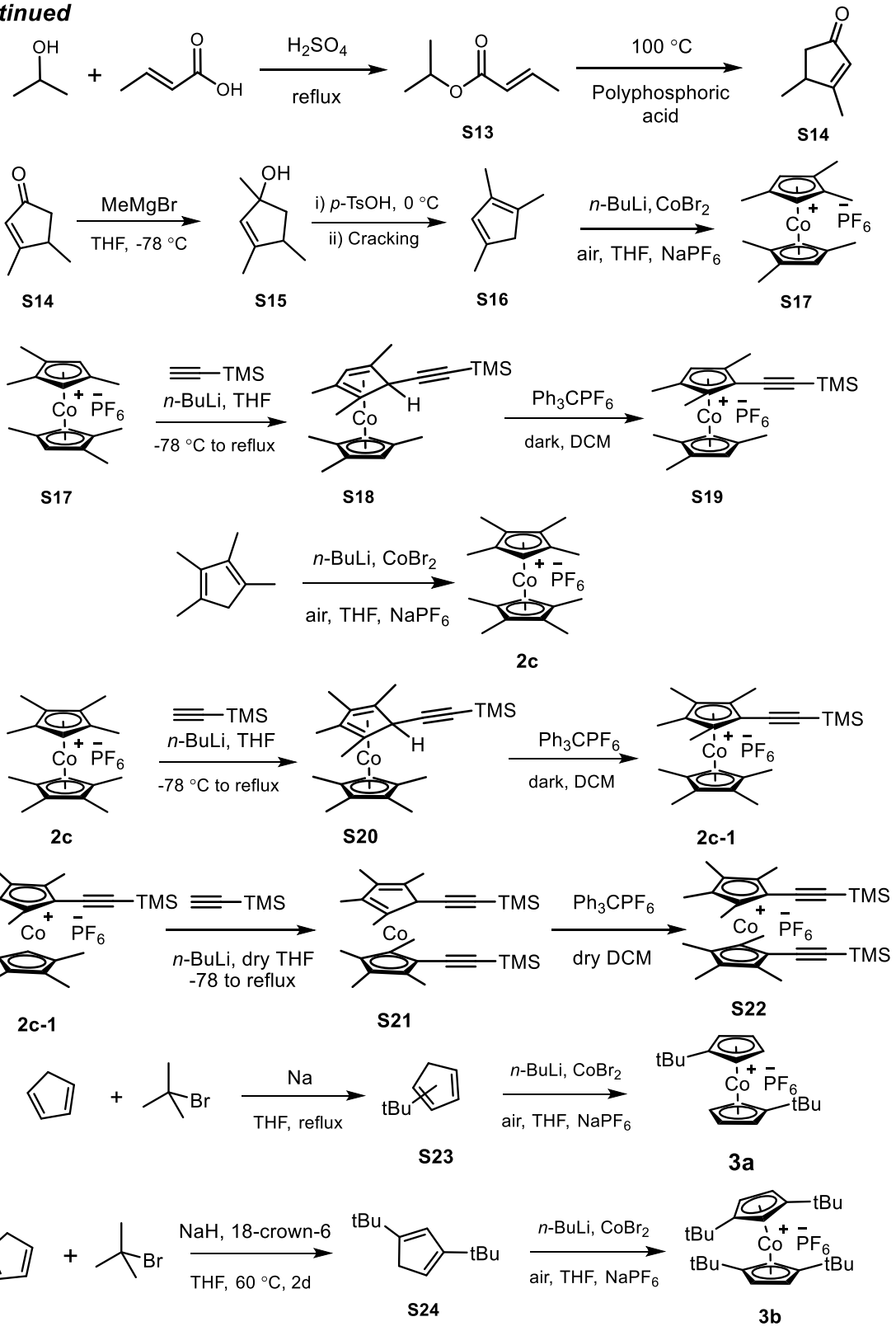

Figure 3.4. Synthesis of cationic cobaltocene derivatives.

(Trimethylsilyl)ethynyl cobaltocenium hexafluorophosphate.

(Trimethylsilyl)ethynyl cobaltocenium hexafluorophosphate was prepared according to the literature.[29-30] **^{1}H NMR** (300 MHz, CD_3CN): δ= 0.27 (s, Si(CH_3)$_3$, 9H), 5.85, 5.68, 5.67 (m, *Cp*, 9H). **^{13}C NMR** (75 MHz, CD_3CN): δ= −0.6 (Si(CH_3)$_3$), 85.9, 87.4, 87.1 (*Cp*), 103.1, 95.5 (-*C*≡*C*-). **MS** *m/z* calculated for $C_{15}H_{18}SiCo^{+}(M^{+})$ 285.33, found 285.

Dimethyl cobaltocenium hexafluorophosphate.

Methylcyclopentadiene (mixture of isomers) was freshly distilled from methylcyclopentadiene dimers prior to use. To a flask charged with 3.9 g sodium (0.168 mol, 1.05 equiv.) and 300 mL THF as solvent, 12.8 g methylcyclopentadiene 0.160 mol, 0.5 equiv.) solution in THF was added dropwise under nitrogen. The resulting mixture refluxed for 24 h. After cooling the mixture to -78 °C, 17.5 g anhydrous $CoCl_2$ powder (0.08 mol, 0.5 equiv.) was added and stirred at room temperature overnight. The solvent was removed by vacuo, yielding a dark brown residue. 300 mL hot water was added, and pressurized air was injected continuously for 3 h. The remaining brown residue was filtered off through celite and gave a yellow aqueous solution. The combined aqueous solutions were washed with 100 mL diethyl ether, decolorized with activated charcoal, and concentrated until the total volume was approximately 20 mL. The concentrated solution was added dropwise to an aqueous solution of sodium hexafluorophosphate (13.4 g $NaPF_6$, 0.08 mol). The yellow powder was filtered off, thoroughly washed with water and then diethyl ether, and dried in vacuo, giving the final product as a yellow powder in 60% yield (17.5 g). Yellow needle-like crystals of dimethyl cobaltocenium was obtained by diffusing

exceedingly thin and mechanically sensitive to manipulation. They are also fracture and lose crystallinity when cooled, so the X-ray diffraction was not carried out for this structure under either room temperature or low-temperature (~265 ± 10 K). **^{1}H NMR** (300 MHz, acetone-d_6): δ= 5.71 (s, *Cp*, 8H), 2.19 (s, -CH_3, 6H). **^{13}C NMR** (75 MHz, acetone-d_6): δ= 104.89, 85.81, 85.87 (*Cp*), 13.21 (-*C*H_3). **HRMS** *m/z* calculated for $C_{12}H_{14}Co^{+}(M^{+})$ 217.0422, found 217.0422.

(Trimethylsilyl)ethynyl-dimethyl cobaltocenium hexafluorophosphate.

A three-neck flask was charged with 20 mL dry THF and trimethylsilylacetylene (400 μL, 2.0 equiv.) under nitrogen. The mixture was cooled to −78 °C, and 2.5 M n-BuLi solution (1.1 mL, 2.0 equiv.) was added dropwise. Stirring continued for 45 min, and dimethyl cobaltocenium (500 mg, 1.38 mmol, 1.0 equiv.) was added. The reaction mixture was slowly warmed to room temperature under vigorous stirring. The solid reactant was fully dissolved after 30 min and the color of the reaction mixture changed to dark red. The solvent was removed in vacuo, and hexane was used to dissolve the product, followed by passing through celite. The nucleophilic addition product was obtained by removing hexane under vacuo and used for the next step without further purification. A flask charged with 30 mL dry dichloromethane, the product from the above step and triphenylcarbenium hexafluorophosphate (1.3 equiv.) were mixed and stirred for 3h under dark at room temperature. The solvent was removed by vacuo and diethyl ether was added to precipitate ethynyldimethyl cobaltocenium hexafluorophosphate. The precipitate was filtered off and thoroughly washed with diethyl ether. Further drying in vacuo afforded a yellow powder (482 mg, 77% yield). **^{1}H NMR** (300 MHz, acetone-d_6): δ= 5.50~6.04 (m, *Cp*, 7H), 2.12, 2.23 (s, -CH_3, 6H) 0.30, 0.26 (s, -Si(CH_3)$_3$, 9H). **^{13}C NMR** (75 MHz, acetone-d_6): δ=

105.88, 104.74 (-*C*≡*C*-), 95.09, 88.64, 85.78, 84.11 (*Cp*), 12.50, 11.36 (-*C*H_3), 0.35 (-Si(*C*H_3)$_3$). **MS** *m/z* calculated for $C_{17}H_{22}SiCo^+(M^+)$ 313.38, found 313.

1,3-Dimethylcyclopenta-1,3-diene.

The synthesis was modified according to a published procedure.[52] A solution of 3-methyl-2-cyclopentenone (10 g, 104 mmol) in dry THF was cooled to -78 °C and treated dropwise with MeMgBr (3M in diethyl ether, 2.0 equiv., 208 mmol) to give a thick white suspension. After stirring for additional 5 h, the color turned yellow. The reaction was quenched by slowly adding saturated NH_4Cl solution. The organic layer was separated and thoroughly washed with water, dried over $MgSO_4$. Solvent was removed in vacuo from the filtrate, giving an orange color liquid. The crude product was immediately passed through a flash column and dried. The light-yellow liquid was treated with *p*-TsOH at 0 °C and stirred overnight. The reaction mixture was washed with DI water, dried over $MgSO_4$, filtered and vacuum dried to give an orange oil. Final product was obtained as a colorless liquid (4.7 g, 48% yield) by fractional distillation, which was used immediately to prepare tetramethyl cobaltocenium hexafluorophosphate. **^{1}H NMR** (300 MHz, $CDCl_3$): δ= 6.04, 5.82 (s/t, -C*H*- in Cp, 2H), 2.86 (d, -CH_2- in Cp, 2H), 2.03, 1.97 (s, -CH_3, 6H).

Tetramethyl cobaltocenium hexafluorophosphate.

A deoxygenated solution of 2.78 g (29.5 mmol) 1,3-dimethylcyclopenta-1,3-diene in 130 mL THF at -78 °C was treated with 11.8 mL (29.5 mmol) of a 2.5 M *n*-butyllithium solution in hexane. The resulting mixture was stirred at this temperature for 3 h. Then 3.23 g (14.7 mmol) of $CoBr_2$ was added, the resulting slurry was warmed to room temperature and stirred overnight. The solvent was removed in vacuo, and 60 mL hot water was added to dissolve the dark brown residue. Pressurized air was injected to the solution continuously

for 4 h to oxidize the product. Then, the aqueous solution was treated with activated charcoal, heated to boil for 30 min, and filtered through celite. A yellow color solution was obtained and concentrated until the total volume was approximately 6 mL. The concentrated solution was added dropwise to an aqueous solution of sodium hexafluorophosphate (2.97 g $NaPF_6$, 17.7 mmol). The solid was obtained by filtration and thoroughly washed with DI water and then ether, dried in vacuo, giving the final product as a yellow powder in 58% yield (3.34 g). Yellow plates of tetramethyl cobaltocenium for X-ray analysis could be obtained by diffusing diethyl ether into a concentrated solution in acetonitrile. **^{1}H NMR** (300 MHz, acetone-d_6): δ= 5.49 (s, *Cp*, 6H), 2.11 (s, -CH_3, 12H). **^{13}C NMR** (75 MHz, acetone-d_6): δ= 103.18, 85.79, 84.89 (*Cp*), 12.78 (-*C*H_3). **HRMS** *m/z* calculated for $C_{14}H_{18}Co^+(M^+)$ 245.0735, found 245.0734.

(Trimethylsilyl)ethynyl-tetramethyl cobaltocenium hexafluorophosphate.

A three-neck flask was charged with 20 mL dry THF and trimethylsilylacetylene (474 μL, 1.3 equiv.) under nitrogen. The mixture was cooled to −78 °C, and 2.5 M *n*-BuLi solution (0.62 mL, 1.2 equiv.) was added dropwise. Stirring continued for 45 min, and tetramethyl cobaltocenium (500 mg, 1.28 mmol, 1.0 equiv.) was added. The reaction mixture was slowly warmed to room temperature under vigorous stirring. The solid reactant was fully dissolved after 30 min and the color of the reaction mixture changed to dark red. The solvent was removed in vacuo, and hexane was used to dissolve the product, followed by passing through celite. The nucleophilic addition product was obtained by removing hexane under vacuo and used for the next step without further purification. A flask charged with 30 mL dry dichloromethane, the product from the above step and triphenylcarbenium hexafluorophosphate (1.2 equiv.) were stirred for 3h under dark at

room temperature. The solvent was removed by vacuo and diethyl ether was added to precipitate ethynyl dimethyl cobaltocenium hexafluorophosphate. The precipitate was filtered off and thoroughly washed with diethyl ether. Further drying in vacuo afforded a yellow powder (505 mg, 81% yield). **^{1}H NMR** (300 MHz, acetone-d_6): δ= 5.28~5.80 (m, *Cp*, 5H), 2.19, 2.10 (s, -CH_3, 12H) 0.31, 0.28 (s, -Si(CH_3)$_3$, 9H). **^{13}C NMR** (75 MHz, acetone-d_6): δ= 103.74 (-*C*≡*C*-) 85.97, 84.45 (*Cp*), 11.92 (-*C*H_3), 0.29 (-Si(*C*H_3)$_3$). **MS** *m/z* calculated for $C_{19}H_{26}SiCo^{+}(M^{+})$ 341.43, found 341.

3,4-Dimethyl-2-cyclopentenone.

The synthesis was modified according to published procedures.[53-54] To prepare crotonic acid isopropyl ester, crotonic acid (10 g) and isopropanol (50 mL) were first mixed together, followed by slowly adding concentrated sulfuric acid (1.2 mL) and heated to reflux and stirred overnight. The solution was neutralized by slowly adding saturated $NaHCO_3$ solution. Diethyl ether was added to extract the product. The organic layer was collected and dried with $MgSO_4$. Diethyl ether was removed in vacuo and the crude product (12.9 g) was obtained as a colorless oil and used in the next step without further purification. A viscous solution of 150 mL polyphosphoric acid was stirred at 100 °C under nitrogen, to which crotonic acid isopropyl ester (10 g) was slowly added, and the reaction mixture was stirred for 3h. The reaction mixture was poured to 600 mL ice water and slowly neutralized with sodium carbonate. The product was extracted with diethyl ether, washed several times with water and subject to vacuum distillation to obtain 3,4-dimethyl-2-cyclopentenone (4.1 g, 48% yield) as a colorless liquid. **^{1}H NMR** (300 MHz, $CDCl_3$): δ= 5.87 (s, C=C*H*-, 1H), 2.80, 2.61 (m, -CH_2, 2H), 2.07 (s, CH_3, 3H), 2.02~1.96 (m, -C*H*-, 1H), 1.17 (d, CH_3, 3H).

1,2,4-Trimethylcyclopenta-1,3-diene.

The synthesis was modified according to published procedures.[55] A solution of 3,4-dimethyl-2-cyclopentenone (5.51 g, 50 mmol) in 25 mL dry THF was cooled to -78 °C and treated dropwise with MeMgBr (25 mL, 75 mmol, 1.5 equiv.) to give a thick white suspension. After stirring for additional 5 h, the color turned yellow. The reaction was quenched by slowly adding saturated NH_4Cl solution. The organic layer was separated and thoroughly washed with water, dried over $MgSO_4$. Solvent was removed in vacuo from the filtrate, giving an orange color liquid. The crude product was immediately passed through a flash column and dried for the dehydration step. The light-yellow liquid was treated with 10 mg of *p*-TsOH at 0 °C and stirred overnight. The reaction mixture was washed with DI water, dried over $MgSO_4$, filtered and vacuum dried to give an orange oil. Final product was obtained by fractional distillation to afford a colorless liquid (2.4 g, 45% yield), which was used immediately to prepare hexamethyl cobaltocenium hexafluorophosphate. **^{1}H NMR** (300 MHz, $CDCl_3$): δ= 5.91 (s, -C*H*- in Cp, 1H), 2.79 (s, -CH_2- in Cp, 2H), 2.01, 1.90, 1.83 (s, -CH_3, 9H).

Hexamethyl cobaltocenium hexafluorophosphate.

A deoxygenated solution of 1.68 g (15.5 mmol) trimethyl cyclopentadiene in 40 mL THF at -78 °C was treated with 7.45 mL (18.6 mmol) of a 2.5 M *n*-butyllithium solution in hexane. The resulting mixture was stirred at this temperature for 3 h. Then 1.70 g (7.76 mmol) of $CoBr_2$ was added, the resulting slurry was warmed to room temperature and stirred overnight. The solvent was removed in vacuo and 30 mL hot water was added to dissolve the dark brown residue. Pressurized air was injected to the solution continuously for 3 h to oxidize the product. Then, the aqueous solution was treated with activated

charcoal, heated to boil for 30 mins and filtered through celite. An orange color solution was obtained and concentrated until the total volume was approximately 5 mL. The concentrated solution was added dropwise to an aqueous solution of sodium hexafluorophosphate (1.30 g $NaPF_6$, 7.76 mmol). The solid was obtained by filtration and thoroughly washed with DI water and then ether, dried in vacuo, giving the final product as a yellow powder in 56% yield (1.80 g). Yellow blocks of hexamethyl cobaltocenium for X-ray analysis could be obtained by diffusing diethyl ether into a concentrated solution in acetonitrile. **^{1}H NMR** (300 MHz, acetone-d_6): δ= 5.29 (s, *Cp*, 4H), 2.02 (s, -CH_3, 18H). **^{13}C NMR** (75 MHz, acetone-d_6): δ= 100.09, 85.44 (*Cp*), 12.33, 10.61 (-*C*H_3). **HRMS** *m/z* calculated for $C_{18}H_{26}Co^+(M^+)$ 273.1048, found 273.1048.

(Trimethylsilyl)ethynyl-tetramethyl cobaltocenium hexafluorophosphate.

A round bottom flask was charged with 15 mL dry THF and 380 μL of trimethylsilylacetylene (2.67 mmol, 2.24 equiv.). The mixture was cooled to -78 °C, and 1.0 mL of 2.5 M *n*-BuLi solution (2.50 mmol, 2.10 equiv.) was added. The reaction mixture was stirred for 1.5 h , and 0.5 g of hexamethyl cobaltocenium (1.19 mmol, 1.0 equiv.) was added. The reaction mixture was slowly warmed to room temperature and then heated to reflux for 2 hrs. The solution turned dark red and all yellow solid dissolved. The solvent was removed in vacuo, and 30 mL hexane was added to re-dissolve the product. Crude product was obtained by passing through celite, dried under vacuum and then used for *endo*-hydride abstraction without further purification. A deoxygenated solution of this compound in dry DCM under dark was treated with 601 mg triphenylcarbenium hexafluorophosphate (1.54 mmol, 1.30 equiv.) portion-wise over 10 min. The reaction mixture was stirred under dark at room temperature overnight. Then the solvent was

removed in vacuo, and the product was obtained by precipitating in diethyl ether several times. The precipitate was filtered off and thoroughly washed with cold water and diethyl ether. After the volatiles were completely removed, 448 mg yellow solid product was obtained with a 73% overall yield for two steps. **^{1}H NMR** (300 MHz, acetone-d_6): δ= 5.47, 5.27, 5.22 (s, *Cp*, 3H), 2.07, 2.02, 1.94, 1.91 (s, -CH_3, 18H), 0.31 (s, -Si(CH_3)$_3$, 9H). **^{13}C NMR** (75 MHz, acetone-d_6): δ= 105.38, 101.30, 99.83, 94.89 (-*C*≡*C*-) 88.53, 86.82, 85.23 (*Cp*), 11.84, 10.85, 10.06, 9.20 (-*C*H$_3$), 0.27 (-Si(*C*H$_3$)$_3$). **MS** *m/z* calculated for $C_{21}H_{30}SiCo^{+}(M^{+})$ 369.49, found 369.

Octamethyl cobaltocenium hexafluorophosphate.

A deoxygenated solution of 5.00 g (40.9 mmol) tetramethyl cyclopentadiene in 65 mL THF cooled to -78 °C was treated with 18.8 mL (47.1 mmol) of a 2.5 M *n*-butyllithium solution in hexane. The resulting mixture was stirred at this temperature for 3 h. Then 4.48 g (20.4 mmol) $CoBr_2$ was added, the resulting slurry was warmed to room temperature and stirred overnight. The solvent was removed in vacuo and 60 mL hot water was added to dissolve the dark brown residue. Pressurized air was injected to the solution continuously for 4 h to oxidize the product. Then, the aqueous solution was treated with activated charcoal, heated to boil for 30 mins, and filtered through celite. An orange color solution was obtained and concentrated until the total volume was approximately 10 mL. The concentrated solution was added dropwise to an aqueous solution of sodium hexafluorophosphate (3.40 g $NaPF_6$, 17.7 mmol). The solid was obtained by filtration and thoroughly washed with DI water and then ether, dried in vacuo, giving the final product as a yellow powder in 71% yield (6.40 g). Yellow needles of octamethyl cobaltocenium for X-ray analysis could be obtained by diffusing diethyl ether into a concentrated solution

in acetonitrile. **^{1}H NMR** (300 MHz, acetone-d_6): δ= 5.10 (s, *Cp*, 2H), 1.96, 1.89 (s, -C*H*$_3$, 24H). **^{13}C NMR** (75 MHz, acetone-d_6): δ= 97.83, 97.23, 84.14 (*Cp*), 10.33, 8.47 (-*C*H$_3$). **HRMS** *m/z* calculated for $C_{18}H_{26}Co^{+}(M^{+})$ 301.1361, found 301.1355.

(Trimethylsilyl)ethynyl-octamethyl cobaltocenium hexafluorophosphate.

A round bottom flask was charged with 300 mL dry THF and 3.64 mL of trimethylsilylacetylene (25.5 mmol, 1.14 equiv.). The mixture was cooled to -78 °C, and 9.40 mL of 2.5 M *n*-BuLi solution (23.5 mmol, 1.05 equiv.) was added. The reaction mixture was stirred for 1.5 h , and 10 g octamethyl cobaltocenium (22.4 mmol, 1 equiv.) was added. The reaction mixture was slowly warmed to room temperature and then heated to reflux for 2 hrs. The solution turned dark red and all yellow solid dissolved. The solvent was removed in vacuo, and 300 mL hexane was added to re-dissolve the product. Crude product was obtained by passing through celite, dried under vacuum and then used for *endo*-hydride abstraction without further purification. A deoxygenated solution of this compound in dry DCM under dark was treated with 8.5 g triphenylcarbenium hexafluorophosphate (21.8 mmol, 0.97 equiv.) portion-wise over 10 min. The reaction mixture was stirred under dark at room temperature overnight. Then the solvent was removed in vacuo, and the product was obtained by precipitating in diethyl ether several times. The precipitate was filtered off and thoroughly washed with cold water and diethyl ether. After the volatiles were completely removed, 8.6 g yellow solid product was obtained with a 71% overall yield for two steps. **^{1}H NMR** (300 MHz, acetone-d_6): δ= 5.09 (s, *Cp*, 1H), 1.99, 1.92, 1.83 (s, -C*H*$_3$, 24H) 0.33 (s, -Si(C*H*$_3$)$_3$, 9H). **^{13}C NMR** (75 MHz, acetone-d_6): δ= 98.53, 96.84 (-*C*≡*C*-) 85.22 (*Cp*), 9.55, 7.58 (-*C*H$_3$), 0.19 (-Si(*C*H$_3$)$_3$). **HRMS** *m/z* calculated for $C_{23}H_{34}SiCo^{+}(M^{+})$ 397.1756, found 397.1755.

1,1'-Bis((trimethylsilyl)ethynyl)-octamethyl cobaltocenium hexafluorophosphate.

A round bottom flask was charged with 20 mL dry THF and 538 µL trimethylsilylacetylene (3.78 mmol, 2.05 equiv.). The mixture was cooled to -78 °C, and 1.47 mL 2.5 M *n*-BuLi solution (3.68 mmol, 2.0 equiv.) was added. The reaction mixture was stirred for 1.5 h, and 1 g trimethylsilylethynyl-octamethyl cobaltocenium hexafluorophosphate (1.84 mmol, 1 equiv.) was added. The reaction mixture was slowly warmed to room temperature and then heated to reflux for 2 hrs. The solution turned dark red and all yellow solid reactant dissolved. The solvent was removed in vacuo, and 30 mL hexane was added to re-dissolve the product. Crude product was obtained by passing through celite, dried under vacuum and then used for *endo*-hydride abstraction without further purification. A deoxygenated solution of this compound in dry DCM under dark was treated with 713 mg triphenylcarbenium hexafluorophosphate (1.84 mmol, 1 equiv.) portion-wise over 10 mins. The reaction mixture was stirred under dark at room temperature overnight. Then the solvent was removed in vacuo, and the product was obtained by recrystallization in a mixed solvent of acetonitrile and diethyl ether for several times. The precipitate was filtered off and thoroughly washed with cold water and diethyl ether. After the volatiles were completely removed, 529 mg yellow solid product was obtained with a 45% overall yield for two steps. **^{1}H NMR** (300 MHz, acetone-d_6): δ= 1.92, 1.89 (s, -CH_3, 24H) 0.30 (s, -Si(CH_3)$_3$, 18H). **^{13}C NMR** (75 MHz, acetone-d_6): δ= 98.60, 97.42 (-*C*≡*C*-) 94.86, 82.08 (*Cp*), 8.66, 7.79 (-*C*H_3), 0.19 (-Si(*C*H_3)$_3$). **MS** *m/z* calculated for $C_{28}H_{42}Si_2Co^+(M^+)$ 493.2157, found 493.2147.

An alternative method to prepare 1,l'-bis(trimethylsilylethynyl)-octamethyl cobaltocenium hexafluorophosphate was to mix trimethyl(tetramethyl-

cyclopentadienylethynyl)silane lithium salt and cobalt bromide. The synthetic procedure and purification process was similar to an early report on 1,l'-bis(trimethylsilylethynyl) ferrocene and ruthenocene.[56] The final product was obtained as a yellow solid in a 40% yield.

***tert*-Butylcyclopentadiene.**

The synthesis was modified according to a reported procedure.[57] To a suspension of 4.2 g (181 mmol) sodium in 100 ml THF, 10 g (12.7 mL, 151 mmol) freshly distilled cyclopentadiene was added dropwise at 0 °C. After stirring for 16 h the solution was heated to reflux and 20.7 g (17.0 mL, 151 mmol) tert-butyl bromide was added dropwise. After additional heating for 1 h, the mixture was cooled to room temperature and hydrolyzed by addition of 100 mL ammonium chloride solution. The organic layer was collected, and the aqueous layer was extracted two times with 50 mL ether. The combined organic layer was dried over $MgSO_4$, filtered and the solvent was removed. The oily residue was fraction-distilled. The resultant colorless product consisted of a mixture of isomers and was isolated in a 50% yield. **^{1}H NMR** (300 MHz, acetone-d_6): δ= 6.55, 6.32, 6.15, 6.03, 5.81 (m, *Cp*, 3H), 2.25 (s, -CH_2, 2H), 0.20 (s, -(CH_3)$_3$, 9H).

Di-*tert*-butyl cobaltocenium hexafluorophosphate.

A deoxygenated solution of 3.23 g (26.4 mmol) tert-butylcyclopentadiene in 60 mL THF at -78 °C was treated with 11.1 mL (27.7 mmol) of a 2.5 M *n*-butyllithium solution in hexane. The resulting mixture was stirred at this temperature for 3 h. Then 2.89 g (13.2 mmol) $CoBr_2$ was added, the resulting slurry was warmed to room temperature and stirred overnight. The solvent was removed in vacuo and 50 mL hot water was added to dissolve the dark brown residue. Pressurized air was injected to the solution continuously for 4 h to

oxidize the product. Then, the aqueous solution was treated with activated charcoal, heated to boil for 30 min, and filtered through celite. An orange color solution was obtained and concentrated until the total volume was approximately 7.0 mL. The concentrated solution was added dropwise to an aqueous solution of sodium hexafluorophosphate (2.22 g $NaPF_6$, 13.2 mmol). The solid was obtained by filtration and thoroughly washed with DI water and then ether, dried in vacuo, giving the final product as a yellow powder in 76% yield (4.50 g). Yellow plates of di-*tert*-butyl cobaltocenium for X-ray analysis could be obtained by diffusing diethyl ether into a concentrated solution in acetonitrile. **^{1}H NMR** (300 MHz, acetone-d_6): δ= 5.87 (s, *Cp*, 8H), 1.36 (s, -CH_3, 18H). **^{13}C NMR** (75 MHz, acetone-d_6): δ= 83.92, 81.76 (*Cp*), 31.74, 30.93 (-*C*(*C*H_3)$_3$). **HRMS** *m/z* calculated for $C_{18}H_{26}Co^+$(M^+) 301.1361, found 301.1360.

1,3-Di-*tert*-butylcyclopenta-1,3-diene.

The synthesis was modified according to an reported procedure.[58] 8.3 g (345 mmol) NaH was mixed with 1.2 g (4.55 mmol) 18-crown-6 and 49.5 mL (440 mmol) *tert*-butyl bromide in 30 mL dry THF as solvent. 3 g (45.4 mmol) freshly distilled cyclopentadiene in 10 mL THF was added dropwise to the solution under nitrogen. The reaction was stirred for 2 days at 60 °C. Then the resulting mixture was cooled to room temperature and diluted with diethyl ether. The precipitated solid was filtered off and washed several times with diethyl ether. The organic phases were collected and combined. The solvent was removed, and the remaining orange liquid was fraction-distilled under vacuum to obtain a colorless liquid product (3.5 g, 43% yield).

Tetra-*tert*-butyl cobaltocenium hexafluorophosphate.

A deoxygenated solution of 3.00 g (16.8 mmol) di-*tert*-butyl-cyclopentadiene in 30 mL THF at-78 °C was treated with 7.4 mL (18.5 mmol) 2.5 M *n*-butyllithium solution in hexane. The resulting mixture was slowly warmed to room temperature and additionally stirred at reflux for 3 h. Then, the solution was cooled to room temperature and 1.84 g (8.4 mmol) anhydrous $CoBr_2$ was added. The resulting slurry was stirred overnight. The solvent was removed in vacuo and 30 mL hot water was added to dissolve the residue. Pressurized air was injected to the solution continuously for 4 h to oxidize the product. Then, the aqueous solution was treated with activated charcoal, heated to boil for 30 min. After filtration through celite, an orange color solution was obtained and concentrated until the total volume was approximately 5 mL. The concentrated solution was added dropwise to an aqueous solution of sodium hexafluorophosphate (1.41 g $NaPF_6$, 8.4 mmol). The solid was obtained by filtration and thoroughly washed with DI water and then ether, dried in vacuo, giving the final product as a yellow powder in 40% yield (1.88 g). Yellow plates of tetra-*tert*-butyl cobaltocenium for X-ray analysis could be obtained by diffusing diethyl ether into a concentrated solution in acetonitrile. **^{1}H NMR** (300 MHz, acetone-d_6): δ= 5.89, 5.79 (s, *Cp*, 6H), 1.40 (s, -C*H*$_3$, 36H). **^{13}C NMR** (75 MHz, acetone-d_6): δ= 78.92 (*Cp*), 32.27, 31.46 (-*C*(*C*H$_3$)$_3$). **HRMS** *m/z* calculated for $C_{26}H_{42}Co^+(M^+)$ 413.2613, found 413.2611.

3.6 References

1. Zhu, T.; Sha, Y.; Adabi, H.; Peng, X.; Cha, Y.; Dissanayake, D. M. M. M.; Smith, M.; Vannucci, A.; Mustain, W. E.; Tang, C., The First Synthesis of a Complete Set of Metallo-Cations Toward Redox- and Alkaline-Stable Metallo-Polyelectrolytes. *manuscript submitted* **2019**.

2. Hara, M., *Polyelectrolytes: science and technology*. CRC Press: 1992.

3. Pack, D. W.; Hoffman, A. S.; Pun, S.; Stayton, P. S., Design and development of polymers for gene delivery. *Nat. Rev. Drug Discov.* **2005,** *4* (7), 581.

4. Shin, D. W.; Guiver, M. D.; Lee, Y. M., Hydrocarbon-based polymer electrolyte membranes: importance of morphology on ion transport and membrane stability. *Chem. Rev.* **2017,** *117* (6), 4759-4805.

5. Whittell, G. R.; Hager, M. D.; Schubert, U. S.; Manners, I., Functional soft materials from metallopolymers and metallosupramolecular polymers. *Nat. Mater.* **2011,** *10* (3), 176.

6. Wojtecki, R. J.; Meador, M. A.; Rowan, S. J., Using the dynamic bond to access macroscopically responsive structurally dynamic polymers. *Nat. Mater.* **2011,** *10* (1), 14.

7. Beck, J. B.; Rowan, S. J., Multistimuli, multiresponsive metallo-supramolecular polymers. *J. Am. Chem. Soc.* **2003,** *125* (46), 13922-13923.

8. Zhu, T.; Xu, S.; Rahman, A.; Dogdibegovic, E.; Yang, P.; Pageni, P.; Kabir, M. P.; Zhou, X.-d.; Tang, C., Cationic Metallo-Polyelectrolytes for Robust Alkaline Anion-Exchange Membranes. *Angew. Chem. Int. Ed.* **2018,** *57* (9), 2388-2392.

9. Grubbs, R. B.; Grubbs, R. H., 50th Anniversary Perspective: Living Polymerization - Emphasizing the Molecule in Macromolecules. *Macromolecules* **2017,** *50* (18), 6979-6997.

10. Zhu, T.; Sha, Y.; Yan, J.; Pageni, P.; Rahman, M. A.; Yan, Y.; Tang, C., Metallo-polyelectrolytes as a class of ionic macromolecules for functional materials. *Nat. Commun.* **2018,** *9* (1), 4329.

11. Yan, Y.; Pageni, P.; Kabir, M. P.; Tang, C., Metallocenium Chemistry and Its Emerging Impact on Synthetic Macromolecular Chemistry. *Synlett* **2016,** *27* (07), 984-1005.

12. Chakraborty, S.; Newkome, G. R., Terpyridine-based metallosupramolecular constructs: tailored monomers to precise 2D-motifs and 3D-metallocages. *Chem. Soc. Rev.* **2018,** *47* (11), 3991-4016.

13. Wang, Y.; Astruc, D.; Abd-El-Aziz, A. S., Metallopolymers for advanced sustainable applications. *Chem. Soc. Rev.* **2019,** *48* (2), 558-636.

14. Gu, H.; Ciganda, R.; Castel, P.; Moya, S.; Hernandez, R.; Ruiz, J.; Astruc, D., Tetrablock metallopolymer electrochromes. *Angew. Chem. Int. Ed.* **2018,** *57* (8), 2204-2208.

15. Zhang, J.; Chen, Y. P.; Miller, K. P.; Ganewatta, M. S.; Bam, M.; Yan, Y.; Nagarkatti, M.; Decho, A. W.; Tang, C., Antimicrobial metallopolymers and their

bioconjugates with conventional antibiotics against multidrug-resistant bacteria. *J. Am. Chem. Soc.* **2014,** *136* (13), 4873-4876.

16. Wilkinson, G., The Preparation and Some Properties of the Cobalticinium Salts. *J. Am. Chem. Soc.* **1952,** *74* (23), 6148-6149.

17. Deck, P. A., Perfluoroaryl-substituted cyclopentadienyl complexes of transition metals. *Coord. Chem. Rev.* **2006,** *250* (9-10), 1032-1055.

18. Williams, R. A.; Tesh, K. F.; Hanusa, T. P., Encapsulated alkaline-earth metallocenes. Synthesis, solution behavior, and solid-state structures of bis (tetraisopropylcyclopentadienyl) calcium and-barium,[(C3H7) 4C5H] 2Ca and [(C3H7) 4C5H] 2Ba. *J. Am. Chem. Soc.* **1991,** *113* (13), 4843-4851.

19. Butenschön, H., Cyclopentadienylmetal complexes bearing pendant phosphorus, arsenic, and sulfur ligands. *Chem. Rev.* **2000,** *100* (4), 1527-1564.

20. Gassman, P. G.; Macomber, D. W.; Hershberger, J. W., Evaluation by ESCA of the electronic effect of methyl substitution on the cyclopentadienyl ligand. A study of titanocenes, zirconocenes, hafnocenes, and ferrocenes. *Organometallics* **1983,** *2* (10), 1470-1472.

21. Pudelski, J. K.; Foucher, D. A.; Honeyman, C. H.; Lough, A. J.; Manners, I.; Barlow, S.; O'Hare, D., Synthesis, Structures, and Properties of Strained, Silicon-Bridged [1] Ferrocenophanes with Methylated Cyclopentadienyl Rings. *Organometallics* **1995,** *14* (5), 2470-2479.

22. Rowland, T. G.; Sztáray, B. l.; Armentrout, P. B., Metal–Cyclopentadienyl Bond Energies in Metallocene Cations Measured Using Threshold Collision-Induced Dissociation Mass Spectrometry. *J. Phys. Chem. A* **2012,** *117* (6), 1299-1309.

23. Frunzke, J.; Lein, M.; Frenking, G., Structures, metal− ligand bond strength, and bonding analysis of Ferrocene derivatives with group-15 heteroligands Fe (H5-E5) 2 and Fecp (H5-E5)(E= N, P, as, Sb). A theoretical study. *Organometallics* **2002,** *21* (16), 3351-3359.

24. Kelly, C. H.; Lein, M., Choosing the right precursor for thermal decomposition solution-phase synthesis of iron nanoparticles: tunable dissociation energies of ferrocene derivatives. *Phys. Chem. Chem. Phys.* **2016,** *18* (47), 32448-32457.

25. Braga, D.; Scaccianoce, L.; Grepioni, F.; Draper, S. M., From order to disorder and return: remarkable molecular and crystal dynamics in solid [(C5H5) 2Co][PF6]. *Organometallics* **1996,** *15* (22), 4675-4677.

26. Herberhold, M.; Chenga, Y.-X.; Jinb, G.-X.; Milius, W., 1, 1'-Di (terf-butyl) metallocenium Cations. *Z. Naturforsch.* **2000,** *55 b*, 814-820.

27. Ren, L.; Hardy, C. G.; Tang, C., Synthesis and Solution Self-Assembly of Side-Chain Cobaltocenium-Containing Block Copolymers. *J. Am. Chem. Soc.* **2010,** *132* (26), 8874-8875.

28. Ren, L.; Zhang, J.; Bai, X.; Hardy, C. G.; Shimizu, K. D.; Tang, C., Preparation of cationic cobaltocenium polymers and block copolymers by "living" ring-opening metathesis polymerization. *Chem. Sci.* **2012,** *3* (2), 580-583.

29. Yan, Y.; Zhang, J.; Qiao, Y.; Tang, C., Facile Preparation of Cobaltocenium‐Containing Polyelectrolyte via Click Chemistry and RAFT Polymerization. *Macromol. Rapid Commun.* **2014,** *35* (2), 254-259.

30. Vanicek, S.; Kopacka, H.; Wurst, K.; Müller, T.; Schottenberger, H.; Bildstein, B., Chemoselective, Practical Synthesis of Cobaltocenium Carboxylic Acid Hexafluorophosphate. *Organometallics* **2014,** *33* (5), 1152-1156.

31. Ryan, M. F.; Richardson, D. E.; Lichtenberger, D. L.; Gruhn, N. E., Gas-phase ionization energetics, electron-transfer kinetics, and ion solvation thermochemistry of decamethylmetallocenes, chromocene, and cobaltocene. *Organometallics* **1994,** *13* (4), 1190-1199.

32. Sheridan, M. V.; Lam, K.; Geiger, W. E., An anodic method for covalent attachment of molecules to electrodes through an ethynyl linkage. *J. Am. Chem. Soc.* **2013,** *135* (8), 2939-2942.

33. Mede, T.; Jäger, M.; Schubert, U. S., "Chemistry-on-the-complex": functional Ru II polypyridyl-type sensitizers as divergent building blocks. *Chem. Soc. Rev.* **2018,** *47* (20), 7577-7627.

34. Geiger, W. E., Electroreduction of cobaltocene. Evidence for a metallocene anion. *J. Am. Chem. Soc.* **1974,** *96* (8), 2632-2634.

35. Mayer, U. F.; Charmant, J. P.; Rae, J.; Manners, I., Synthesis and Structures of Strained, Neutral [d7] and Cationic [d6] Hydrocarbon-Bridged [n] Cobaltocenophanes (n= 2, 3). *Organometallics* **2008,** *27* (7), 1524-1533.

36. Noor, F.; Wüstholz, A.; Kinscherf, R.; Metzler‐Nolte, N., A cobaltocenium‐peptide bioconjugate shows enhanced cellular uptake and directed nuclear delivery. *Angew. Chem. Int. Ed.* **2005,** *44* (16), 2429-2432.

37. Hugar, K. M.; Kostalik IV, H. A.; Coates, G. W., Imidazolium cations with exceptional alkaline stability: a systematic study of structure–stability relationships. *J. Am. Chem. Soc.* **2015,** *137* (27), 8730-8737.

38. Womble, C. T.; Kang, J.; Hugar, K. M.; Coates, G. W.; Bernhard, S.; Noonan, K. J., Rapid Analysis of Tetrakis (dialkylamino) phosphonium Stability in Alkaline Media. *Organometallics* **2017,** *36* (20), 4038-4046.

39. You, W.; Padgett, E.; MacMillan, S. N.; Muller, D. A.; Coates, G. W., Highly conductive and chemically stable alkaline anion exchange membranes via ROMP of trans-cyclooctene derivatives. *Proc. Natl. Acad. Sci. U.S.A.* **2019,** *116*, 9729-9734.

40. You, W.; Hugar, K. M.; Coates, G. W., Synthesis of Alkaline Anion Exchange Membranes with Chemically Stable Imidazolium Cations: Unexpected Cross-Linked Macrocycles from Ring-Fused ROMP Monomers. *Macromolecules* **2018,** *51* (8), 3212-3218.

41. Kwasny, M. T.; Zhu, L.; Hickner, M. A.; Tew, G. N., Thermodynamics of counterion release is critical for anion exchange membrane conductivity. *J. Am. Chem. Soc.* **2018,** *140* (25), 7961-7969.

42. Zha, Y.; Disabb-Miller, M. L.; Johnson, Z. D.; Hickner, M. A.; Tew, G. N., Metal-cation-based anion exchange membranes. *J. Am. Chem. Soc.* **2012,** *134* (10), 4493-4496.

43. Gu, S.; Wang, J.; Kaspar, R. B.; Fang, Q.; Zhang, B.; Coughlin, E. B.; Yan, Y., Permethyl Cobaltocenium (Cp* 2 Co+) as an Ultra-Stable Cation for Polymer Hydroxide-Exchange Membranes. *Sci. Rep.* **2015,** *5*, 11668.

44. Chen, N.; Zhu, H.; Chu, Y.; Li, R.; Liu, Y.; Wang, F., Cobaltocenium-containing polybenzimidazole polymers for alkaline anion exchange membrane applications. *Polym. Chem.* **2017,** *8* (8), 1381-1392.

45. Kwasny, M. T.; Zhu, L.; Hickner, M. A.; Tew, G. N., Utilizing thiol‐ene chemistry for crosslinked nickel cation‐based anion exchange membranes. *J. Polym. Sci., Part A: Polym. Chem.* **2018,** *56* (3), 328-339.

46. Noonan, K. J. T.; Hugar, K. M.; Kostalik, H. A.; Lobkovsky, E. B.; Abruña, H. D.; Coates, G. W., Phosphonium-Functionalized Polyethylene: A New Class of Base-Stable Alkaline Anion Exchange Membranes. *J. Am. Chem. Soc.* **2012,** *134* (44), 18161-18164.

47. Tsai, T.-H., Ionic Copolymers for Alkaline Anion Exchange Membrane Fuel Cells (AAEMFCs). *Doctoral Dissertations* **2014**.

48. Marino, M.; Kreuer, K., Alkaline stability of quaternary ammonium cations for alkaline fuel cell membranes and ionic liquids. *ChemSusChem* **2015,** *8* (3), 513-523.

49. Mohanty, A. D.; Bae, C., Mechanistic analysis of ammonium cation stability for alkaline exchange membrane fuel cells. *J. Mater. Chem. A* **2014,** *2* (41), 17314-17320.

50. Zhang, J.; Pellechia, P. J.; Hayat, J.; Hardy, C. G.; Tang, C., Quantitative and Qualitative Counterion Exchange in Cationic Metallocene Polyelectrolytes. *Macromolecules* **2013,** *46* (4), 1618-1624.

51. Vanicek, S.; Kopacka, H.; Wurst, K.; Müller, T.; Schottenberger, H.; Bildstein, B., Chemoselective, Practical Synthesis of Cobaltocenium Carboxylic Acid Hexafluorophosphate. *Organometallics* **2014,** *33* (5), 1152-1156.

52. McKnight, A. L.; Waymouth, R. M., Ethylene/norbornene copolymerizations with titanium CpA catalysts. *Macromolecules* **1999,** *32* (9), 2816-2825.

53. Laurenson, J. A.; Parkinson, J. A.; Percy, J. M.; Rinaudo, G.; Roig, R., Multigramme synthesis and asymmetric dihydroxylation of a 4-fluorobut-2E-enoate. *Beilstein J. Org. Chem.* **2013,** *9* (1), 2660-2668.

54. Fendrick, C. M.; Schertz, L. D.; Mintz, E. A.; Marks, T. J.; Bitterwolf, T.; Horine, P.; Hubler, T.; Sheldon, J.; Belin, D., Large‐Scale Synthesis of 1, 2, 3, 4, 5‐Penta‐Methylcyclopentadiene. *Inorg. Synth.* **1992**, 193-198.

55. Mironov, V.; Sobolev, E.; Elizarova, A. N., Some general characteristic properties of substituted cyclopentadienes. *Tetrahedron* **1963,** *19* (12), 1939-1958.

56. Pudelski, J. K.; Callstrom, M. R., Structure, reactivity, and electronic properties of [4] ferrocenophanes and [4] ruthenocenophanes prepared via a novel heteroannular cyclization reaction. *Organometallics* **1994,** *13* (8), 3095-3109.

57. Paradies, J.; Kehr, G.; Fröhlich, R.; Erker, G., Ansa-metallocene polymerization catalysts derived from [2+ 2] cycloaddition reactions of bis (1-methylethenyl-cyclopentadienyl) zirconium systems. *Proc. Natl. Acad. Sci. U.S.A.* **2006,** *103* (42), 15333-15337.

58. Dehmlow, E. V.; Bollmann, C., Verbesserte präparative Darstellung von Polyisopropyl-und Poly-tert-butylcyclopentadienen/Improved Preparation of Polyisopropyl-and-tert-butylcyclopentadienes. *Zeitschrift für Naturforschung B* **1993,** *48* (4), 457-460.

CHAPTER 4

REDOX- AND ALKALINE-STABLE METALLO-POLYELECTROLYTES FOR ENERGY STORAGE DEVICES [1]

[1] Zhu, T.; Sha, Y.; Adabi, H.; Peng, X.; Cha, Y.; Dissanayake, D. M. M. M.; Smith, M. D.; Vannucci, A. K.; Mustain, W. E.; Tang, C., The First Synthesis of a Complete Set of Metallo-Cations Toward Redox- and Alkaline-Stable Metallo-Polyelectrolytes. *Manuscript submitted*, **2019.**

4.1 Abstract

Mechanically strong, ionically conductive, and chemically stable polyelectrolytes are of paramount importance to energy storage devices. Herein, we report a class of metallo-polyelectrolyte membranes with octamethyl cobaltocenium cation and polyethylene backbone for alkaline anion-exchange membrane fuel cells. We show that the new metallo-polyelectrolyte membrane exhibits superior properties in ionic conductivity, mechanical flexibility as well as alkaline and redox stability. The device performance of these polyelectrolytes under highly basic and oxidative environments is competitive with many organo-polyelectrolytes.

4.2 Introduction

Fuel cells are of one clean power sources that converts chemical energy into electricity with high efficiency.[2] Alkaline anion-exchange exchange membrane fuel cells (AEMFCs) have been highly touted for practical use because of the potential use of non-precious metal catalysts for the oxygen reduction reaction (ORR) and better tolerance towards carbon dioxide.[3] However, lacking advanced alkaline anion-exchange membranes (AEMs) with robust mechanical properties, excellent alkaline- and redox- stability, as well as high ionic conductivity is the major challenge to the realization of high-performance and durable AEMFCs.

Over the past years, considerable efforts have been made to develop alkaline-stable cations and highly-conductive polyelectrolyte membranes.[4] However, traditional quaternary ammonium cations are found to degrade rapidly under highly basic conditions due to Hofmann elimination and nucleophilic substitution reactions, as well as the formation of Ylide or other chemical rearrangements.[4] Thus, many other organic cations

have been investigated to address the issue of poor chemical stability in alkaline media, especially over long-term and elevated temperatures. Recently, Yan and Li reported piperidinium based AEMs as promising materials to address the alkaline stability problem.[5-6] Coates and Steven designed highly conductive and chemically stable AEMs with multi-substituted imidazolium cations.[7-8] On the other hand, the advance in organometallic chemistry also enables many metallo-cations and metallo-polyelectrolytes as a promising solution to this issue.[9-10] Till now, there are mainly two types of metal-containing cations reported for polyelectrolyte membranes: (1) cationic metallocenes (or metallocenium cations), which contain covalent bonds between metal cations and cyclopentadienyl (Cp); (2) coordination metal complexes, which utilize coordination interactions between terpyridine ligands and metal cations.[11-16] However, none of them have been applied at device level, largely due to synthetic difficulty and inferior property.

In this work, we report the preparation of robust metallo-polyelectrolyte AEMs based on alkaline and redox-stable octamethyl cobaltocenium cation. These membranes exhibited excellent mechanical property, alkaline stability, and ionic conductivity. The electrochemical performance of these metal-containing AEMs was also characterized in alkaline anion-exchange membrane fuel cells, which demonstrated the great potential of a family of metallo-polyelectrolytes to be explored in this area.

4.3 Results and Discussion

Given the successful synthesis and understanding of physiochemical properties of cobaltocenium derivatives (Chapter 3), we intended to design a class of polyelectrolytes with cobaltocenium as cations and further correlate macromolecular properties with redox and chemical stability of cations. Cobaltocenium-containing polyelectrolytes have been

utilized as AEMs that show a good alkaline stability under inert atmosphere and reasonable ionic conductivity, which could be useful for fabricating electrochemical devices, such as AEMFCs.[4, 17] Because of the excellent stability of the substituted cobaltocenium cations in alkaline and oxidative atmosphere, we believe that they could be applied in constructing solid polyelectrolytes that would be much more stable than traditional organic polyelectrolytes.[5-6, 8, 17-18]

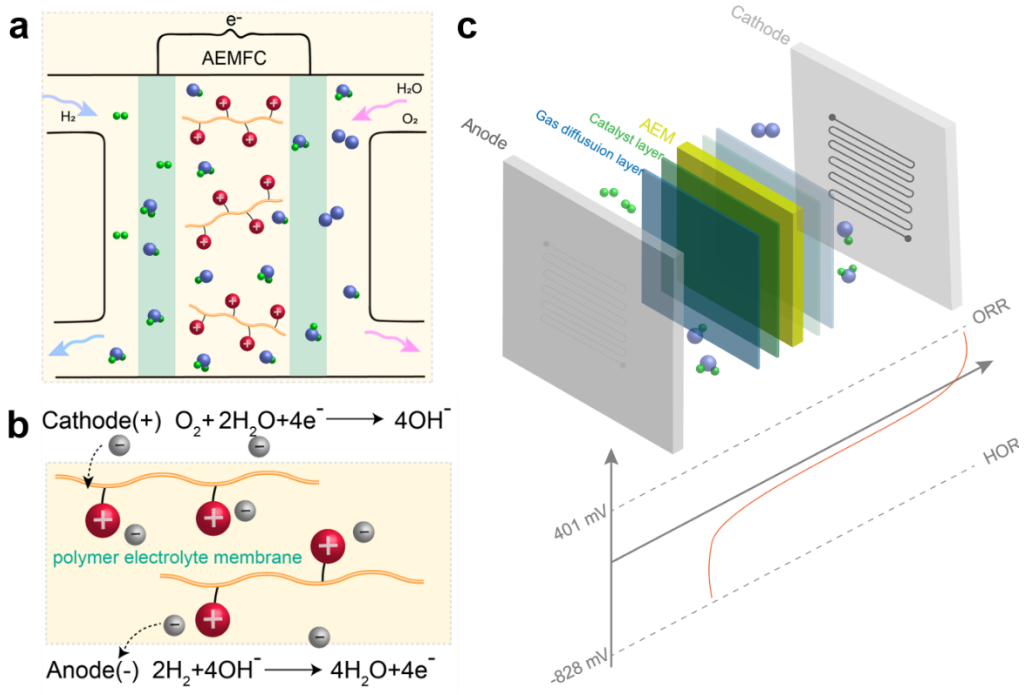

Figure 4.1. Schematic illustration of **a.** an AEMFC device; **b.** ion transport, ORR and HOR reactions in an AEMFC; **c.** the voltage changes in an AEMFC.

However, it is important that the redox potential of the cation is outside the operating voltage window of fuel cell devices. In AEMFCs, the hydrogen oxidation reaction (HOR) potential at the anode is -828 mV (*vs.* SHE for all potentials mentioned here), and oxygen reduction reaction (ORR) potential at the cathode is 401 mV. Thus, a cation has to be redox stable over these wide operation potentials, which would preclude many redox-active cations (**Figure 4.1**).[17] For example, unsubstituted cobaltocenium can

be reduced to neutral cobaltocene complex at HOR relevant potentials. Despite the fact that it is thermodynamically more stable, tetra-*tert*-butyl cobaltocenium was not chosen due to its redox potential overlapping with the HOR. On the other hand, alkyl substituents were chosen rather than other functional groups because heteroatoms are more vulnerable for side reactions under oxidative and alkaline conditions. Based on the redox properties observed in our CV studies, octamethyl cobaltocenium is redox stable over the entire potential range for operating AEMFCs and provides a larger operating window compared to other cations. Besides, octamethyl cobaltocenium also exhibits high alkaline stability. Thus, it was chosen to construct polyelectrolytes as AEMs (labeled as omccAEM).

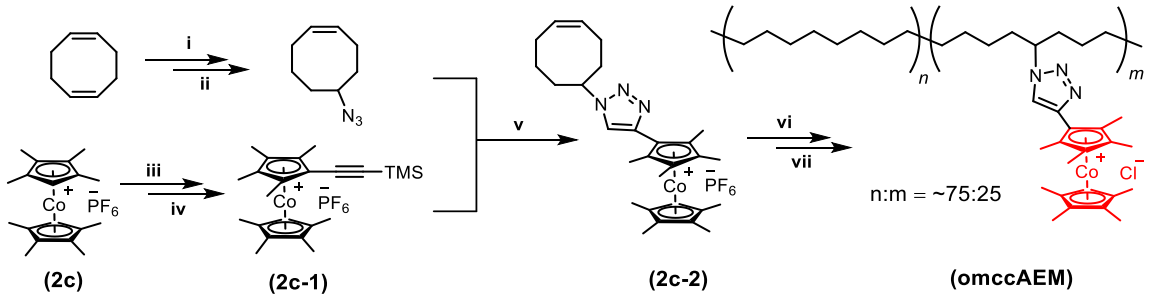

Figure 4.2. Synthesis of octamethyl cobaltocenium polyelectrolytes as AEMs. (synthesis details. **i**: HBr/HAc; **ii**: NaN_3, DMF, 70 ˚C; **iii**: ethynyltrimethylsilane, *n*-BuLi, THF; **iv**: triphenylcarbenium hexafluorophosphate, DCM; **v**: $CuSO_4$, Na ascorbate, THF/H_2O; **vi**: Grubbs III catalyst, DMAc/xylenes, *p*-toluenesulfonyl hydrazide, Bu_3N; **vii**: aqueous NH_4Cl, ion-exchange resin, 60 ˚C)

As shown in **Figure 4.2**, octamethyl cobaltocenium cyclooctene monomer (**2c-2**) was firstly prepared by a copper-catalyzed click reaction between 5-azidocyclooct-1-ene and ethynyl octamethyl cobaltocenium hexafluorophosphate (**2c-1**). Then, metallo-polyelectrolytes were prepared by ring-opening metathesis polymerization (ROMP) of monomer (**2c-2**) with *cis*-cyclooctene as a co-monomer, followed by backbone

hydrogenation and ion exchange. The monomer and copolymers with hexafluorophosphate counterion were characterized by ^{1}H NMR spectroscopy (**Figure 4.3**).

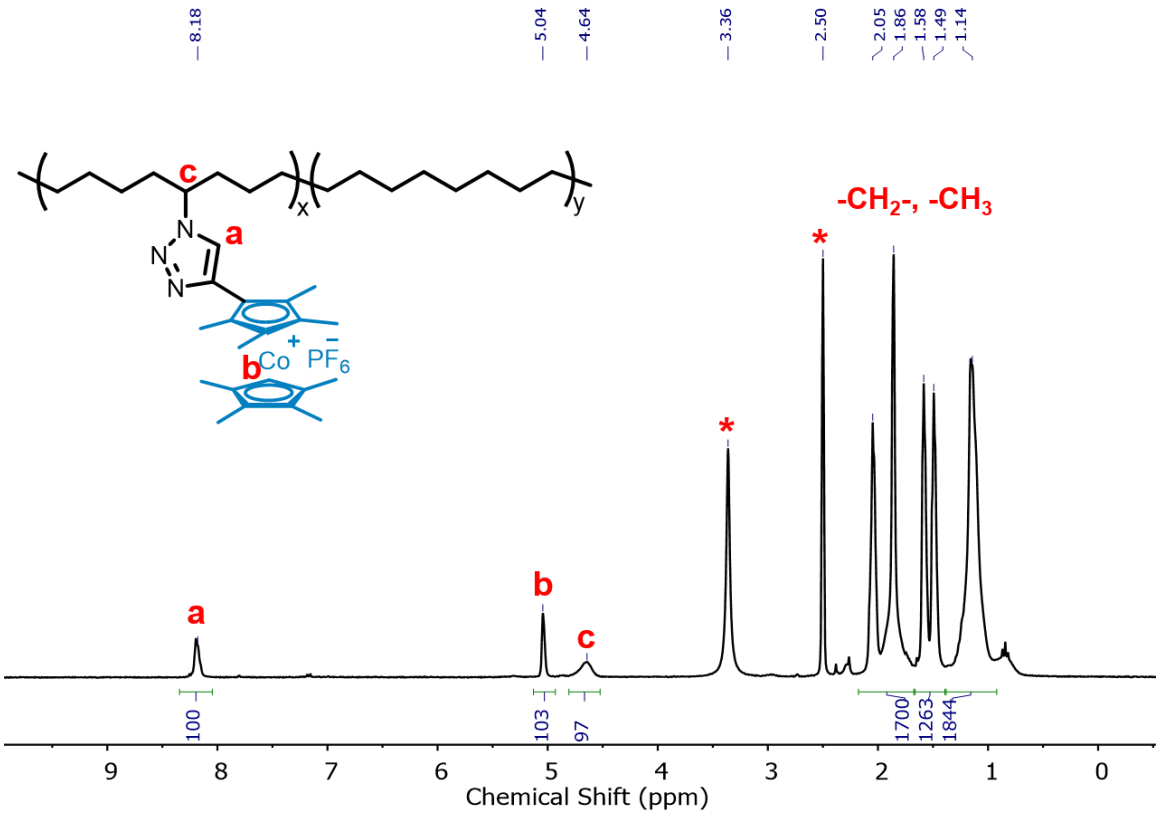

Figure 4.3. ^{1}H NMR spectrum of hydrogenated octamethyl cobaltocenium polymer in DMSO-d_6.

As shown in **Figure 4.4 a**, these metallo-polyelectrolyte membranes exhibit robust mechanical properties, probably due to the presence of a flexible polyethylene-like backbone with a tunable side chain composition. For example, omccAEM has a tensile strain of 390 % and a tensile stress of 21 MPa at 100% RH under ambient temperature. With such excellent mechanical properties, it would allow to make membranes very thin, e.g. ~40 μm thick, which is desirable for facilitating the water back-diffusion and supporting a high current density in a fuel cell.[5, 19-21]

Wide-angle X-ray diffraction (WAXD) was used to probe crystallization behavior of omccAEM. The crystalline and amorphous peaks were deconvoluted *via* peak fitting (**Figure 4.4 b**). Two sharp crystalline peaks at $2\theta \sim 21.4^{\circ}$ and 23.7° correspond to polyethylene backbones.[22] Atomic force microscopy (AFM) and small-angle X-ray scattering (SAXS) were used to correlate the chemical structures and morphology for multi-substituted cobaltocenium based AEMs (**Figure 4.4 c**). The dark regions in AFM phase image represent the soft matrix from hydrophobic polyethylene backbone, whereas the brighter ones represent hard domains from hydrophilic metal-containing side-chains. The SAXS pattern for omccAEM (with chloride counterions) shows a broad scattering peak around $q^* = 1.01$ nm^{-1} with a *d*-spacing ($2\pi/q^*$) of 6.2 nm.[23] Moreover, distinct microphase separation between hydrophilic and hydrophobic domains was observed by both atomic force microscopy (AFM) and small-angle X-ray scattering (SAXS). Such phase-separated morphology is critical to facilitate ion-transport by forming connected ion-transport channels in polyelectrolyte membranes.[9, 15, 24]

Water management properties also pay a critical role in fuel cell performance.[21, 25] AEMs are expected to facilitate sufficient water back diffusion from anode to cathode to support oxygen reduction reaction, however, taking excess of water also results in membranes to be dimensionally unstable over long-term. **Figure 4.4 d** shows the water uptake and swelling ratio of omccAEM membrane in DI water at different temperature. Due to the hydrophobic nature of polyethylene backbone, omccAEM membrane exhibited relatively low water uptake (<50%) and swelling ratio (<10%) from room temperature to elevated temperature, which allows the membrane to be dimensionally stable in an AEMFC.

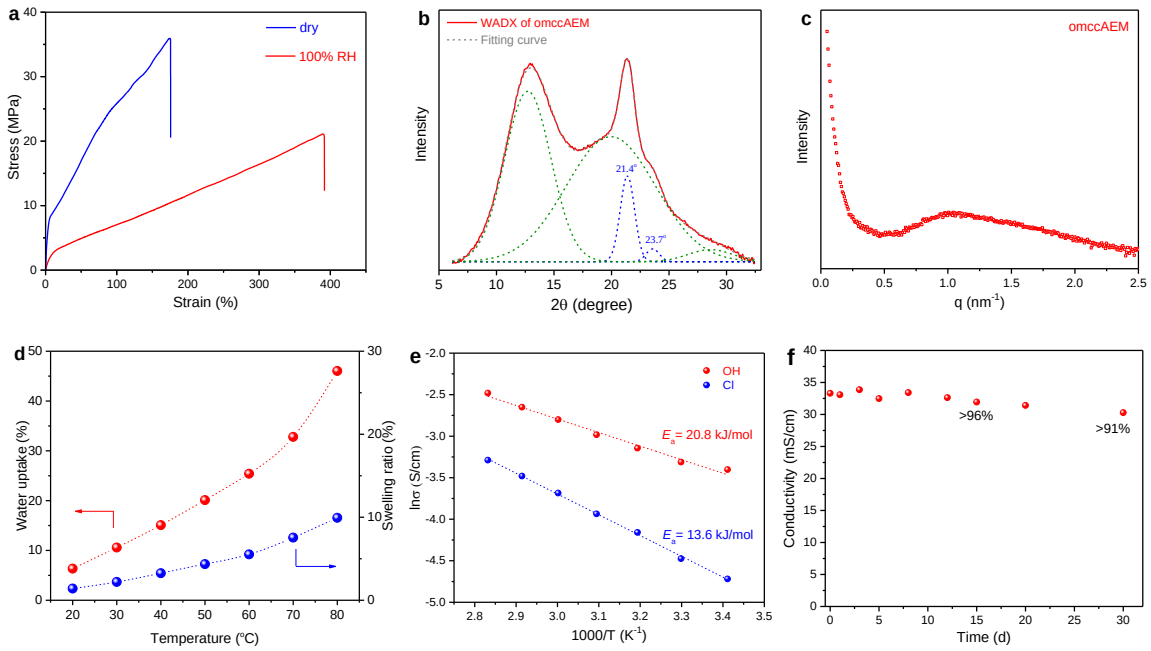

Figure 4.4. a. Stress-strain curves of omccAEM membrane in a dry state and a hydrated condition; **b.** WADX pattern of omccAEM membrane (red line: experimental data; grey line: fitting sum curve; green and blue lines: fitting multi-peaks, where blue line is considered as a crystalline peak); **c.** SAXS profile of omccAEM membrane; **d.** water uptake and swelling ratio for omccAEM membrane at different temperature; **e.** Arrhenius plots for conductivity of omccAEM with chloride and hydroxide as a function of temperature under fully hydrated conditions; **f.** room temperature conductivity as a function of immersion time of omccAEM in 3M KOH aqueous solution at 60 ˚C.

The temperature-dependent ionic conductivity of omccAEM with hydroxide and chloride counterions was measured under fully hydrated conditions. Membranes with chloride and hydroxide counterions showed increased conductivity at elevated temperature, which can be rationalized by faster ion migration and higher water uptake. The hydroxide conductivity is 33.3 and 83.7 mS/cm at room temperature and 80 ˚C, respectively. The ionic conductivity also followed an Arrhenius relationship as shown in **Figure 4.4 e**. The activation energy (E_a) for hydroxide and chloride transport was calculated to be 20.8 and 13.6 kJ/mol, which was comparable to the results with similar polymeric architectures.[7, 15] Moreover, polyethylene is well known for its high resistance towards base and oxidants, because it is composed with only chemically inert carbon-

carbon bonds. Earlier work on organo-polyelectrolytes with polyethylene backbone exhibited exceptional stability under basic conditions.[7, 15, 26-27] It should be noted that the omccAEM with inert polyethylene backbone and a highly stable cobaltocenium cation also preserved the hydroxide conductivity (91% retention) after testing in a 3 M KOH solution at 60 ˚C for 30 days under open air (**Figure 4.4 f**).

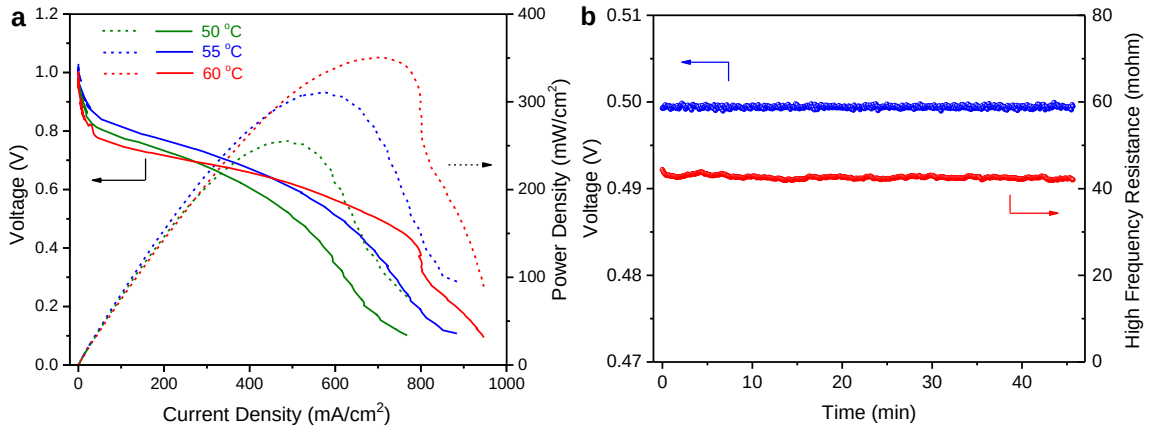

Figure 4.5. a. Polarization curves and power densities for omccAEM in a H_2/O_2 fuel cell (Anode: 0.8 mg PtRu/C cm^{-2}, Cathode: 0.49 mg Pt/C cm^{-2} on 5% PTFE GDL); **b.** high frequency resistance curves for omccAEM in a H_2/O_2 fuel cell under constant voltage at 55 ˚C.

The electrochemical performance of the omccAEM was investigated in an AEMFC operating with H_2 and O_2 reacting gases. **Figure 4.5** show the high frequency resistance (HFR) and device performance at several temperature, respectively. To the best of our knowledge, this is the first test of metallo-polyelectrolytes at a device level. In **Figure 4.5 a**, the polarization curves and power density curves show that the performance of the cell improved as the temperature increased. A maximum peak power density of 350 mW cm^{-2} was achieved with the metallo-polyelectrolyte membrane fuel cell, which is comparable to a variety of AEMs with organic cations reported recently.[6, 8, 19, 28-30] This is very promising and it is likely that refinement in the structure of metallo-polyelectrolyte membranes will

allow further increases in ionic conductivity and water transport properties and even higher fuel cell performance.

4.4 Conclusions

In summary, a class of mechanically robust, ionically conductive and chemically stable metallo-polyelectrolyte membrane has been successfully synthesized by ring opening-metathesis polymerization with sequential backbone hydrogenation. The resulting polyelectrolyte membranes contain semicrystalline polyethylene backbone and highly stable metallo-cation. The electrochemical evaluations by AEMFCs confirm that these metallo-polyelectrolytes yield comparable performance with organo-polyelectrolytes. We are actively working on modifying the macromolecular scaffolds to afford greater enhancements in membrane properties for energy storage, and the results of these efforts will be presented in due course.

4.5 Experimental Details

Materials

N,*N*-dimethylacetamide, *n*-butyllithium solution (2.5 M in hexanes), sodium hexafluorophosphate, 1,2,3,4-tetramethyl-1,3-cyclopentadiene (~85%), *cis*-cyclooctene, Grubbs catalyst 3rd generation, *p*-toluenesulfonic anhydride and methanol-d_3 were purchased from Sigma-Aldrich and used as received. Cobalt(II) bromide (anhydrous) was purchased from Beantown Chemical. Acetonitrile, hexane, methanol, dichloromethane, tetrahydrofuran, xylenes, tributylamine, anhydrous copper(II) sulfate, sodium ascorbate and acetone were purchased from VWR. Chloroform-*d*, acetone-d_6, acetonitrile-d_3, and dimethyl sulfoxide DMSO-d_6 were purchased from Cambridge Isotope Laboratories. 5-

Bromocyclooct-1-ene and 5-azidocyclooct-1-ene were synthesized according to our early work.[15] Ion exchange procedures to prepare small molecules and polyelectrolytes with hydrophilic counterions (Cl^- and OH^-) followed our early work.[15, 31]

Characterization

^1H NMR (300 MHz) and ^{13}C NMR (75 MHz) spectra were recorded on a Varian Mercury 300 spectrometer using chloroform-d_3 ($CDCl_3$), or dimethyl sulfoxide(DMSO-d_6) as solvents. All chemical shifts in ^1H and ^{13}C NMR were compared to deuterated solvents or tetramethylsilane (TMS) as a reference. High-resolution mass spectra (HRMS) and ESI mass spectra (MS) were collected at the University of South Carolina mass spectrometry center.

Wide angle X-ray diffraction (WAXD) and small angle X-ray diffraction (SAXS) experiments were conducted using a SAXSLab Ganesha at the South Carolina SAXS Collaborative. A Xenocs GeniX3D microfocus source was used with a Cu target to generate a monochromic beam with a wavelength of 0.154 nm. The instrument was calibrated using National Institute of Standards and Technology (NIST) reference material 640c silicon powder with the peak position at 2θ of 28.44°. A Pilatus 300 K detector (Dectris) was used to collect the two-dimensional (2D) scattering patterns. The 2D images were azimuthally integrated to yield the scattering vector and intensity with SAXSGUI software. The conversion of the resulting intensity versus q data was converted to 2θ using the formula $q=4\pi\lambda^{-1}\sin\theta$, where λ is the X-ray wavelength and 2θ is the total scattering angle.

Water uptake and swelling behavior of membranes were measured from 20 to 80 ˚C. Dry membranes with chloride counterion were firstly weighed to obtain the dry weight (m_{dry}) and dry length (X_{dry}). Then, these membranes were immersed in a water bath at different temperature for 10 min. The samples were wiped dry with paper towel and quickly measured the wet weight (m_{wet}) and the wet length (X_{wet}) at certain temperature. The water uptake and swelling ratio were calculated according to the equations:

$$\text{water uptake} = \frac{m_{wet} - m_{dry}}{m_{dry}} \times 100\%$$

$$\text{swelling ratio} = \frac{X_{wet} - X_{dry}}{X_{dry}} \times 100\%$$

Mechanical properties of anion-exchange membranes (AEMs) were characterized with an Instron 5543A testing instrument. Membranes with chloride counterion were dried under vacuum or pre-wetted under 100% RH for 24 hours before the measurements. Dog-bone shaped specimens were cut from membranes with a length of 20 mm, a width of 5 mm, and a thickness of ~40 μm. All the samples were tested with a crosshead speed of 20 mm/min.

The ionic conductivity of AEMs was measured by a four-probe method in DI water under various temperature using TrueData-EIS (Fuel Con) RE232 potentiostat. Membranes in a chloride or hydroxide form (3 cm × 0.5 cm) were thoroughly washed with DI water and immersed in DI water under nitrogen for 1h before the test. The impedance was measured from 200 μHz to 50 kHz, providing the total resistance of the membrane R (Ω) under different conditions. The conductivity was calculated based on geometry and total resistance according to the following equation, in which L (cm) refers to the distance

between two current carrying electrodes and A (cm^2) means the cross-section area of the membrane between electrodes.

$$\sigma = \frac{L}{RA}$$

Temperature-dependent conductivity of membranes in a chloride or hydroxide form was measured with multiple samples and by heating and cooling DI water media for several cycles (20 to 80 ˚C). For the long-term stability test, the samples were stored in a 3M KOH solution at 60 ˚C under air over time. Before the conductivity test, these samples were cooled to room temperature and thoroughly washed with DI water. The KOH solution was replaced with fresh one after each measurement.

Gas diffusion electrode (GDE) fabrication, membrane-electrode assembly (MEA) and AEM fuel cell (AEMFC) testing: Prior to the formulation of a catalyst ink, an ETFE-g-poly (VBTMAC) powder ionomer was first grounded with a well-cleaned mortar and pestle for 5 min to reduce the number of aggregated particles.[21] Next, metal catalyst and 1.0 mL of DI water were added to the grounded ionomer and grounded for an additional 10 min until a visually homogeneous catalyst slurry was formed. The ETFE powder mass comprised of 20% of the total solid mass of all GDEs. After the slurry was homogenized, 1.5 mL of isopropanol was added into the mortar followed by another 10 min grinding. A final 5 mL of isopropanol was added to the mortar and the final ink mixture was transferred to a PTFE-lined vial and sonicated for 1 hour in an ice bath. The prepared ink was then sprayed onto the gas diffusion layer (GDL) (Toary 60) using an air-assisted sprayer (Iwata) to fabricate GDEs. 40% Pt on Vulcan carbon (Alfa Aesar HiSPEC 4000, Pt nominally 40% wt., supported on Vulcan XC-72R carbon) and Pt-Ru catalyst (Alfa Aesar HiSPEC 10000,

Pt nominally 40% wt., and Ru, nominally 20% wt., supported on Vulcan XC-72R carbon) were used as electrocatalysts for cathode and anode, respectively. Both the anode and cathode GDEs, and membrane were hydrated in DI water for 20 min and then soaked three times in 1.0 M KOH to remove impurities and ion exchange the cationic groups before cell assembly. AEMFCs with 5 cm^2 active area were assembled in a single cell hardware with a single channel serpentine flow field. The average thickness of anode and cathode were measured to be 203 and 205 μm, respectively. Thus, 152 μm Teflon gaskets were used on anode and cathode, respectively, to keep the pinch around 25% of the total GDE thickness. The AEMFCs were tested on a Scribner 850e fuel cell test station under a flow rate of H_2/O_2 at 1.0 L/min. The temperature of the heated gas follow lines between the fuel cell test stand and the cell were maintained at 5°C above the respective gas dew points. The cell was pre-operated at a voltage of 0.5 V for break-in and the relative humidity (RH) of both the cathode and anode was adjusted to help the cell to be operated at optimal conditions. Polarization curves were collected under the potentiometric control at a scan rate of 10 mV/s.

Synthetic procedures

Octamethyl cobaltocenium copolymer (2c-3)

Octamethyl cobaltocenium-containing copolymers were synthesized by ring-opening metathesis polymerization (ROMP). Monomer (**2c-2**) (250 mg, 0.41 mmol) and cyclooctene (133.0 mg, 1.21 mmol) were dissolved in 2 mL solvent of dimethylacetamide (DMAc) and xylene (1:1 by volume) and purged with nitrogen for 20 min. The reaction temperature was slowly increased to 65 ºC, and then 2 mg Grubbs III catalyst in 0.2 mL

DMAc was added into the reaction mixture. The reaction was stirred under this temperature for 3 h and then quenched with 0.5 mL ethyl vinyl ether (EVE). The copolymer (**2c-3**) was obtained by precipitation three times in cold methanol and dried overnight under vacuum (yield: 90%). **^{1}H NMR** (300 MHz, DMSO-d_6): δ= 8.66 (s, -C*H*- in triazole, 1H), 5.17~5.52 (broad, -C*H*=C*H*- in backbone), 4.96 (s, *Cp*, 1H), 4.50~4.77 (broad, -C*H*- in cyclooctene, 1H), 1.05~2.24 (m, -CH_2- in backbone, -CH_3 in octamethyl cobaltocenium cations).

Hydrogenated octamethyl cobaltocenium copolymer (2c-4)

A flask loaded with copolymer (**2c-3**) (300 mg) and 12 mL of DMAc/xylene (1:1 by volume) was purged nitrogen for 20 min under room temperature. Then, *p*-toluenesulfonyl hydrazide (4.0 equiv. per double bond) and tributylamine (5.0 equiv. per double bond) were added into the reaction solution. The reaction mixture was heated to 100 ºC and stirred overnight. The clear yellow solution was cooled to room temperature and precipitated into cold diethyl ether. Then, the yellow fiber-like polymer (**2c-4**) was washed three times with methanol and dried overnight under vacuum (yield 97%). **^{1}H NMR** (300 MHz, DMSO-d_6): δ= 8.18 (s, -C*H*- in triazole, 1H), 5.04 (s, *Cp*, 1H), 4.53~4.80 (broad, -C*H*- in cyclooctene, 1H), 0.96~2.14 (-CH_2- in backbone, -CH_3 in octa-methyl cobaltocenium cations).

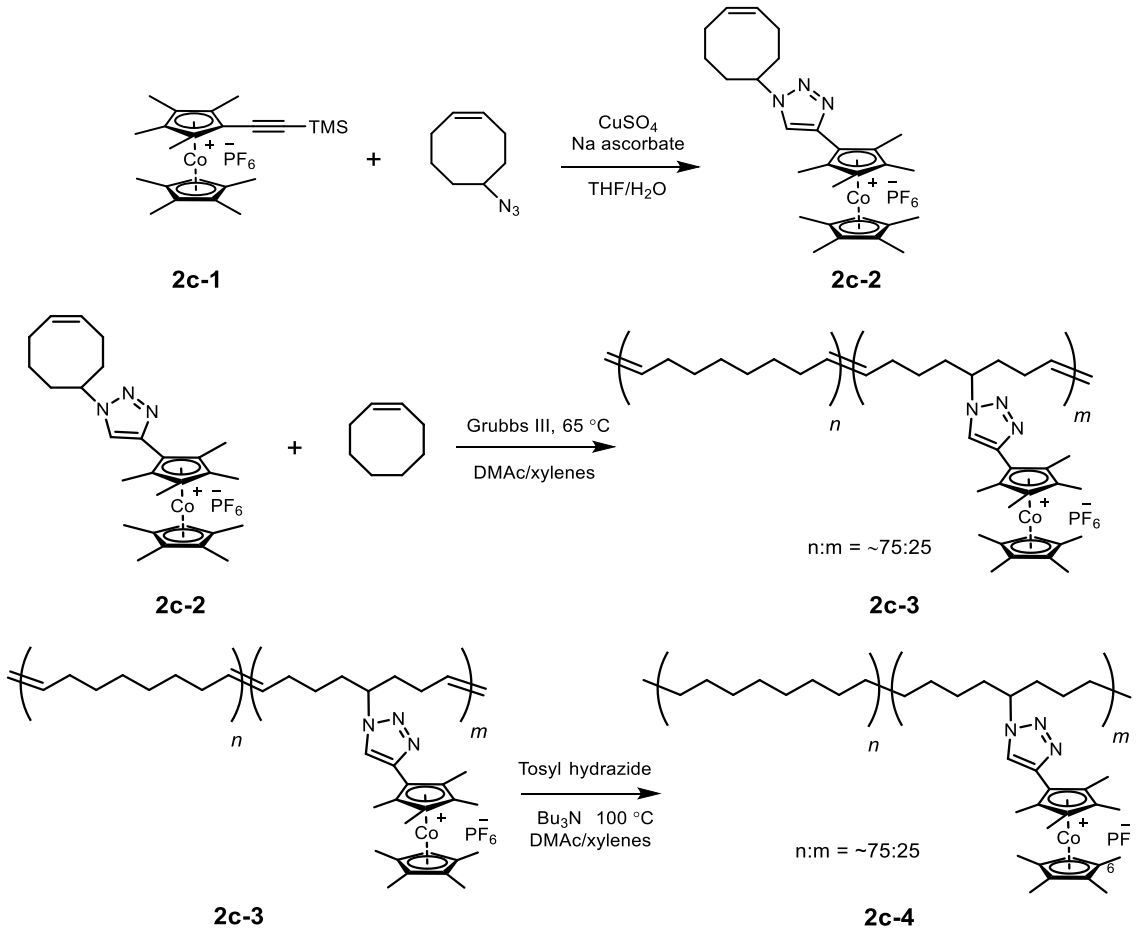

Figure 4.6. Synthesis of octamethyl cobaltocenium AEMs.

4.6 References

1. Zhu, T.; Sha, Y.; Adabi, H.; Peng, X.; Cha, Y.; Dissanayake, D. M. M. M.; Smith, M.; Vannucci, A.; Mustain, W. E.; Tang, C., The First Synthesis of a Complete Set of Metallo-Cations Toward Redox- and Alkaline-Stable Metallo-Polyelectrolytes. *Manuscript submitted* **2019**.

2. Larminie, J.; Dicks, A.; McDonald, M. S., *Fuel cell systems explained*. J. Wiley Chichester, UK: 2003; Vol. 2.

3. Varcoe, J. R.; Slade, R. C., Prospects for alkaline anion‐exchange membranes in low temperature fuel cells. *Fuel Cells* **2005,** *5* (2), 187-200.

4. Couture, G.; Alaaeddine, A.; Boschet, F.; Ameduri, B., Polymeric materials as anion-exchange membranes for alkaline fuel cells. *Prog. Polym. Sci.* **2011,** *36* (11), 1521-1557.

5. Wang, J.; Zhao, Y.; Setzler, B. P.; Rojas-Carbonell, S.; Yehuda, C. B.; Amel, A.; Page, M.; Wang, L.; Hu, K.; Shi, L., Poly (aryl piperidinium) membranes and ionomers for hydroxide exchange membrane fuel cells. *Nat. Energy* **2019,** *4*, 392–398.

6. Chu, X.; Shi, Y.; Liu, L.; Huang, Y.; Li, N., Piperidinium-functionalized Anion Exchange Membranes and its application in Alkaline Fuel Cell and Water Electrolysis. *J. Mater. Chem. A* **2019,** *7*, 7717-7727.

7. You, W.; Padgett, E.; MacMillan, S. N.; Muller, D. A.; Coates, G. W., Highly conductive and chemically stable alkaline anion exchange membranes via ROMP of trans-cyclooctene derivatives. *Proc. Natl. Acad. Sci. U.S.A.* **2019,** *116*, 9729-9734.

8. Fan, J.; Willdorf-Cohen, S.; Schibli, E. M.; Paula, Z.; Li, W.; Skalski, T. J. G.; Sergeenko, A. T.; Hohenadel, A.; Frisken, B. J.; Magliocca, E.; Mustain, W. E.; Diesendruck, C. E.; Dekel, D. R.; Holdcroft, S., Poly(bis-arylimidazoliums) possessing high hydroxide ion exchange capacity and high alkaline stability. *Nat. Commun.* **2019,** *10* (1), 2306.

9. Zhu, T.; Sha, Y.; Yan, J.; Pageni, P.; Rahman, M. A.; Yan, Y.; Tang, C., Metallo-polyelectrolytes as a class of ionic macromolecules for functional materials. *Nat. Commun.* **2018,** *9* (1), 4329.

10. Wang, Y.; Astruc, D.; Abd-El-Aziz, A. S., Metallopolymers for advanced sustainable applications. *Chem. Soc. Rev.* **2019,** *48* (2), 558-636.

11. Kwasny, M. T.; Zhu, L.; Hickner, M. A.; Tew, G. N., Thermodynamics of counterion release is critical for anion exchange membrane conductivity. *J. Am. Chem. Soc.* **2018,** *140* (25), 7961-7969.

12. Zha, Y.; Disabb-Miller, M. L.; Johnson, Z. D.; Hickner, M. A.; Tew, G. N., Metal-cation-based anion exchange membranes. *J. Am. Chem. Soc.* **2012,** *134* (10), 4493-4496.

13. Gu, S.; Wang, J.; Kaspar, R. B.; Fang, Q.; Zhang, B.; Coughlin, E. B.; Yan, Y., Permethyl Cobaltocenium (Cp* 2 Co+) as an Ultra-Stable Cation for Polymer Hydroxide-Exchange Membranes. *Sci. Rep.* **2015,** *5*, 11668.

14. Chen, N.; Zhu, H.; Chu, Y.; Li, R.; Liu, Y.; Wang, F., Cobaltocenium-containing polybenzimidazole polymers for alkaline anion exchange membrane applications. *Poly. Chem.* **2017,** *8* (8), 1381-1392.

15. Zhu, T.; Xu, S.; Rahman, A.; Dogdibegovic, E.; Yang, P.; Pageni, P.; Kabir, M. P.; Zhou, X.-d.; Tang, C., Cationic Metallo-Polyelectrolytes for Robust Alkaline Anion-Exchange Membranes. *Angew. Chem. Int. Ed.* **2018,** *57* (9), 2388-2392.

16. Kwasny, M. T.; Zhu, L.; Hickner, M. A.; Tew, G. N., Utilizing thiol ‐ ene chemistry for crosslinked nickel cation ‐ based anion exchange membranes. *J. Polym. Sci. A* **2018,** *56* (3), 328-339.

17. Varcoe, J. R.; Atanassov, P.; Dekel, D. R.; Herring, A. M.; Hickner, M. A.; Kohl, P. A.; Kucernak, A. R.; Mustain, W. E.; Nijmeijer, K.; Scott, K., Anion-exchange membranes in electrochemical energy systems. *Energy Environ. Sci.* **2014,** *7* (10), 3135-3191.

18. Noh, S.; Jeon, J. Y.; Adhikari, S.; Kim, Y. S.; Bae, C., Molecular Engineering of Hydroxide Conducting Polymers for Anion Exchange Membranes in Electrochemical Energy Conversion Technology. *Acc. Chem. Res.* **2019,** *52* (9), 2745-2755.

19. Wang, L.; Peng, X.; Mustain, W. E.; Varcoe, J. R., Radiation-grafted anion-exchange membranes: the switch from low-to high-density polyethylene leads to remarkably enhanced fuel cell performance. *Energy Environ. Sci.* **2019,** *12*, 1575-1579.

20. Mustain, W. E., Understanding how high-performance anion exchange membrane fuel cells were achieved: Component, interfacial, and cell-level factors. *Curr. Opin. Chem. Electrochem.* **2018,** *12*, 233-239.

21. Omasta, T. J.; Park, A. M.; LaManna, J. M.; Zhang, Y.; Peng, X.; Wang, L.; Jacobson, D. L.; Varcoe, J. R.; Hussey, D. S.; Pivovar, B. S., Beyond catalysis and membranes: visualizing and solving the challenge of electrode water accumulation and flooding in AEMFCs. *Energy Environ. Sci.* **2018,** *11* (3), 551-558.

22. Krimm, S.; Tobolsky, A. V., Quantitative x‐ray studies of order in amorphous and crystalline polymers. Quantitative x‐ray determination of crystallinity in polyethylene. *J. Polym. Sci.* **1951,** *7* (1), 57-76.

23. Huang, F.; Largier, T. D.; Zheng, W.; Cornelius, C. J., Pentablock copolymer morphology dependent transport and its impact upon film swelling, proton conductivity, hydrogen fuel cell operation, vanadium flow battery function, and electroactive actuator performance. *J. Membr. Sci.* **2018,** *545*, 1-10.

24. Shin, D. W.; Guiver, M. D.; Lee, Y. M., Hydrocarbon-based polymer electrolyte membranes: importance of morphology on ion transport and membrane stability. *Chem. Rev.* **2017,** *117* (6), 4759-4805.

25. Omasta, T.; Wang, L.; Peng, X.; Lewis, C.; Varcoe, J.; Mustain, W. E., Importance of balancing membrane and electrode water in anion exchange membrane fuel cells. *J. Power Sources* **2018,** *375*, 205-213.

26. You, W.; Hugar, K. M.; Coates, G. W., Synthesis of Alkaline Anion Exchange Membranes with Chemically Stable Imidazolium Cations: Unexpected Cross-Linked Macrocycles from Ring-Fused ROMP Monomers. *Macromolecules* **2018,** *51* (8), 3212-3218.

27. Noonan, K. J. T.; Hugar, K. M.; Kostalik, H. A.; Lobkovsky, E. B.; Abruña, H. D.; Coates, G. W., Phosphonium-Functionalized Polyethylene: A New Class of Base-Stable Alkaline Anion Exchange Membranes. *J. Am. Chem. Soc.* **2012,** *134* (44), 18161-18164.

28. Jeon, J. Y.; Park, S.; Han, J.; Maurya, S.; Mohanty, A. D.; Tian, D.; Saikia, N.; Hickner, M. A.; Ryu, C. Y.; Tuckerman, M. E.; Paddision, S. J.; Kim, Y. S.; Bae, C., Synthesis of Aromatic Anion Exchange Membranes by Friedel–Crafts Bromoalkylation and Cross-Linking of Polystyrene Block Copolymers. *Macromolecules* **2019,** *52* (5), 2139-2147.

29. Akiyama, R.; Yokota, N.; Miyatake, K., Chemically Stable, Highly Anion Conductive Polymers Composed of Quinquephenylene and Pendant Ammonium Groups. *Macromolecules* **2019,** *52* (5), 2131-2138.

30. Zhu, L.; Peng, X.; Shang, S. L.; Kwasny, M. T.; Zimudzi, T. J.; Yu, X.; Saikia, N.; Pan, J.; Liu, Z. K.; Tew, G. N., High Performance Anion Exchange Membrane Fuel Cells Enabled by Fluoropoly (olefin) Membranes. *Adv. Funct. Mater.* **2019,** *29*, 1902059.

31. Zhang, J.; Pellechia, P. J.; Hayat, J.; Hardy, C. G.; Tang, C., Quantitative and Qualitative Counterion Exchange in Cationic Metallocene Polyelectrolytes. *Macromolecules* **2013,** *46* (4), 1618-1624.

CHAPTER 5

SUMMARY AND OUTLOOK[1]

[1] Zhu, T.; Sha, Y.; Yan, J.; Pageni, P.; Rahman, M. A.; Yan, Y.; Tang, C., Metallo-Polyelectrolytes as A Class of Ionic Macromolecules for Functional Materials. *Nat. Commun.* ***2018,*** *9,* 4329. Adapted with permission from Springer Nature. Copyright © 2018 Springer Nature

5.1 DISSERTATION SUMMARY

Metallo-polyelectrolytes represent an emerging class of polymeric materials with unique properties compared to traditional polyelectrolytes and neutral metallopolymers. Exclusive dependence on fossil fuels in recent decades have expedited research towards developing more environmentally friendly and cost-effective energy storage and conversion systems. Solid polyelectrolyte membranes with good mechanical property, ionic conductivity and chemical stability are in urgent need for a range of electrochemical devices. In this thesis, we demonstrated ROMP of cobaltocenium-containing cyclooctene monomers followed by backbone hydrogenation as a versatile template to prepare metallo-polyelectrolyte membranes with excellent mechanical properties and alkaline stability. To broaden this area, a combination of computational and experiment design toward a set of metallo-cations with tunable electronic and redox properties was presented. The exploration of redox- and alkaline- stable cations further allows us to prepare new solid polyelectrolyte membranes with unprecedented properties. Finally, we reported the first-ever tests of these polyelectrolytes in a device under highly alkaline, oxidative and humid environments with performance competitive with well-established organo-polyelectrolytes. We believe the utilization of metallo-cations instead of traditional quaternary ammonium cations for solid polyelectrolyte membranes could circumvent the long-term stability issue for solid electrolyte membranes and bring new functions. However, the major limitation at current stage is large molar mass of metallo-cations (e.g. 301 g/mol for octamethyl cobaltocenium, compared to 74 g/mol for trimethyl quaternary ammonium cation), which results in significant lower IEC with similar mass ratio of charged groups. On the other hand, current practices in the preparation of synthetic

polyelectrolytes are mostly unsustainable, even though they are targeted for sustainable applications (e.g. clean power sources). Thus, exploring more efficient and economy synthetic pathways for synthetic polyelectrolytes are of vital importance.

5.2 FUTURE DIRECTION

The field of metallo-polyelectrolytes is just beginning to take off, as a result of their fascinating electronic, physicochemical and redox properties that are recently discovered as quite differently from organo-polyelectrolyte counterparts. The unique electronic properties of metal centers endow metallo-polyelectrolytes some of unprecedented ionic binding with a variety of (macro)molecular substrates. They could complex with small antibiotics, oppositely charged polyelectrolytes such as DNA and peptides, as well as cell membranes or crosslinked networks. The redox properties further allow metallo-polyelectrolytes to access many functions that traditional organo-polyelectrolytes cannot. Metal cations also possess unusual physiochemical stability, which could be well utilized in applications requiring robust ion exchange and transport. Given these rich properties, we summarize below specific applications and challenges, and provide future perspectives of metallo-polyelectrolytes.

Quantitative analysis of ionic binding strength of metallo-polyelectrolytes with molecular substrates is largely missing. While similar dilemma is faced with the entire field of polyelectrolytes, our understanding on metallo-polyelectrolytes is almost exclusively qualitative. For organo-polyelectrolytes, quantitative interaction strength of polyelectrolyte complexes (PECs) has been directly probed by the ability of salts added to break ion pairs using spectroscopic methods. The Schlenoff group have pioneered on the salt-water plasticization of PECs (“saloplasticity”) to extrude dense shapes suitable for many types of

measurements, including ion equilibria.[2-3] However, quantitative binding with small molecules or membranes is critically needed. An establishment of representative phase diagram would be a challenging, but worthy task to explore.[4] There is an urgent need to establish quantitative physical chemistry of metallo-polyelectrolytes.

Theoretical models are needed to construct and predict key influential parameters on polyelectrolyte complexation.[5-6] These models could combine with experimental analysis to augment the understanding at molecular and macroscopic levels. A mean-field model of complex coacervation from weakly charged polymers has been established by Voorn and Overbeek.[7] Parameters include chain length, charge density and concentrations of polymers and salts. Random phase approximation allows high charge densities and connectivity of polymer segments, as studied in early 2000.[8-9] Later, an off-lattice approach describing polyelectrolyte complexation for polyelectrolytes with pH-dependent charges was constructed by Biesheuvel and Cohen Stuart.[10] Very recently, a coarse-grained model is proposed to simulate coacervation as a function of polymer length and overall salt concentration by the de Palbo group.[11] These models could help estimate the total free energy of mixing as well as mixing entropy and enthalpy terms. However, these models only deal with organo-polyelectrolytes. New models or advanced versions of the above models must take consideration of metal cations and their unique electronic and redox properties.

Grand challenges would be dealing with more complex biological interfaces. For example, multiple mechanisms of action have been proposed for antimicrobial activity of metallo-polyelectrolytes. However, the intrinsic free energy change such as enthalpy and entropy change as well as solubility equilibrium, which ultimately interferes key

biochemical processes, is still not quantitively studied. A more comprehensive understanding is needed to direct the design of macromolecular metal complexes, i.e., macromolecular structures, complex types and metal moieties. Another example involves ion transport. Theoretical modelling could help design new metallo-polyelectrolytes with better phase-separate structures for improved electrochemical performance.

Nevertheless, the fields of polymer and macromolecular sciences have overseen the enormous potential of metallo-polyelectrolytes for a broad range of fundamental scientific mysteries and practical applications. Much work on the chemistry, biology, physics and engineering of metallo-polyelectrolytes is expected in the coming years to fulfill the ever-increasing demands for functional advanced materials.

5.3 References

1. Zhu, T.; Sha, Y.; Yan, J.; Pageni, P.; Rahman, M. A.; Yan, Y.; Tang, C., Metallo-polyelectrolytes as a class of ionic macromolecules for functional materials. *Nat. Commun.* **2018,** *9* (1), 4329.

2. Shamoun, R. F.; Hariri, H. H.; Ghostine, R. A.; Schlenoff, J. B., Thermal Transformations in Extruded Saloplastic Polyelectrolyte Complexes. *Macromolecules* **2012,** *45* (24), 9759-9767.

3. Fu, J.; Fares, H. M.; Schlenoff, J. B., Ion-Pairing Strength in Polyelectrolyte Complexes. *Macromolecules* **2017,** *50* (3), 1066-1074.

4. Rumyantsev, A. M.; Kramarenko, E. Y.; Borisov, O. V., Microphase Separation in Complex Coacervate Due to Incompatibility between Polyanion and Polycation. *Macromolecules* **2018,** *51* (17), 6587-6601.

5. Spruijt, E.; Westphal, A. H.; Borst, J. W.; Cohen Stuart, M. A.; van der Gucht, J., Binodal compositions of polyelectrolyte complexes. *Macromolecules* **2010,** *43* (15), 6476-6484.

6. Van der Gucht, J.; Spruijt, E.; Lemmers, M.; Stuart, M. A. C., Polyelectrolyte complexes: bulk phases and colloidal systems. *J. Colloid Interface Sci* **2011,** *361* (2), 407-422.

7. Overbeek, J. T. G.; Voorn, M., Phase separation in polyelectrolyte solutions. Theory of complex coacervation. *J. Cell. Physiol* **1957,** *49* (S1), 7-26.

8. Castelnovo, M.; Joanny, J.-F., Formation of polyelectrolyte multilayers. *Langmuir* **2000,** *16* (19), 7524-7532.

9. Kudlay, A.; Ermoshkin, A. V.; Olvera de La Cruz, M., Complexation of oppositely charged polyelectrolytes: effect of ion pair formation. *Macromolecules* **2004,** *37* (24), 9231-9241.

10. Biesheuvel, P. M.; Cohen Stuart, M. A., Electrostatic free energy of weakly charged macromolecules in solution and intermacromolecular complexes consisting of oppositely charged polymers. *Langmuir* **2004,** *20* (7), 2785-2791.

11. Andreev, M.; Prabhu, V. M.; Douglas, J. F.; Tirrell, M.; de Pablo, J. J., Complex Coacervation in Polyelectrolytes from a Coarse-Grained Model. *Macromolecules* **2018,** *51* (17), 6717-6723.

APPENDIX A – PERMISSION TO REPRINT

Figure A.1. Copyright release for Chapter 1 and Chapter 5.

Order Completed

Thank you for your order.

This Agreement between University of South Carolina -- Tianyu Zhu ("You") and John Wiley and Sons ("John Wiley and Sons") consists of your license details and the terms and conditions provided by John Wiley and Sons and Copyright Clearance Center.

Your confirmation email will contain your order number for future reference.

printable details

License Number	4678250296350
License date	Sep 29, 2019
Licensed Content Publisher	John Wiley and Sons
Licensed Content Publication	Angewandte Chemie International Edition
Licensed Content Title	Cationic Metallo-Polyelectrolytes for Robust Alkaline Anion-Exchange Membranes
Licensed Content Author	Chuanbing Tang, Xiao-dong Zhou, Mohammad Pabel Kabir, et al
Licensed Content Date	Jan 16, 2018
Licensed Content Volume	57
Licensed Content Issue	9
Licensed Content Pages	5
Type of use	Dissertation/Thesis
Requestor type	Author of this Wiley article
Format	Print and electronic
Portion	Full article
Will you be translating?	No
Title of your thesis / dissertation	CATIONIC COBALTOCENE DERIVATIVES AND POLYELECTROLYTES FOR ENERGY STORAGE APPLICATIONS
Expected completion date	Dec 2019
Expected size (number of pages)	150
Requestor Location	University of South Carolina 631 Sumter Street Horizon I Room 210 COLUMBIA, SC 29208 United States Attn: University of South Carolina

Figure A.2. Copyright release for Chapter 2.

APPENDIX B – CRYSTAL STRUCTURES

X-Ray Structure Determination of $Co(C_5H_5)_2(PF_6)$

Crystals of the compound formed as abundant yellow plates, some quite large (>1 mm), most of which were visibly twinned. The crystals are sensitive to mechanical manipulation and visibly deform unless handled gently. They cannot be cleaved without degradation of single crystallinity. Several crystals were examined, all flash-cooled to 100 K. Most gave diffraction patterns consistent with multiple domains. Upon removing the screened crystals from the diffractometer cold stream, extensive fracturing was evident when viewed with a polarizing microscope. This is likely the result of the temperature-induced phase transition known to occur in this material. Eventually a seemingly untwinned yellow plate single crystal was found. Examination of the diffraction pattern showed some weak unindexed reflections, but they were not significantly overlapped with those of the major domain. The best refinement model (below) neglects these reflections. No contribution from a minor twin domain was found with the TwinRotMat program. X-ray intensity data were collected at 100(2) K using a Bruker D8 QUEST diffractometer equipped with a PHOTON-100 CMOS area detector and an Incoatec microfocus source (Mo Kα radiation, λ = 0.71073 Å). The raw area detector data frames were reduced and corrected for absorption effects using the Bruker APEX3, SAINT+ and SADABS programs.[1, 2] The structure was solved with SHELXT. Subsequent difference Fourier calculations and full-matrix least-squares refinement against F^2 were performed with SHELXL-2018[3] using OLEX2.[4]

The compound crystallizes in the monoclinic system. The pattern of systematic absences in the intensity data was consistent with the space group $P2_1/c$, which was confirmed by structure solution. The structure has been determined previously at 243 K and is also isostructural with the ferrocenium analog at 120 K.[5, 6] The asymmetric unit

consists of half each of two cobaltocenium ($Co(C_5H_5)_2^+$) cations and one hexafluorophosphate anion. Both unique cobalt centers are located on crystallographic inversion centers. As shown in **Figure S1**, cation Co2 is disordered and was modeled with two orientations. Only the unique $C_5H_5^-$ ring is affected, and it was modeled with two equally occupied components (C6-C10 A/B). All non-hydrogen atoms were refined with anisotropic displacement parameters. Hydrogen atoms were located in different Fourier maps before being placed in geometrically idealized positions and included as riding atoms with *d*(C-H) = 0.95 Å and *U*iso(H) = 1.2*U*eq(C). The largest residual electron density peak in the final difference map is 0.60 $e^-/Å^3$, located 1.10 Å from Co2.

Table B.1. Crystal data and structure refinement for $Co(C_5H_5)_2(PF_6)$

Empirical formula	$C_{10}H_{10}CoF_6P$
Formula weight	334.08
Temperature/K	100(2)
Crystal system	monoclinic
Space group	$P2_1/c$
a/Å	13.2837(17)
b/Å	9.1759(12)
c/Å	9.2520(12)
α/°	90
β/°	96.293(3)
γ/°	90
Volume/$Å^3$	1120.9(3)
Z	4
$\rho_{calc}g/cm^3$	1.980
μ/mm^{-1}	1.731
F(000)	664.0
Crystal size/mm^3	0.2 × 0.08 × 0.02

Radiation	MoKα (λ = 0.71073)
2Θ range for data collection/°	3.084 to 52.876
Index ranges	-16 ≤ h ≤ 16, -11 ≤ k ≤ 11, -11 ≤ l ≤ 10
Reflections collected	12519
Independent reflections	2303 [R_{int} = 0.0484, R_{sigma} = 0.0329]
Data/restraints/parameters	2303/0/212
Goodness-of-fit on F^2	1.076
Final R indexes [I>=2σ (I)]	R_1 = 0.0368, wR_2 = 0.0739
Final R indexes [all data]	R_1 = 0.0570, wR_2 = 0.0807
Largest diff. peak/hole / e $Å^{-3}$	0.60/-0.42

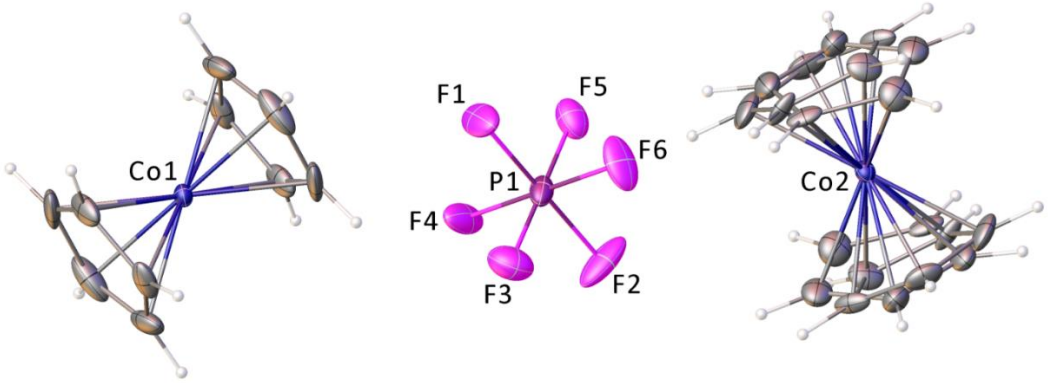

Figure B.1. Molecular structure of **1** showing displacement ellipsoids drawn at the 60% probability level. Both Co centers on crystallographic inversion centers. Cp rings of Co2 disordered over two equally populated orientations.

X-Ray Structure Determination of $Co(C_5H_3(CH_3)_2)_2][PF_6]$

X-ray intensity data from a yellow plate were collected at 100(2) K using a Bruker D8 QUEST diffractometer equipped with a PHOTON-100 CMOS area detector and an Incoatec microfocus source (Mo Kα radiation, λ = 0.71073 Å). The raw area detector data frames were reduced and corrected for absorption effects using the Bruker APEX3, SAINT+ and SADABS programs.[1, 2] The structure was solved with SHELXT. Subsequent

difference Fourier calculations and full-matrix least-squares refinement against F^2 were performed with SHELXL-2018[3] using OLEX2.[4]

The compound crystallizes in the tetragonal system. The pattern of systematic absences in the intensity data was consistent with the space groups *I*4, *I*-4 and *I*4/*m*. The non-centrosymmetric group *I*-4 was eventually confirmed by successful solution and refinement, and by trial refinements in lower space groups (see below). The asymmetric unit consists of ¼ of one $Co(Me_2Cp)_2^+$ cation and ¼ of one PF_6^- anion. Both species are located on sites of crystallographic S_4 point symmetry. The $Co(Me_2Cp)_2^+$ cation is disordered about the S_4 axis. One Me_2Cp grouping exists in the asymmetric unit, and four are generated by the S_4 axis. Atoms of the Me_2Cp group were refined with half-occupancy, but with no other restraints. All non-hydrogen atoms were refined with anisotropic displacement parameters. Hydrogen atoms bonded to carbon were located in difference Fourier maps before being placed in geometrically idealized positions and included as riding atoms with *d*(C-H) = 0.95 Å and *U*iso(H) = 1.2*U*eq(C) for aromatic hydrogen atoms and *d*(C-H) = 0.98 Å and *U*iso(H) = 1.5*U*eq(C) for methyl hydrogens. The methyl hydrogens were allowed to rotate as a rigid group to the orientation of maximum observed electron density. The largest residual electron density peak in the final difference map is 0.50 $e^-/Å^3$, located 2.03 Å from C2. The absolute structure (Flack) parameter near convergence was 0.17(3), consistent with a minor inversion twinning component. An inversion matrix was included in the final refinement cycles. Efforts to resolve the Me_2Cp group disorder by solution and refinement in lower space groups, including *C*2 and *P*1 (No. 1), were unsuccessful. The same disorder appeared in all lower symmetry groups. The

structure is therefore genuinely disordered and the space group *I*-4 was retained as the best symmetry description for the structure.

Table B.2. Crystal data and structure refinement for $[Co(C_5H_3(CH_3)_2)_2][PF_6]$

Empirical formula	$C_{14}H_{18}CoF_6P$
Formula weight	390.18
Temperature/K	100(2)
Crystal system	tetragonal
Space group	I-4
a/Å	10.8185(3)
b/Å	10.8185(3)
c/Å	6.6735(2)
α/°	90
β/°	90
γ/°	90
Volume/Å^3	781.07(5)
Z	2
ρ_{calc}g/cm^3	1.659
μ/mm^{-1}	1.255
F(000)	396.0
Crystal size/mm^3	0.4 × 0.3 × 0.18
Radiation	MoKα (λ = 0.71073)
2Θ range for data collection/°	5.326 to 60.042
Index ranges	$-15 \leq h \leq 14$, $-15 \leq k \leq 15$, $-9 \leq l \leq 9$
Reflections collected	18295
Independent reflections	1149 [R_{int} = 0.0349, R_{sigma} = 0.0137]
Data/restraints/parameters	1149/0/86
Goodness-of-fit on F^2	1.142
Final R indexes [I>=2σ (I)]	R_1 = 0.0197, wR_2 = 0.0495
Final R indexes [all data]	R_1 = 0.0211, wR_2 = 0.0502

Largest diff. peak/hole / e Å^{-3}	0.50/-0.40
Flack parameter	0.17(3)

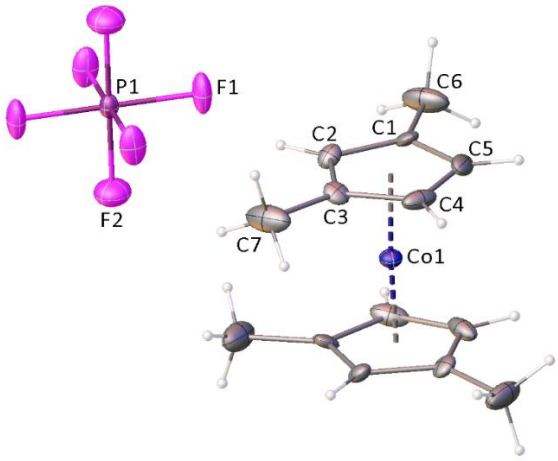

Figure B.2. Molecular structure of **2b** showing displacement ellipsoids drawn at the 40% probability level. Images of one possible Me_2Cp grouping arrangement in the cation.

X-Ray Structure Determination of $[Co(C_5H_2(CH_3)_3)_2][PF_6]$

X-ray intensity data from a yellow block were collected at 100(2) K using a Bruker D8 QUEST diffractometer equipped with a PHOTON-100 CMOS area detector and an Incoatec microfocus source (Mo Kα radiation, λ = 0.71073 Å). Strong diffuse scattering in the form of continuous streaks connecting Bragg spots was observed in the diffraction frames. This apparently arises because of a form of occupational disorder affecting only the cobalt atomic position in the derived structural model (below). The diffuse streaking was observed regardless of data collection temperature, as the effect was also observed at room temperature using fresh crystals that had never been cooled. The raw area detector data frames were reduced and corrected for absorption effects using the Bruker APEX3, SAINT+ and SADABS programs.[1, 2] The structure was solved with SHELXT.[3] Subsequent difference Fourier calculations and full-matrix least-squares refinement against F^2 were performed with SHELXL-2018[3] using OLEX2.[4]

The compound crystallizes in the space group $C222_1$ of the orthorhombic system. The initial structure solution revealed all carbon atoms of one Me_3Cp ring, one P and three F atoms of the hexafluorophosphate anion and two apparent metal atom sites. The PF_6^- anion is located on a crystallographic C_2 axis of rotation. The two possible metal sites were both located at distances from the Me_3Cp ring atoms typical of cobalt-cyclopentadiene groups (*ca*. 2.05 Å). Both metal atom sites are also located on crystallographic C_2 axes. Refinement of both metal sites with full occupancy gave abnormally large displacement parameters, poor *R*-values and unusual difference Fourier map features. Refinement of the metal site occupancies resulted in a significant decrease from unity occupancy for both sites (Co1A ~ 0.72 and Co1B ~ 0.28), a precipitous decrease in *R*-values and a normalization of the difference map. This implies one cobalt atom which is disordered over two partially occupied sites with a total occupancy near 1.0. This was interpreted as a whole-molecule (cation) disorder. In the structure, the Me_3Cp rings are ordered in planes parallel to the crystallographic ***bc*** plane at $x \sim 0.25$. The Me_3Cp rings further are aligned into stacked columns running along the crystallographic ***a*** axis. Since all Me_3Cp rings are equivalent by symmetry, the distance between adjacent Me_3Cp rings in a column is always 3.30 Å (half the ***a*** axis length), regardless of whether the ring above or below is considered. The cobalt atomic positions are disordered halfway between the Me_3Cp planes, with unequally distributed occupancies located at $x = 0$ (Co1A, 71.9% occupancy) and $x = 0.5$ (Co1B, 28.1% occupancy). The most reasonable interpretation of the disorder model is that entire stacked $Co(Me_3Cp)_2^+$ columns contain either all Co1A or all Co1B, with 72% of the columns containing Co1A and 28% containing Co1B in a disordered arrangement. The Co1A and Co1B cations are enantiomers, implying that upon crystallization, a partial

resolution of the racemic solution mixture has taken place, generating a disordered structure. Such disorder correlates with the diffuse scattering seen in the area detector diffraction frame images, discussed above. For the final refinement model, the total cobalt occupancy was constrained to sum to one, giving anisotropic displacement parameters of reasonable magnitude and form. All non-hydrogen atoms were refined with anisotropic displacement parameters. Hydrogen atoms bonded to carbon were located in difference Fourier maps. The two unique arene hydrogen atoms were refined freely. Methyl hydrogens were placed in geometrically idealized positions and included as riding atoms with *d*(C-H) = 0.98 Å and freely refined isotropic displacement parameters. They were allowed to rotate as a rigid group to the orientation of maximum observed electron density. The largest residual electron density peak in the final difference map is 0.67 $e^-/Å^3$, located 1.02 Å from Co1B. Examination of the diffraction frames, including synthetic precession images, did not reveal superstructure reflections consistent with a larger unit cell. Solution attempts in lower symmetry space groups (including *P*1, No. 1) likewise did not resolve the disorder.

Table B.3. Crystal data and structure refinement for $[Co(C_5H_2(CH_3)_3)_2][PF_6]$

Empirical formula	$C_{16}H_{22}CoF_6P$
Formula weight	418.23
Temperature/K	100(2)
Crystal system	orthorhombic
Space group	$C222_1$
a/Å	6.5974(2)
b/Å	15.3006(5)
c/Å	16.7260(6)
α/°	90
β/°	90
γ/°	90

Volume/Å^3	1688.39(10)
Z	4
ρ_{calc}g/cm^3	1.645
μ/mm^{-1}	1.167
F(000)	856.0
Crystal size/mm^3	0.48 × 0.34 × 0.22
Radiation	MoKα (λ = 0.71073)
2Θ range for data collection/°	4.87 to 65.208
Index ranges	-10 ≤ h ≤ 9, -23 ≤ k ≤ 23, -25 ≤ l ≤ 25
Reflections collected	26861
Independent reflections	3087 [R_{int} = 0.0322, R_{sigma} = 0.0153]
Data/restraints/parameters	3087/0/138
Goodness-of-fit on F^2	1.204
Final R indexes [I>=2σ (I)]	R_1 = 0.0332, wR_2 = 0.0824
Final R indexes [all data]	R_1 = 0.0345, wR_2 = 0.0830
Largest diff. peak/hole / e Å^{-3}	0.67/-0.76
Flack parameter	0.47(3)

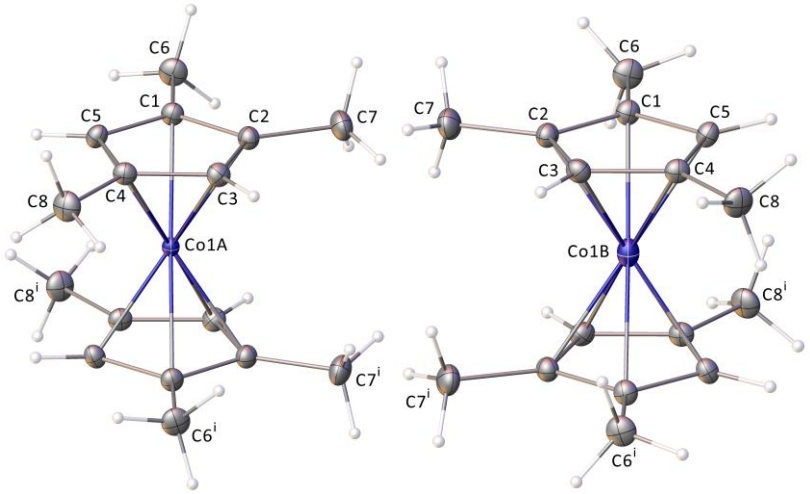

Figure B.3. Molecular structure of **S17** showing displacement ellipsoids drawn at the 50% probability level.Co1A and Co1B cations are enantiomers. Counterions are omitted for clarity.

X-Ray Structure Determination of [Co(C$_5$H(CH$_3$)$_4$)$_2$][PF$_6$]

X-ray intensity data from a yellow needle were collected at 100(2) K using a Bruker D8 QUEST diffractometer equipped with a PHOTON-100 CMOS area detector and an Incoatec microfocus source (Mo Kα radiation, λ = 0.71073 Å). The raw area detector data frames were reduced and corrected for absorption effects using the Bruker APEX3, SAINT+ and SADABS programs.[1, 2] The structure was solved with SHELXT. Subsequent difference Fourier calculations and full-matrix least-squares refinement against F^2 were performed with SHELXL-2018[3] using OLEX2.[4]

The compound crystallizes in the orthorhombic system. The pattern of systematic absences in the intensity data was consistent with several space groups; *Cmce* (No. 64) was found by the solution program XT and was confirmed by refinement. The asymmetric unit consists of (formally) ¼ of one $[Co(C_5H(CH_3)_4)_2]^+$ cation and ¼ of one PF_6^- anion. Both species are located on sites of crystallographic C_{2h} point symmetry. The cobaltocenium cation is ordered on its site. The PF_6^- phosphorus atom is also ordered but the fluorine atoms are disordered, defining four orientations of the anion. Two crystallographically independent sets of two F atoms each per asymmetric unit were refined. F1 is disordered over two positions with occupancies F1A/F1B = 0.56(6)/0.44(6). F2 is disordered over four positions; two in the asymmetric unit with occupancies F2A/F2B = 0.22(3)/0.28(3) and two additional symmetry-equivalent F2 sites generated by a mirror plane. All P-F bonds were restrained to similar distances. All non-hydrogen atoms were refined with anisotropic displacement parameters. Hydrogen atoms bonded to carbon were located in difference Fourier maps before being placed in geometrically idealized positions and included as riding atoms with *d*(C-H) = 0.95 Å and *U*iso(H) = 1.2*U*eq(C) for the arene hydrogen atom and *d*(C-H) = 0.98 Å and *U*iso(H) = 1.5*U*eq(C) for methyl hydrogens. The methyl

hydrogens were allowed to rotate as a rigid group to the orientation of maximum observed electron density. The largest residual electron density peak in the final difference map is 0.38 $e^-/Å^2$, located 0.73 Å from C3.

Table B.4. Crystal data and structure refinement for $[Co(C_5H(CH_3)_4)_2][PF_6]$

Empirical formula	$C_{18}H_{26}CoF_6P$
Formula weight	446.29
Temperature/K	100(2)
Crystal system	orthorhombic
Space group	Cmce
a/Å	13.1710(4)
b/Å	11.3315(4)
c/Å	12.6496(4)
α/°	90
β/°	90
γ/°	90
Volume/$Å^3$	1887.92(11)
Z	4
$\rho_{calc}g/cm^3$	1.570
μ/mm^{-1}	1.049
F(000)	920.0
Crystal size/mm^3	0.28 × 0.22 × 0.2
Radiation	MoKα (λ = 0.71073)
2Θ range for data collection/°	5.732 to 60.126
Index ranges	$-18 \leq h \leq 18$, $-15 \leq k \leq 15$, $-17 \leq l \leq 17$
Reflections collected	35896
Independent reflections	1440 [R_{int} = 0.0534, R_{sigma} = 0.0187]
Data/restraints/parameters	1440/6/91
Goodness-of-fit on F^2	1.271
Final R indexes [I>=2σ (I)]	R_1 = 0.0335, wR_2 = 0.0720

Final R indexes [all data]	$R_1 = 0.0388$, $wR_2 = 0.0737$
Largest diff. peak/hole / e Å^{-3}	0.38/-0.30

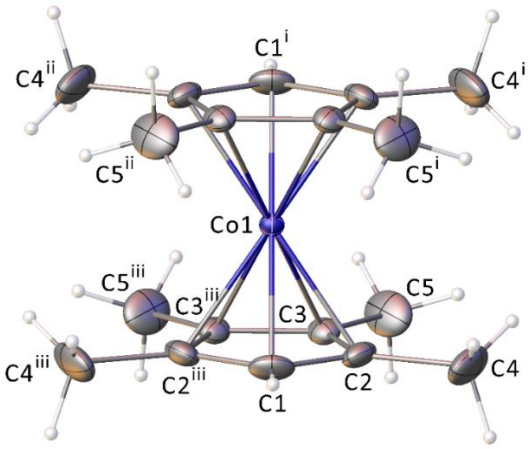

Figure B.4. Molecular structure of **2c** showing displacement ellipsoids drawn at the 50% probability level. Counterions are omitted for clarity.

X-Ray Structure Determination of $[Co(C_5H_4C(CH_3)_3)_2][PF_6]$

X-ray intensity data from a yellow plate were collected at 100(2) K using a Bruker D8 QUEST diffractometer equipped with a PHOTON-100 CMOS area detector and an Incoatec microfocus source (Mo Kα radiation, λ = 0.71073 Å). The raw area detector data frames were reduced and corrected for absorption effects using the Bruker APEX3, SAINT+ and SADABS programs.[1, 2] The structure was solved with SHELXT. Subsequent difference Fourier calculations and full-matrix least-squares refinement against F^2 were performed with SHELXL-2018[3] using OLEX2.[4]

The compound crystallizes in the monoclinic system. The pattern of systematic absences in the intensity data was consistent with the space groups *C*2, *Cm*, and *C*2/*m*. The centrosymmetric space group *C*2/*m* was confirmed by structure solution. The asymmetric unit consists of (formally) ¼ of one $[Co(C_5H_4C(CH_3)_3)_2]^+$ cation and ¼ of one hexafluorophosphate anion. Both species are located on positions of crystallographic 2/*m*

(C_{2h}) point symmetry. All non-hydrogen atoms were refined with anisotropic displacement parameters. Hydrogen atoms were located in difference Fourier maps before being placed in geometrically idealized positions and included as riding atoms with *d*(C-H) = 0.95 Å and *U*iso(H) = 1.2*U*eq(C) for aromatic hydrogen atoms and *d*(C-H) = 0.98 Å and *U*iso(H) = 1.5*U*eq(C) for methyl hydrogens. The largest residual electron density peak in the final difference map is 0.41 $e^-/Å^3$, located 0.75 Å from C4.

Table B.5. Crystal data and structure refinement for $[Co(C_5H_4C(CH_3)_3)_2](PF_6)$

Empirical formula	$C_{18}H_{26}CoF_6P$
Formula weight	446.29
Temperature/K	100(2)
Crystal system	monoclinic
Space group	C2/m
a/Å	11.6313(4)
b/Å	9.8968(4)
c/Å	8.6586(3)
α/°	90
β/°	105.259(2)
γ/°	90
Volume/$Å^3$	961.58(6)
Z	2
$\rho_{calc}g/cm^3$	1.541
μ/mm^{-1}	1.030
F(000)	460.0
Crystal size/mm^3	0.46 × 0.22 × 0.08
Radiation	MoKα (λ = 0.71073)
2Θ range for data collection/°	4.876 to 56.598
Index ranges	$-15 \leq h \leq 15$, $-13 \leq k \leq 13$, $-11 \leq l \leq 11$
Reflections collected	17749

Independent reflections	1266 [R_{int} = 0.0390, R_{sigma} = 0.0165]
Data/restraints/parameters	1266/0/71
Goodness-of-fit on F^2	1.086
Final R indexes [I>=2σ (I)]	R_1 = 0.0228, wR_2 = 0.0586
Final R indexes [all data]	R_1 = 0.0253, wR_2 = 0.0603
Largest diff. peak/hole / e Å^{-3}	0.41/-0.28

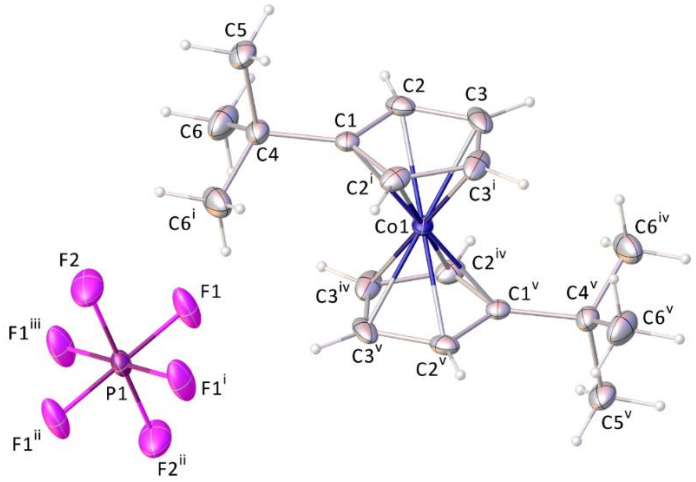

Figure B.5. Molecular structure of **3a** showing displacement ellipsoids drawn at the 50% probability level. Superscripts denote symmetry-equivalent atoms. Both species have C_{2h} point symmetry.

X-Ray Structure Determination of [Co(C$_5$H$_3$(C(CH$_3$)$_3$)$_2$)$_2$](PF$_6$)

X-ray intensity data from a yellow needle were collected at 100(2) K using a Bruker D8 QUEST diffractometer equipped with a PHOTON-100 CMOS area detector and an Incoatec microfocus source (Mo Kα radiation, λ = 0.71073 Å). The raw area detector data frames were reduced and corrected for absorption effects using the Bruker APEX3, SAINT+ and SADABS programs.[1, 2] The structure was solved with SHELXT. Subsequent difference Fourier calculations and full-matrix least-squares refinement against F^2 were performed with SHELXL-2018[3] using OLEX2.[4]

The compound crystallizes in the monoclinic system. The pattern of systematic absences in the intensity data was consistent with the space group $P2_1/c$, which was verified by structure solution. The asymmetric unit consists of one cobaltocenium cation and one hexafluorophosphate anion. The PF_6^- anion is disordered and was modeled using three components. Anisotropic displacement parameters for nearly superimposed P and F atoms were held equal, and the total PF_6^- group occupancy was constrained to sum to 1.0. The occupancies refined to A/B/C = 0.506(3)/0.216(2)/0.277(3). The geometry of each of the two minor components (B/C) was restrained to be similar to that of the major component (A) using SHELX SAME instructions. All non-hydrogen atoms were refined with anisotropic displacement parameters. Hydrogen atoms bonded to carbon were located in difference Fourier maps before being placed in geometrically idealized positions and included as riding atoms with *d*(C-H) = 0.95 Å and *U*iso(H) = 1.2*U*eq(C) for aromatic hydrogen atoms and *d*(C-H) = 0.98 Å and *U*iso(H) = 1.5*U*eq(C) for methyl hydrogens. The methyl hydrogens were allowed to rotate as a rigid group to the orientation of maximum observed electron density. The largest residual electron density peak in the final difference map is 0.89 $e^-/Å^3$, located 0.84 Å from Co1.

Table B.6. Crystal data and structure refinement for $[Co(C_5H_3(C(CH_3)_3)_2)_2](PF_6)$

Empirical formula	$C_{26}H_{42}CoF_6P$
Formula weight	558.49
Temperature/K	100(2)
Crystal system	monoclinic
Space group	$P2_1/c$
a/Å	10.1801(5)
b/Å	25.8207(13)
c/Å	11.3019(6)

α/°	90
β/°	112.920(2)
γ/°	90
Volume/Å^3	2736.2(2)
Z	4
ρ_{calc}g/cm^3	1.356
μ/mm^{-1}	0.739
F(000)	1176.0
Crystal size/mm^3	0.54 × 0.42 × 0.38
Radiation	MoKα (λ = 0.71073)
2Θ range for data collection/°	4.84 to 56.64
Index ranges	-13 ≤ h ≤ 13, -34 ≤ k ≤ 34, -15 ≤ l ≤ 15
Reflections collected	118472
Independent reflections	6721 [R_{int} = 0.0667, R_{sigma} = 0.0269]
Data/restraints/parameters	6721/64/365
Goodness-of-fit on F^2	1.077
Final R indexes [I>=2σ (I)]	R_1 = 0.0422, wR_2 = 0.0936
Final R indexes [all data]	R_1 = 0.0521, wR_2 = 0.0974
Largest diff. peak/hole / e Å^{-3}	0.89/-0.53

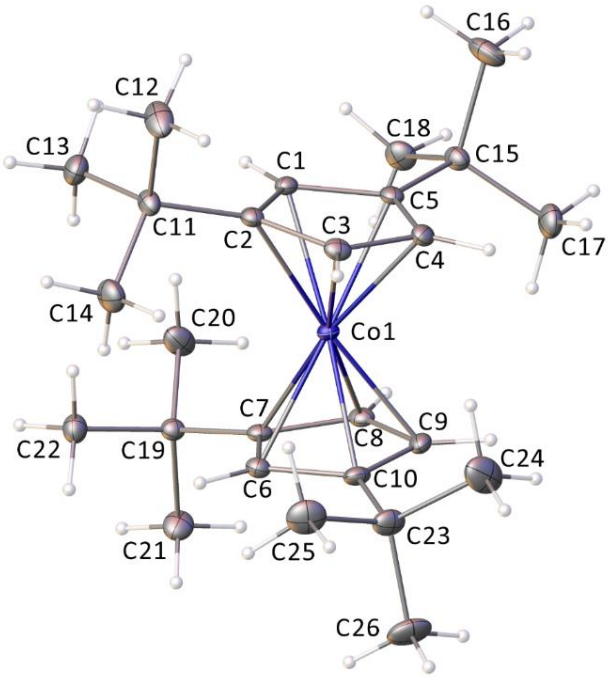

Figure B.6. Molecular structure of **3b** displacement ellipsoids drawn at the 40% probability level. Counterions are omitted for clarity.

References

1. Krause, L., Herbst-Irmer, R., Sheldrick, G. M., Stalke, D. Comparison of Silver and Molybdenum Microfocus X-Ray Sources for Single-Crystal Structure Determination. *J. Appl. Crystallogr.* **48**, 3-10 (2015).
2. Bruker AXS, I. *Apex3 Version 2018.1-0 and Saint+ Version 8.38a.* (2016).
3. Sheldrick, G. M. Shelxt–Integrated Space-Group and Crystal-Structure Determination. *Acta Crystallogr. A* **71**, 3-8 (2015).
4. Dolomanov, O. V., Bourhis, L. J., Gildea, R. J., Howard, J. A., Puschmann, H. Olex2: A Complete Structure Solution, Refinement and Analysis Program. *J. Appl. Crystallogr.* **42**, 339-341 (2009).
5. Braga, D., Scaccianoce, L., Grepioni, F., Draper, S. M. From Order to Disorder and Return: Remarkable Molecular and Crystal Dynamics in Solid [(C5h5) 2co][Pf6]. *Organometallics* **15**, 4675-4677 (1996).
6. Posner, S. R., Lorson, L. C., Gell, A. R., Foxman, B. M. Experimental Establishment of Mother–Daughter Orientation Relationships and Twinning Effects in Phase Transitions: A Great Legacy from Jack Gougoutas and Peggy Etter. *Crystal Growth & Design* **15**, 3407-3416 (2015).